EUROPEAN MASTER in
Theoretical Chemistry and Computational Modelling

THE INTERACTION BETWEEN BeX_2 (X = H, F, Cl) MOLECULES AND ETHYLENE/ACETYLENE

A STUDY ON BERYLLIUM BONDS

-MASTER THESIS-

Estefanía Fernández Villanueva
(Universidad de Valladolid)

Supervisor: **Dr. Manuel Yañez Montero**
(Universidad Autónoma de Madrid)

Universidad de Valladolid

UAM UNIVERSIDAD AUTONOMA DE MADRID

Agradecimientos

En primer lugar me gustaría darles las gracias de corazón a mis directores Antonio Largo Cabrerizo y Carmen Barrientos Benito, así como al resto de los miembros del Grupo de Química Computacional de la Universidad de Valladolid, no sólo por la ayuda que en todo momento me ofrecen y me han ofrecido desde el mismo día en que consultara a Antonio, hace ya dos años, sobre el máster cuya tesis estoy aquí presentando, sino sobre todo por la paciencia y en especial la cercanía y calidez más allá de toda relación profesional.

En segundo lugar quisiera agradecer a mis supervisores Manuel Yáñez Montero y Otilia Mo que me aceptaran en su grupo durante la estancia en la que se desarrolló este trabajo de fin de máster y, por supuesto, por toda su ayuda en la realización y estudio del mismo, pero por encima de todo querría agredecerles la infinita paciencia y comprensión mostradas.

En tercer lugar me gustaría agradecerles a mis padres tanto los medios para la realización del máster como el apoyo y la confianza que siempre me han proporcionado.

Además, desearía dar las gracias a todos los compañeros del máster, que durante estos dos años han compartido conmigo no sólo conocimientos sino emociones de todo tipo. La internacionalidad es una de las mejores cualidades de este máster, y gracias a ello he conocido a personas maravillosas y sorprendentes.

También me gustaría darle las gracias a mi compañera Vicky, no solo por intentar ayudarme siempre sino por esa alegría que lleva a todo lo que hace. Se te echa de menos.

A mi amiga Noelia, por estar siempre pendiente de mí, por comprenderme y por siempre estar ahí para lo que sea. Gracias, guapa.

Finalmente, me gustaría agradecer a Javi su apoyo incondicional, su paciencia y su cariño. Un simple gracias, una simple frase puede parecer muy poco para todo lo ha hecho por mí, pero es que para todo eso simplemente no hay palabras. Gracias.

A todos, muchísimas gracias, de verdad.

INDEX

RESUMEN

En estudios recientes se ha mostrado la existencia de un nuevo tipo de 'interacciones no covalentes', llamadas 'enlaces de Berilio'[1], cuyas propiedades químicas parecen indicar un futuro prometedor en áreas como la ciencia de materiales. Estos enlaces de Berilio se producen como aductos entre moléculas de berilio que actúan como ácidos de Lewis y otras moléculas que actúan como bases de Lewis. En este marco, el presente estudio analiza el enlace entre las pequeñas moléculas BeX_2 (X = H, F, Cl) actuando como ácidos y el acetileno o etileno actuando como bases. Para un primer estudio se utilizan métodos DFT, seguidos de optimizaciones a nivel MP2 y CCSD, usándose para todos los métodos la base 6-311+G(d,p), y adicionalmente se realizan cálculos a nivel MP2 y CCSD con la base aug-cc-pVTZ para proporcionar resultados más precisos para la energía. Finalmente, se usan los programas AIMAll y NBO para llevar a cabo análisis topológicos y de orbitales naturales de enlace que permitan el estudio de la natura del enlace. Efectivamente, se encuentra que existe un enlace relativamente fuerte de berilio en cada uno de los complejos y también se observan las principales participaciones de los orbitales y las deformaciones de cada molécula características de los enlaces de berilio. Dentro de cada serie, sin embargo, la tendencia seguida por la densidad del enlace de berilio y la de la energía de interacción del complejo son opuestas. Sospechamos que la deformación sufrida por la subunidad de berilio juega un papel importante en este, a priori, extraño comportamiento, y es necesario investigar más esta cuestión para poder explicarla.

ABSTRACT

Recent studies have shown the existence of a new type of 'non-covalent interactions', called Beryllium bonds[1], whose chemical properties seem to indicate a promising future in material science. These Beryllium bonds are found to be established as an adduct formation between beryllium molecules that act as Lewis acids and other molecules that act as Lewis bases. In this general framework, the present study analyses the bonding between the small BeX_2 (X = H, F, Cl) molecules acting as acids and acetylene or ethylene acting as bases. DFT methods are used for early studies, followed by MP2 and CCSD optimization calculations, all of them with the 6-311+G(d,p) basis set, and additional MP2 and CCSD(T) calculations with the aug-cc-pVTZ basis are employed to provide more precise energy results. Finally, topological and natural bond orbital analyses with AIMAll and NBO programs are carried out to study the nature of the bonding. It is indeed found that there is a relatively strong beryllium bond in each of the corresponding complexes and its expected characteristics regarding the orbitals main participations and the deformation of the moieties are also observed. Within each of the series, however, the trends followed by the density of the beryllium bond and the interaction energy of the complex are opposing. We suspect the deformation undergone by the beryllium subunit plays a key role in this *a priori* strange behavior, and further researches are required to clarify this point.

1. INTRODUCTION

The term "bond" represents one of the most basic concepts in chemistry. It has been usually and roughly defined just as some type of force that keeps some atoms together, but nowadays a more common and correct description states that a bond is "an interaction that stabilizes the system".

There are many types of bonds, and they all are usually classified in two main groups: the strong ones and the weak ones. Strong bonds are, at the same time, divided into the covalent and the ionic ones. The latter are characteristic of crystals, while covalent bonds are characteristic of molecules -though in molecules a mixture of ionic and covalent nature is actually very common-. Following this classification, the weak bonds that take place either within of between molecules are collected in the general term "non-covalent bonds" or "non-covalent interactions".

However, it is known that there are a lot of different non-covalent interactions with very different properties, and it is also known that most of them are very important, for they are responsible of the stabilization and correct functionality of practically all molecular assemblies, not only artificial but natural ones, such as the DNA.

One of the most important non-covalent interactions, that nearly has the strength of a conventional covalent bond[2], is the hydrogen bond. We are all well aware of how important the hydrogen bond is in life, starting by its role in our essential water to our essential DNA passing by synthetic polymers and drugs, etc., that we use in our everyday life.

Well, the characteristics of a hydrogen bond are not necessarily exclusive to them.

In fact, the same type of interaction can be found whenever a not very electronegative element with low-lying empty orbitals is covalently bonded to a more electronegative one. The difference in electronegativity makes the element more positive, and another atom –from a different molecule- with negative net charge can feel the electrostatic attraction, which is the predominant force in a hydrogen bond. Besides, the low empty orbitals of the element allows it to behave as a good electron acceptor, which then makes possible the secondary but important force that characterizes the hydrogen bond: the covalent backbonding from the lone pairs of the atom of the molecule nearby to the mentioned low empty orbitals of the element.

Beryllium is an element that fulfill these requirements, and it also has been shown that BeX_2 derivatives are good Lewis acids[3], which therefore makes the molecule in principle capable of forming this type of non-covalent interaction with molecules that act as Lewis basis.

As a matter of fact, the group of Estructura Molecular y Reactividad Química at the Universidad Autónoma de Madrid leaded by Professor Manuel Yañez Montero has recently discovered this new type of non-covalent interaction in Beryllium complexes, and the group found out that it indeed has several similarities with the hydrogen bond. Due to these similarities, they decided to call it "Beryllium bond".

In the paper entitled *Beryllium Bonds, Do They Exist?* of 2009, which is cited several times in the present work, Yañez et al. analyzed the complexes between BeX_2 (Z=H, F, Cl, OH) with different Lewis basis and discussed the beryllium bonds existence and its characteristics[1].

The conclusions of that study are the background of this work, and I'd like to briefly review here the most important ideas:

The similarity between beryllium bonds and hydrogen bonds are firstly about their nature. As said before, there is a predominant electrostatic component, but the group also found evidence that indicated a non-negligible covalent contribution for beryllium bonds, as there also is in hydrogen bonds. In beryllium bonds, however, this was associated to an electron transfer from the lone pairs of the Lewis base toward the empty p orbital of the beryllium atom and the σ_{BeX*} antibonding orbital instead of just from the lone-pairs of the hydrogen bond acceptor to the antibonding orbital of the hydrogen bond donor. As a consequence of the electron transfer to the p orbitals of beryllium, the BeX_2 subunit of the complex is distorted. Also, since there is an electron transfer to an antibonding orbital of BeX, these bonds lengthen, and there is a red shift of the BeX_2 antisymmetric stretch. However, a blue shift of the symmetric stretch is also noticed. This is due to the fact that the stretch is coupled with the stretching of the berlyllium bond, so that a compression of the beryllium bond leads to a symmetric elongation of Be-X bonds. Therefore, the stronger the beryllium bond is the larger the blue shifting of the Be-X symmetric stretch becomes. This can be used as an experimental signature of beryllium bonds, as the red-shifting of the XH stretching is used for hydrogen bonds. Finally, an important difference they found is that beryllium bonds are, in general, significantly stronger that hydrogen bonds.

The fact that beryllium bonds have similar or even more strength than hydrogen bonds already opens the door to a vast new world of possibilities, for beryllium bonds have then enough strength to become the building blocks of new ensembles and, in the end, this can give rise to new materials, with new or specifically modulated properties. This possible application alone would suffice to make this topic worth studying, if not only for the progress of our knowledge and science in general, but beryllium also has other interesting properties that need to be studied to take advantage of them.

In fact, beryllium cation can behave as what has been called 'tetrahedral proton', and can displace H^+ in the situations where the proton acts as such[4].

In addition, in these cases the tetrahedral coordination of beryllium allows to produce chiral-at-metal complexes, i.e. molecules where the stereogenic center is the beryllium atom, so that if the rest of the complex has another stereogenic center, two diasteromeric complexes can be generated with different properties.
Besides, this behavior of the beryllium cation may be related to the beryllium disease, for which the causes are still unknown.

Finally, beryllium bonds have been shown to be able to modulate the strength of other non-covalent interactions such as the already mentioned hydrogen bonds[5].

The aim of this work is to contribute to the next step on the research on beryllium bonds by studying the possible existence of them –and their characteristics- between BeX_2 (X = H, F, Cl) molecules and small unsaturated hydrocarbons that can act as Lewis bases, specifically acetylene and ethylene.

2. METHODOLOGY

All of the calculations of this research have been carried out within the Centro de Computación Científica at the Universidad Autónoma de Madrid.

This center has more than a hundred servers with more than 1400 cores specifically dedicated to research, and it is characterized by the great variety in both the servers and the processors, for we can find servers of different trademarks (HP, Dell, Sun, SGI…) and both AMD and Intel processors (AMD Opteron, Intel Xeon, Intel Itanium).

All of the calculations have been done with the Gaussian 09 program package[6] in a Linux-based environment.

In order to study the interaction between the beryllium atom of BeX_2 (X = H, F, Cl) and the CC bonds of ethylene (C_2H_4) or acetylene (C_2H_2) an initial geometry for the system must be set. Since the two molecules are symmetric, a symmetric system as a whole is also expected from their interaction. However, a symmetric system can be achieved with several dispositions in both the cases of ethylene and acetylene, with a change in the direction of the planes of the molecules (being perpendicular all the same):

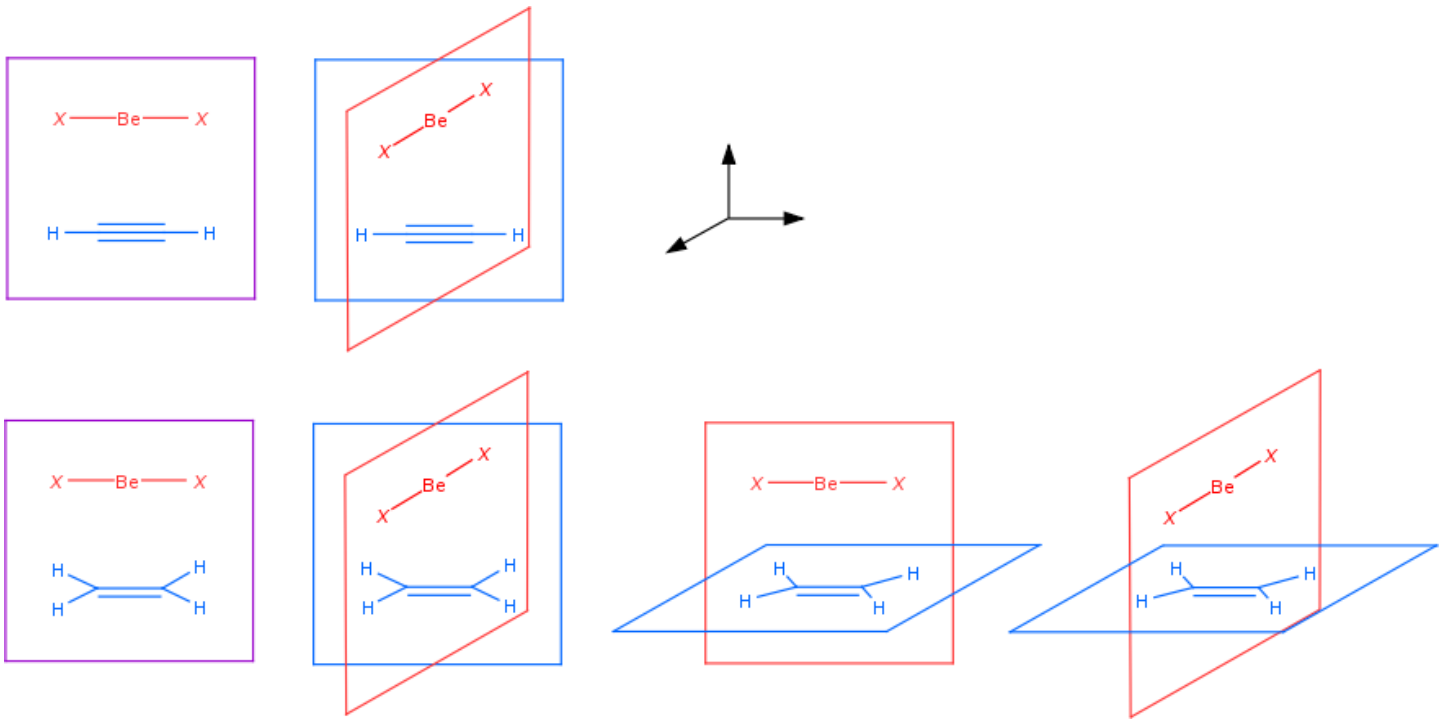

Figure 1. Possible relative symmetric dispositions of the two molecules. Notice that since C_2H_2 and BeX_2 are linear there are more planes that would fit, but these ones were chosen for the sake of clarity.

However, the dispositions showed in figure 1 are not the actual geometries expected for the complexes, for if a bond forms between the molecules, each of the two molecules -now the subunits of the complex- will experiment a deformation.

In both cases the CH bonds of acetylene or ethylene are expected to be bent towards the outside, and so are also the BeX bonds. Therefore, the BeX_2 molecule will not be linear anymore, nor will the acetylene/ethylene remain linear/planar.

The magnitude of this deformation is an indication of the strength of the beryllium bond between the molecules, so that the stronger the deformation is, the stronger the beryllium bond is likely to be. This deformation occurs due to the charge transfer from the high electronic density of the triple or double CC bond of acetylene or ethylene, respectively, towards the empty low p orbital of the beryllium atom. This produces a small change in the hybridization of both the acetylene/ethylene and the beryllium orbitals, for they have now electronic density in a new direction of space and need to adapt the directions of the rest in order to avoid repulsion forces and maintain the stability. Besides, the more electronic density displaced towards the beryllium bond, the stronger will the beryllium bond be and the more will the orbitals need to modify in order to adapt to the new situation, giving rise to the statement that the more deformation the system acquires, the stronger the beryllium bond is. In addition to this, in a beryllium bond there is also a charge transfer from the CC bond of acetylene/ethylene to the antibonding orbitals of BeX, σ_{BeX^*} and therefore the Be-X bonds lengthen. It is easy to see that the more long the BeX bond becomes, the more strong the beryllium bond is likely to be.

Finally, although maybe obvious, it is important to remark that, despite this deformation, the system as a whole will maintain a C_{2v} symmetry.

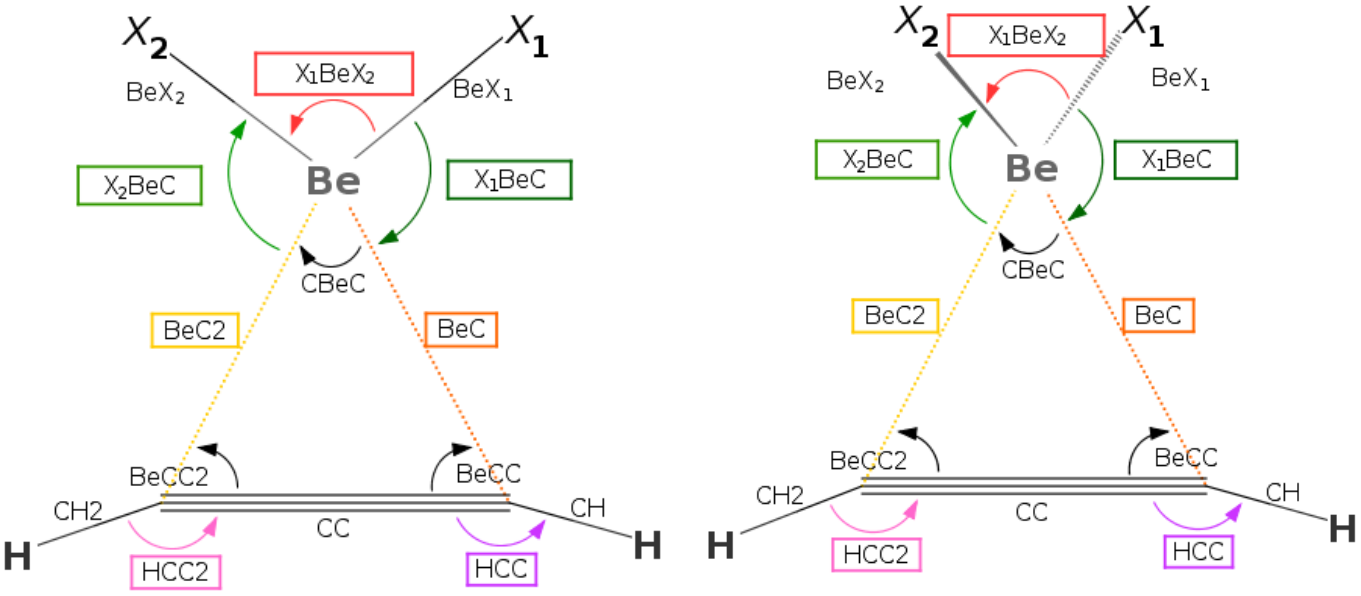

Figure 2. Possible symmetric dispositions between BeX_2 (X=H,F,Cl) molecules and acetylene. Since X_1=X_2 the system is symmetric and the different distances and angles will also be symmetric.

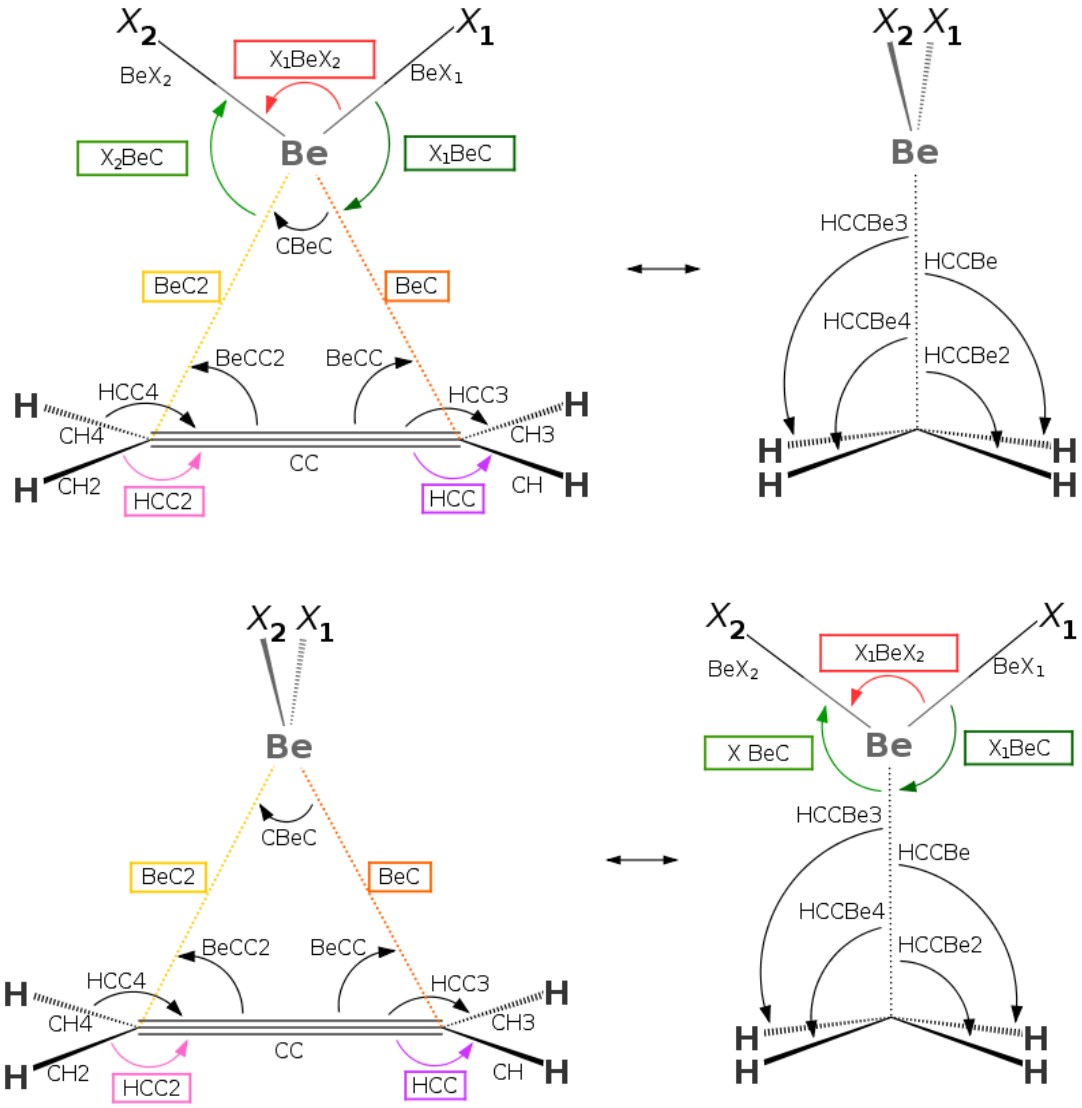

Figure 3. Possible symmetric dispositions between BeX_2 (X=H,F,Cl) molecules and ethylene. Since XH_1=XH_2 the system is symmetric and the different distances and angles will also be symmetric.

Please notice that the two first dispositions for the BeX_2-C_2H_4 system showed in Figure 1 are not showed in Figure 3. The reason is that they were very likely to be more unstable –if they were stable at all- than the other two. Nevertheless a few calculations[1] were done with those initial dispositions and they were definitely discarded.

Since two possible dispositions remained for each case, optimization calculations were carried out with density functional theory in order to find which one was more stable for each system, if any of them was.

[1] At B3LYP/6-311+G(d,p) level.

The functionals chosen were B3LYP (the known hybrid functional that combines Becke's exchange functional and Lee, Yand and Parr correlation functional)[7-11] and M06 and M06-2X (meta-GGA hybrid functionals of Truhlar and Zhao)[12].

B3LYP was chosen because it usually gives good values for the molecular properties with fast non-expensive calculations and thus it is nowadays used in most initial calculations. M06 and M06-2X functionals were selected because they are semi-local, and usually give good results for main group, organometallics, kinectics and –the part of our interest- non-covalent bonds. Dispersion is somewhat taken into account in these functionals because of the way they are defined: they have many parameters which, in addition to be constrained to reproduce the uniform electron gas limit behavior, are empirically fitted using many data sets, and these data sets correspond not only to thermochemistry but also to non-covalent interactions and kinetics. The main difference between them is the amount of HF exchange energy they include, as it is explained later in section 3.

The basis used with these functionals was the small 6-311+G(d,p) basis of Pople[13] for not much precision was needed at this point.

Once these calculations of optimization were done, a preferential structure for each system was found. For these optimal structures, second order Moller-Plesset perturbation theory (MP2)[14-17] and coupled cluster singles and doubles (CCSD)[18-23] calculations were carried out to obtain more precise values of the molecular properties and, at the same time, compare the values obtained with the four used methods.

In order to be able to compare results, however, additional calculations were needed to obtain the interaction enthalpy of the beryllium bond of the system, also known as dissociation energy, and its vertical dissociation energy as well.

The dissociation energy of the system (D_0 or ΔH_{int}) is mathematically calculated as the negative of the enthalpy obtained by subtracting from the enthalpy of the complex the enthalpy of the two isolated monomers (in their isolated equilibrium geometry):

$$D_0 = -\left(\Delta H^0_{complex} - \sum_i^{molec} \Delta H^0_i \right) \qquad (2.1)$$

It is usually defined either as the energy that the system loses when the bond is made or as the energy it is needed to break it (homolytically), although that is not entirely true. The vertical dissociation energy (E_{int} or ΔH_{vert}) or interaction energy is actually the one that accounts for the energy of the bond and only the bond, because it is defined as the energy required to separate the interacting subunits at infinite distance but keeping frozen the structure they have in the complex. The point is that the dissociation energy D_0 also collects the energy of relaxation of the two subunits from their structure within the complex to their isolated equilibrium structures, which are just that, relaxation energies, not part of the energy of the beryllium bond. Since these relaxation energies

are always negative, it is easy to see that $E_{int} > D_0$, and that the vertical dissociation energy E_{int} can be calculated by adding the absolute values of the relaxation energies of the subunits to the dissociation energy D_0 of the complex:

$$E_{\text{int}} = D^0_{complex} - \sum_i^{molec} \Delta H_i^{relax} \tag{2.2}$$

$$\sum_i^{molec} \Delta H_i^{relax} = \sum_i^{molec} \Delta H_i^{complex} - \sum_i^{molec} \Delta H_i^0 \tag{2.3}$$

Thus, in order to obtain the values of D_0 and E_{int}, the corresponding optimization calculations were done for each isolated molecule at the four methods, as well as single-point calculations for the isolated molecules at the frozen geometry they have within each of the complexes and also at the four methods. In all of these calculations the 6-311+G(d,p) was logically maintained.

It is worth noting that the values of D_0 will vary a lot from one complex to another because they depend on the relaxation energies of the subunits, whose substituents are different, while the change in E_{int} should show a smaller but very important change that will indicate how does the strength of the beryllium bond vary with the substituents of the two molecules of the complex.

Apart from these calculations, a deeper study of the bonds was made by using Natural Bond Order theory and Atoms In Molecules theory.

The NBO[24, 25] analysis gives an idea of the participation of each atomic orbital in the molecular bonds. These calculations were carried out from Gaussian with the NBO 5.0 program[26].

The Bader analysis of AIM theory[27-29] allows us to determine if there really is a bond between a pair of atoms and helps in defining its nature. These calculations were made with the AIMAll program package[30].

Finally, to obtain the most precise results for the energy, additional single-point calculations were carried out at the MP2 and CCSD(T)[21] levels of theory using the aug-cc-pVTZ basis set of Dunning[31, 32] and starting with the optimized geometry found previously with the 6-311+G(d,p) basis in each case.

The MOLDEN program package[33] was also used during the whole research for the visualization of structures and the identification of frequencies.

3. THEORETICAL FOUNDATIONS

3.1. BASIS SETS.

Generally, in quantum chemistry methods, the wavefunction of the system is expressed as a linear combination of certain basis functions. These basis functions constitute the basis set. If the basis set is complete, any mathematical function can be exactly represented this way, but achieving this would involve an infinite number of functions, which is not possible computationally. Therefore a finite basis is used as an approximation. The type and size of the chosen basis can determine the accuracy of the calculation.

Two of the first and simplest basis sets are Slater Type Orbitals (STO) and Gaussian Type Orbitals (GTO).

STO[34] have the general form:

$$\phi_{\xi,n,l,m}(r,\theta,\varphi) = NY_{l,m}(\theta,\varphi)r^{n-1}e^{-\xi\cdot r} \qquad (3.1.1)$$

where N is a normalization constant, $Y_{l,m}(\theta,\varphi)$ are the spherical harmonics and ξ is the effective nuclear charge. The exponential dependence on r gives a good description of the maximum of the function, on the nucleus and a rapid convergence. However, two electron integrals centered on three or four atoms cannot be solved analytically, and as a result the use of STO has been limited to the treatment of atoms and diatomic molecules mostly.

GTO were proposed by Boys[35] in order to overcome the disadvantages of STO, and indeed with this basis all the integrals can be calculated analytically. Its functions have the general form:

$$\phi_{\xi,n,l,m}(r,\theta,\varphi) = NY_{l,m}(\theta,\varphi)r^{(2n-2-l)}e^{-\xi\cdot r^2} \text{ or } \phi_{\xi,n,l,m}(r,\theta,\varphi) = Nx^{l_x}y^{l_y}z^{l_z}e^{-\xi\cdot r^2} \qquad (3.1.2)$$

where the sum $l_x + l_y + l_z$ determines the type of orbital, being an s orbital if it is equal to 0, a p orbital if it is equal to 1 and so on.

The exponential dependence on r^2 does not describe correctly the behavior at the nucleus. In addition, GTO decrease too quickly with the nuclear-electron distance, and the long distance region of the orbital is also not well reproduced.

3.1.1. MINIMAL BASIS SET.

The most common minimal basis sets are STO-NG basis sets. It was proposed by Pople and coworkers[36] and consists in a combination of the two basis set mentioned before. The basis set uses a set of GTOs (N = 3-6) to fit by least squares to a STO function:

$$\phi_{STO-NG} = \sum_i a_i \varphi_{i,GTO} \tag{3.1.3}$$

Where $\varphi_{i,GTO}$ is a gaussian function and is called primitive, while the STO-NG are called contracted. The expansion can include as many terms as desired, but from N = 3 the inclusion of more terms does not provide much improvement compared to the increase in the computational cost. That is why the most used is the STO-3G.

In minimal basis set the number of functions used are the minimum one to describe the core and valence orbitals of the atoms, but not any virtual orbitals. As a consequence the results obtained are very rough, for a minimal basis set is not flexible enough to describe correctly the atoms in a molecular environment.

3.1.2. SPLIT-VALENCE BASIS SET.

Following the idea that in most chemical bonds the valence electrons are the one which mainly participate, in these basis sets the atomic orbitals corresponding to the valence atomic orbitals are described with more than one basis function. They usually are split in two parts, an inner compact one and an outer and diffuse other. If the split is in two basis functions, the basis is called double zeta, DZ, in a reference to the two exponents of the two basis functions. Similarly we can have a triple zeta, quadruple zeta and so on basis set. The coefficients of each of these functions can be varied and thus the size of the orbital changes, allowing the adjustment to a particular molecular environment.

The most common basis sets of this type are Pople basis sets[37].

The notation of these basis sets is X-YZG, where G stands for Gaussian, X represents the number of primitive Gaussians of each core atomic orbital basis functions, and Y and Z indicate as well the number of primitive Gaussian functions that form each valence function, but each of Y and Z are composed of two basis functions instead of one. The hyphen implies its split-valence character. These are, then double zeta basis sets, but more number can be added indicating triple zeta, quadruple zeta and so on.

However, in some cases additional flexibility is needed to the correct description of the system. In those cases polarization and diffuse functions are used.

Polarization functions are orbitals with higher angular momentum than the ones an atom has in its ground state. It owes its name to the fact that it provides the atom with new directions that can accommodate the electron density in cases where it is deformed such

as in polarization processes. Polarization is usually notated with an asterisk following the normal notation of the basis set or alternatively by adding a P. An additional set of p orbitals on each hydrogen is indicated by a second asterisk or alternatively by adding 2P. Also, the orbitals added can be notated in parenthesis, firstly for the heavy atoms and secondly for hydrogen atoms. For instance, a 6-31G(d) basis set is equal to 6-31G* and indicates that each core atomic orbital is described by a function with 6 Gaussian primitive functions, that the valence atomic orbitals are split in two, each of which is described by two functions, the first two with 3 Gaussian primitives and the second two with 1 Gaussian primitive. In addition, heavy atoms have a d polarization function.

Diffuse functions are needed in cases where the atomic orbitals reach farther distances from the nuclei due to it having more charge, as in ionic atoms, or in the case of weakly bonded systems. In general, they are included as an s function and a set of p functions for each atom of the system, with the exponents obtained variationally for the anion or hydride anion of the corresponding atoms. In Pople basis sets the inclusion of diffuse functions is denoted by a symbol +, if they have been added to heavy atoms only, and with two symbols ++ if they have also been added to hydrogens.

One of the most common basis sets used, and one of the two that have been used in the present work in 6-311+G(d,p). This basis, therefore, indicates that each core atomic orbital is described by a function with 6 Gaussian primitive functions, that the valence atomic orbitals are split in three, each of which is described by two functions, the first two with 3 Gaussian primitives and the remaining four with 1 Gaussian primitive each. In addition, heavy atoms are described with a diffuse function, and for heavy atoms and hydrogen atoms a d and p polarization function, respectively, is included.

3.1.3. CORRELATION CONSISTENT BASIS SETS

These basis sets were developed by Dunning[31, 32]. They are designed to converge systematically to the complete basis set. The notation for them is ‘cc-pVXZ’ where cc-p stands for correlation consistent polarized, the V stands indicates they are only valence basis sets and X can be D, T, Q, etc which stands for double zeta, triple zeta, quadruple zeta and so on. These basis set include progressively more polarized functions, and for instance cc-pVDZ includes 2s and 1p orbital to describe hydrogens while cc-pVTZ includes 3s, 2p and 1d.

However, these basis set do not include diffuse functions. When they are needed, an extra function with a smaller exponent is added for each angular momentum of each atom, and the basis set adds ‘aug-‘ in front of its name. For instance, a basis set used in the present work is aug-cc-pVTZ, which describes H with 3s, 2p, 1d and additional diffused orbitals 1s, 1p, 1d, while Be is described by 4s, 3p, 2d, 1f and additional disffused orbitals 1s, 1p, 1d, 1f.

3.2. DENSITY FUNCTIONAL THEORY

The density functional theory owes its name to the use of functionals, i.e. functions of another function, of the electron density, and is a method that allows the properties of many electron systems to be determined.

The main idea of DFT is using the electron density, which only depends on 3 spatial coordinates, instead of the complex wavefunction to solve Schrödinger's equation.

Since the Hamiltonian depends only on the total number of electrons and the positions and atomic numbers of the nuclei, it is reasonable to think that the electronic density could well define the Hamiltonian, calculating the energy with the electron density. However, the exact mathematical relation between energy and electron density is unknown, and some approximations must be done. In spite of them, though, DFT is nowadays known as one of the most versatile methods available in computational chemistry due to the very accurate results it provides at a very low computational cost.

The probability density is the probability of certain random variable to take on a given value per unit volume at a certain point. Applied to this case, we can define a probability density function ρ that describes the probability of having certain number of electrons per unit volume at a given point, which, in quantum chemistry, is equal to the squared wave function of the system. For instance, if we had a system with a single electron of α spin described by the spin orbital $\Psi(\vec{x}) = \phi(\vec{r})\alpha(s)$, then we would have the following expression for the probability density function: $\rho(\vec{x}) = |\Psi(\vec{x})|^2$. Therefore, the probability of finding that determined electron in a certain given volume, for instance $d\boldsymbol{x} = d\boldsymbol{r}\cdot ds$ would be the product of the probability density by the volume dx:

$$\rho(\vec{x})d\vec{x} = |\Psi(\vec{x})|^2 d\vec{x} = \Psi^*(\vec{x})\Psi(\vec{x})d\vec{x} \qquad (3.2.1)$$

However, if we only want to know how the electron is distributed in space no matter what spin it has, then we can integrate out the spin, i.e. make the integration over the spin as if the spatial part was constant. Since the one-electron spin functions form an orthonormal basis, we obtain the following expression:

$$\int \rho(\vec{x})d\vec{x} = \int \rho(\vec{x})d\vec{r}ds = \phi^*(\vec{r})\phi(\vec{r})d\vec{r}\int \alpha^*(s)\alpha(s)ds = |\phi(\vec{r})|^2 d\vec{r} \qquad (3.2.2)$$

The new probability density we obtain as a result, $P(\vec{r}) = |\phi(\vec{r})|^2$, is the one that has been called electron density, that only depends on the spatial part of the wave function of the electron, which is the only part we need in order to describe the energy of the system.

Now, in order to generalize the expression, let's consider a system with N electrons described by the wave function $\Psi(\vec{x}_1, \vec{x}_2, ..., \vec{x}_N)$, where $\vec{x}_i$ represents the spatial and spin coordinates of electron *i*:

$$\rho(\vec{x}_1, \vec{x}_2, ..., \vec{x}_N) d\vec{x}_1 d\vec{x}_2 ... d\vec{x}_N = \left|\Psi(\vec{x}_1, \vec{x}_2, ..., \vec{x}_N)\right|^2 d\vec{x}_1 d\vec{x}_2 ... d\vec{x}_N \quad (3.2.3)$$

$$\rho(\vec{x}_1, \vec{x}_2, ..., \vec{x}_N) d\vec{x}_1 d\vec{x}_2 ... d\vec{x}_N = \Psi^*(\vec{x}_1, \vec{x}_2, ..., \vec{x}_N)\Psi(\vec{x}_1, \vec{x}_2, ..., \vec{x}_N) d\vec{x}_1 d\vec{x}_2 ... d\vec{x}_N \quad (3.2.4)$$

The expression above is then the probability of finding a first electron in a volume of $d\boldsymbol{x}_1 = d\boldsymbol{r}_1 ds_1$ and at the same time a second electron in a volume of $d\boldsymbol{x}_2 = d\boldsymbol{r}_2 ds_2$ and so on up to the last electron in a volume of $d\boldsymbol{x}_N = d\boldsymbol{r}_N ds_N$.

However, since the Hamiltonian is a two-electron operator we only need to know the probability of one electron and two electrons simultaneously, not all of them. Therefore we can integrate out unwanted coordinates, just as with the spin coordinate. Thus, the probability of finding the first electron in volume $d\boldsymbol{x}_1$ regardless of where the rest of electrons simultaneously are is given by:

$$\rho_1(\vec{x}_1) d\vec{x}_1 = d\vec{x}_1 \int \Psi^*(\vec{x}_1, \vec{x}_2, ..., \vec{x}_N)\Psi(\vec{x}_1, \vec{x}_2, ..., \vec{x}_N) d\vec{x}_2 ... d\vec{x}_N \quad (3.2.5)$$

Since electrons are indistinguishable particles the probability of finding any electron instead of a determined one is N times larger:

$$\rho_1(\vec{x}) d\vec{x} = N d\vec{x} \int \Psi^*(\vec{x}_1, \vec{x}_2, ..., \vec{x}_N)\Psi(\vec{x}_1, \vec{x}_2, ..., \vec{x}_N) d\vec{x}_2 ... d\vec{x}_N \quad (3.2.6)$$

$\rho_1(\vec{x}) d\vec{x}$ is the one-particle density function of the system.

Notice that the subscript 1 on the x is no longer there because we now consider any electron in a single, arbitrary and infinitesimal volume $d\boldsymbol{x}$ at position vector **x**. Again, we can obtain the spin-less electron density function by integrating out the remaining spin coordinate:

$$P_1(\vec{r}) = \int \rho_1(\vec{x}\ ) ds \quad (3.2.7)$$

Similarly, we can obtain the expression for the two-electron electronic density function as the probability of finding an arbitrary electron in volume $d\boldsymbol{x}_1$ and simultaneously another in $d\boldsymbol{x}_2$ by integrating over all coordinates except $\mathbf{x}_1$ and $\mathbf{x}_2$. Also bear in mind that the electron pairs are undistinguishable as well, and mathematically the amount of possible ways to choose two different electrons is given by a permutation:

$$\rho_2(\vec{x}_1, \vec{x}_2) d\vec{x}_1 d\vec{x}_2 = d\vec{x}_1 d\vec{x}_2 \int \Psi^*(\vec{x}_1, \vec{x}_2, ..., \vec{x}_N)\Psi(\vec{x}_1, \vec{x}_2, ..., \vec{x}_N) d\vec{x}_3 ... d\vec{x}_N; \quad (3.2.8)$$

$$ {}_N P_2 = \frac{N!}{(N-2)!} = \frac{N(N-1)(N-2)!}{(N-2)!} = N(N-1) \tag{3.2.9} $$

$$ \rho_2(\vec{x}_1, \vec{x}_2) dx_1 dx_2 = N(N-1) d\vec{x}_1 d\vec{x}_2 \int \Psi^*(\vec{x}_1, \vec{x}_2, ..., \vec{x}_N) \Psi(\vec{x}_1, \vec{x}_2, ..., \vec{x}_N) d\vec{x}_3 ... d\vec{x}_N \tag{3.2.10} $$

Notice that subscripts 1 and 2 in the last equation are to differentiate the two arbitrary infinitesimal volumes $d\boldsymbol{x}_1$ and $d\boldsymbol{x}_2$ at positions $\mathbf{x}_1$ and $\mathbf{x}_2$ respectively, and they are not referred to specific electrons 1 and 2 anymore.

Finally we can obtain the spin-less electron density by integrating out the two spin coordinates s_1 and s_2:

$$ P_2(\vec{r}_1, \vec{r}_2) = \int \rho_2(\vec{x}_1, \vec{x}_2) ds_1 ds_2 \tag{3.2.11} $$

This function accounts for the correlated movement of interacting electrons.

Since the one-electron operator $\hat{h}(\vec{r}_i)$ of the Hamiltonian contains a differential operator, in order to solve the Schrödinger equation we need also the density matrix for one-electron terms. The first-order or Fock-Dirac density matrix is defined as:

$$ \rho_1(\vec{x}_1'; \vec{x}_1) = N \int \Psi^*(\vec{x}'_1, \vec{x}_2, ..., \vec{x}_N) \Psi(\vec{x}_1, \vec{x}_2, ..., \vec{x}_N) d\vec{x}_2 ... d\vec{x}_N \tag{3.2.12} $$

As we have seen before we can integrate out the spin in order to have a spin-less version, which in this case is called first-order reduced density matrix:

$$ P_1(\vec{r}_1'; \vec{r}_1) = \int \rho_1(\vec{x}_1'; \vec{x}_1) ds_1' ds_1 \tag{3.2.13} $$

The diagonal of this matrix is equal to the density function but the rest of the elements have no physical meaning. Also, the sum of the diagonal elements is equal to the total number of electrons N:

$$ tr\ P_1 = \int P_1(\vec{r}_1'; \vec{r}_1) d\vec{r}_1 = \int P_1(\vec{r}_1) d\vec{r}_1 = N \tag{3.2.14} $$

The time-independent Schrödinger equation is, in general:

$$ \hat{H}\Psi = E\Psi \tag{3.2.15} $$

Where Ψ is the wave function, which contains all the information of the system, and $\hat{H}$ is the Hamiltonian operator, which contains the kinetic $\left(\hat{T}\right)$ and potential $\left(\hat{V}\right)$energy terms:

$$\hat{H} = \hat{T} + \hat{V} = \hat{T}_n + \hat{T}_e + \hat{V}_{ee} + \hat{V}_{nn} + \hat{V}_{ne} \tag{3.2.16}$$

Where n is the label for nuclear coordinates (**R**) and e is the label for electron coordinates (**r**).

It is well known that since the nuclei are much heavier than the electrons the latter move much faster and they can barely feel the movement of the nuclei, and due to that we can decouple nuclear and electronic velocities, in what is known as the Born-Oppenheimer approximation. Therefore, an electronic Hamiltonian is defined by separating the term of the kinetic energy of the nuclei:

$$\hat{H}_{el} = \hat{T}_e + \hat{V}_{ee} + \hat{V}_{nn} + \hat{V}_{ne} \tag{3.2.11}$$

$$\hat{H}_{el}\Psi\left(\vec{r},\vec{R}\right) = E_e\Psi(\vec{r},\vec{R}) \tag{3.2.12}$$

This means that the Hamiltonian depends now only parametrically on the coordinates of the nuclei. For a system of N electrons and M nuclei, we can write the electronic Hamiltonian as follows:

$$\hat{H}_{el} = \sum_{i=1}^{N} -\frac{\hbar^2}{2m_e}\nabla_i^2 + \sum_i\sum_{j>i}\frac{e^2}{4\pi\varepsilon_0\left|r_i - r_j\right|} + \sum_k\sum_{l>k}\frac{Z_k Z_l e^2}{4\pi\varepsilon_0\left|R_k - R_l\right|} - \sum_k\sum_i\frac{Z_k e^2}{4\pi\varepsilon_0\left|R_k - r_i\right|} \tag{3.2.13}$$

Where e and m_e stand for charge and mass of an electron, Z_k and Z_l stand for the charge of the nuclei, ε_0 is the permittivity of free space and $\hbar$ is the reduced Planck's constant.

To make things easier, we can use atomic units. That way the elementary constants m_e, e and $\hbar$ are equal to 1, the corresponding length unit would be Bohr's radius a_0 = 1 bohr = $5.292 \cdot 10^{-11}$m and the energy would be in Hartrees E_H = 1 Hartree = 27.21 eV. Using these units the electronic Hamiltonian simplifies to:

$$\hat{H}_{el} = \sum_{i=1}^{N}\left(-\frac{1}{2}\nabla_i^2 - \sum_{k=1}^{M}\frac{Z_k}{\left|R_k - r_i\right|}\right) + \sum_i\sum_{j>i}\frac{1}{\left|r_i - r_j\right|} + \sum_k\sum_{l>k}\frac{Z_k Z_l}{\left|R_k - R_l\right|} = \tag{3.2.14}$$

$$= \sum_{i=1}^{N}\left(-\frac{1}{2}\nabla_i^2 - \sum_{k=1}^{M}\frac{Z_k}{\left|R_k - r_i\right|}\right) + \frac{1}{2}\sum_{ij}\frac{1}{\left|r_i - r_j\right|} + \sum_k\sum_{l>k}\frac{Z_k Z_l}{\left|R_k - R_l\right|} \tag{3.2.15}$$

$$\hat{H}_{el} = \sum_{i=1}^{N}\hat{h}(i) + \sum_i\sum_{j>i}\hat{g}(i,j) + E_{nuc} = \sum_{i=1}^{N}\hat{h}(i) + \frac{1}{2}\sum_{ij}\hat{g}(i,j) + E_{nuc} \tag{3.2.16}$$

Since equation (3.2.12) is an eigenvalue problem, for a certain given geometry many eigenvalues E_k will be obtained. The lowest E_k corresponds to the ground state, while higher ones correspond to excited states. Therefore, by varying the geometries we would obtain high-dimensional potential energy surfaces for each state, so that, for instance, a minima found for the ground state surface $E_0(\mathbf{R}_1, \mathbf{R}_2, \ldots, \mathbf{R}_M)$ would correspond to a energetically stable geometry, while the first-order saddle points would correspond to transition structures.

In order to solve the Schrödinger's equation (3.2.12) we have to obtain the electronic energy as the expectation value of the electronic Hamiltonian:

$$\hat{H}_{el}\Psi\left(\vec{r},\vec{R}\right)=E_e\Psi(\vec{r},\vec{R}) \tag{3.2.17}$$

$$E_e=\left\langle\Psi\left(\vec{r},\vec{R}\right)\middle|\hat{H}_{el}\middle|\Psi\left(\vec{r},\vec{R}\right)\right\rangle \tag{3.2.18}$$

By substituting in the last equation the expression for the electronic Hamiltonian, we finally arrive to an expression of the expected value of the electron density in terms of the first-order density matrix and of the two-electron density:

$$E_e=\int_{r'=r}\left(-\frac{1}{2}\nabla^2\left(\vec{r}\right)+\hat{v}\left(\vec{r}\right)\right)\rho_1\left(\vec{r}';\vec{r}\right)dr+\frac{1}{2}\int\int\frac{\rho_2\left(\vec{r}_1,\vec{r}_2\right)}{\left|\vec{r}_1-\vec{r}_2\right|}d\vec{r}_1d\vec{r}_2+E_{nuc} \tag{3.2.19}$$

Notice that in the previous section we used P instead of ρ to remark the difference between the densities depending on **r** and depending on **x**. Since from now on we will only deal with the density depending on r, we recover the general notation ρ for the density.

The two-electron density $\rho_2\left(\vec{r}_1,\vec{r}_2\right)$contains information about the correlated motion of two electrons. Since it's a probability, if the electrons were independent this density would be equal to the product of the densities of each separated electron, but since that is not the case, we have a conditional probability $\gamma(\vec{r}_1,\vec{r}_2)$:

$$\rho_2\left(\vec{r}_1,\vec{r}_2\right)=\rho(\vec{r}_1)\gamma(\vec{r}_1,\vec{r}_2) \tag{3.2.20}$$

The exchange-correlation density $\Gamma_{XC}\left(\vec{r}_1,\vec{r}_2\right)$ is defined as:

$$\Gamma_{XC}\left(\vec{r}_1,\vec{r}_2\right)=\rho_2\left(\vec{r}_1,\vec{r}_2\right)-\rho(\vec{r}_1)\rho(\vec{r}_2) \tag{3.2.21}$$

Therefore, dividing by $\rho(\vec{r}_1)$:

$$\frac{\Gamma_{XC}(\vec{r}_1,\vec{r}_2)}{\rho(\vec{r}_1)} = \gamma(\vec{r}_1,\vec{r}_2) - \rho(\vec{r}_2) = \rho_{XC}(\vec{r}_1,\vec{r}_2) \tag{3.2.22}$$

We obtain the density $\rho_{XC}(\vec{r}_1,\vec{r}_2)$, which is known as the Exchange-Correlation hole. It designates a region around an electron where the presence of another electron is excluded to some extent. This hole can be a Fermi hole, if the electrons considered are of the same spin, or a Coulomb hole, if the electrons have different spin:

$$\rho_{XC}(\vec{r}_1,\vec{r}_2) = \rho_{XC}^{\alpha\alpha}(\vec{r}_1,\vec{r}_2) + \rho_{XC}^{\alpha\beta}(\vec{r}_1,\vec{r}_2) \tag{3.2.23}$$

We can then separate $\rho_2(\vec{r}_1\ ,\vec{r}_2)$ of equation (3.2.19) in two terms, and the expression for the electronic energy would be as follows:

$$E_e = \int_{r_1'=r_1} \left(-\frac{1}{2}\nabla^2(\vec{r}_1)\right)\rho_1(\vec{r}_1',\vec{r}_1)d\vec{r}_1 + \int \hat{v}(\vec{r}_1)\rho_1(\vec{r}_1)d\vec{r}_1 + \frac{1}{2}\iint \frac{\rho(\vec{r}_1)\rho(\vec{r}_2)}{|\vec{r}_1 - \vec{r}_2|}d\vec{r}_1 d\vec{r}_2$$
$$+ \frac{1}{2}\iint \frac{\rho(\vec{r}_1)\rho_{XC}(\vec{r}_1,\vec{r}_2)}{|\vec{r}_1 - \vec{r}_2|}d\vec{r}_1 d\vec{r}_2 + E_{nuc} \tag{3.2.24}$$

In this expression the first term accounts for the kinetic energy of the electrons $\hat{T}_e(\rho)$, the second term is the electron-nuclear potential energy $\hat{V}_{ne}(\hat{v},\rho)$, the third corresponds to the classical Coulomb electron repulsion $\hat{J}(\rho)$ and the fourth one represents the non-classical electronic exchange-correlation energy $\hat{E}_{NC}(\rho)$. Notice that then we have divided the potential energy between the electrons $\hat{V}_{ee}(\rho)$ in two terms:

$$\hat{V}_{ee}(\rho) = \hat{J}(\rho) + \hat{E}_{NC}(\rho) \tag{3.2.25}$$

And therefore:

$$E_e = \hat{T}_e(\rho) + \hat{V}_{ne}(v,\rho) + \hat{J}(\rho) + \hat{E}_{NC}(\rho) + \hat{E}_{nuc} \tag{3.2.26}$$

It is possible then to express the energy as a function of first and secon-order density functions and density matrices, and therefore it can be said that the energy is a functional of the density.

3.2.1. HOHENBERG AND KOHN THEOREMS.

The Hohenberg and Kohn theorems gave rise to the DFT methodology, because with them the theory became useful: the first theorem showed its applicability and the second paved the way for the mathematical equations to make it work.

The first Hohenberg-Kohn theorem[38] states that, for non-generate ground states, the external electron-nuclei potential $v_{ext}(\mathbf{r})$, and hence the total energy, is a unique functional of the electron density n(r). The demonstration of the theorem is achieved by reduction ad absurdum. The very important consequence of this theorem is that, since $v_{ext}(\mathbf{r})$ and N completely define de Hamiltonian of the system, the electrons determine not only this potential and the energy but also all the electronic properties of the ground state of the system. Furthermore, this means that any observable of a stationary non-degenerate ground state can be written as a functional of the electron density of the ground state and be calculated exactly.

Since for a specific external potential $v_{ext}(\mathbf{r})$ the energy is a functional of the density, the terms of equation (3.2.26) that don't depend directly on this external potential, namely the kinetic energy of the electrons $\hat{T}_e(\rho)$ and the repulsion potential of the electrons $\hat{V}_{ee}(\rho)$, are gathered, to simplify, in what is called the Hohenberg-Kohn functional $F_{HK}(\rho)$:

$$E_v(\rho) = \int \hat{v}(\vec{r})\rho_1(\vec{r})d\vec{r} + F_{HK}(\rho) + E_{nuc} \qquad (3.2.27)$$

Since this Hohenberg-Kohn functional does not depend on N or $v_{ext}(\mathbf{r})$, it will be the same for all of the systems that the theorem is valid for.

The second theorem corresponds to the variational principle for the energy E(ρ), and states that the electron density of a non-degenerate ground state can be calculated exactly by determining the density that minimizes the energy of the ground state.
The variational principle grants that any density used gives an energy greater or equal to the exact energy of the ground state. In order to obtain the exact density of the ground state we have to find the density that minimizes the energy, i.e. the one that makes zero the derivative of the energy with respect to the density:

$$\frac{\partial E_v(\rho)}{\partial \rho} = 0 \qquad (3.2.28)$$

In this approach the second-reduced density matrix is intended to be applied directly, without previous knowledge of the N-electron wave function from which it is derived. This is a problem because one has to know that there exists indeed an N-electron wave

function that could result in such electron density. In order to ensure this, one has to determine what Coleman called the N-representability conditions[39] that the second reduced density matrix has to fulfill.

One way of solving this problem is by means of the Lagrange undetermined multipliers method.
We have a functional E of the variable function P. Applied to this case the method proposes an equation with an added parameter, the solution of which will give the values of the parameter and ρ for the energy to be stationary (and therefore granting the existence of a corresponding stationary state or wave function):

$$E_v(\rho) - \mu\left(\int \rho(\vec{r})d\vec{r} - N\right) \tag{3.2.29}$$

Where μ is the undetermined Lagrange multiplier and, as we know $\int \rho(\vec{r})d\vec{r} - N = 0$.
However, the stationary energy we need has to be the lowest one, and therefore the derivative of the previous equation has to be zero:

$$\partial\left[E_v(\rho) - \mu\left(\int \rho(\vec{r})d\vec{r} - N\right)\right] = 0 \tag{3.2.30}$$

The differential of a functional has the form: $\partial F = \int \frac{\partial F(f)}{\partial f(x)}\partial f(x)dx$ Therefore:

$$\partial\left[E_v(\rho) - \mu\left(\int \rho(\vec{r})d\vec{r} - N\right)\right] = \int \frac{\partial E_v(\rho)}{\partial \rho(\vec{r})}\partial\rho(\vec{r})d\vec{r} - \mu\int \partial\rho(\vec{r})d\vec{r} = 0 \tag{3.2.31}$$

$$\int\left(\frac{\partial E_v(\rho)}{\partial \rho(\vec{r})} - \mu\right)\partial\rho(\vec{r})d\vec{r} = 0 \tag{3.2.32}$$

The minimum value for the undetermined Lagrange multiplier μ is defined as:

$$\mu = \frac{\partial E_v(\rho)}{\partial \rho(\vec{r})} \tag{3.2.33}$$

Introducing the expression of the energy of equation (3.4.3):

$$\mu = \frac{\partial E_v(\rho)}{\partial \rho(\vec{r})} = \hat{v}(\vec{r}) + \frac{\partial F_{HK}(\rho)}{\partial \rho(\vec{r})} + \frac{\partial E_{nuc}(\rho)}{\partial \rho(\vec{r})} = \hat{v}(\vec{r}) + \frac{\partial F_{HK}(\rho)}{\partial \rho(\vec{r})} \tag{3.2.34}$$

This constitutes the fundamental equation of density functional theory.

The problem now is that the exact mathematical relation between the functional and the density is unknown. More specifically, the exact form of $\hat{T}_e(\rho)$ is unknown.

3.2.2. KOHN AND SHAM METHOD

Kohn and Sham[40] considered separating this unknown kinetic energy in a known term and an unknown term. The known term would correspond to a system of reference in where the electron-electron interactions are not considered, but defined by the electron density of the real system. In this way we would have a Hartree-Fock exact value for this kinetic energy $\hat{T}_r$, which would be the same as part of the kinetic density of our system, for they would have the same density. The other term, $\hat{T}_c$, would account for some electron correlation and would remain inexact:

$$\hat{T}_e = \hat{T}_r + \hat{T}_c \tag{3.2.35}$$

Therefore:

$$E_v(\rho) = \hat{T}_r(\rho) + \int \hat{v}(\vec{r})\rho_1(\vec{r})d\vec{r} + E_{nuc} + \hat{J}(\rho) + \hat{E}_{NC}(\rho) + \hat{T}_c(\rho) \tag{3.2.36}$$

$$E_v(\rho) = \hat{T}_r(\rho) + \int \hat{v}(\vec{r})\rho_1(\vec{r})d\vec{r} + E_{nuc} + \hat{J}(\rho) + \hat{E}_{NC}(\rho) + \hat{T}_e(\rho) - \hat{T}_s(\rho) \tag{3.2.37}$$

$$E_v(\rho) = \hat{T}_r(\rho) + \int \hat{v}(\vec{r})\rho_1(\vec{r})d\vec{r} + E_{nuc} + \hat{J}(\rho) + \hat{E}_{XC}(\rho) \tag{3.2.38}$$

Since it accounts for some electron correlation, it can be gathered to $\hat{E}_{NC}(\rho)$ in what constitutes the exchange-correlation energy. Applying the fundamental equation of DFT we have:

$$\frac{\partial E_v(\rho)}{\partial\rho(\vec{r})} = \frac{\partial T_r(\rho)}{\partial\rho(\vec{r})} + \hat{v}(\vec{r}) + 0 + \int \frac{\rho(\vec{r}_2)}{|\vec{r}_1 - \vec{r}_2|} d\vec{r}_2 + \frac{\partial E_{XC}(\rho)}{\partial\rho(\vec{r})} = \mu \tag{3.2.39}$$

We can simplify this expression by defining the following potentials:

$$\hat{v}_C(\vec{r}) = \hat{v}(\vec{r}) + \int \frac{\rho(\vec{r}_2)}{|\vec{r}_1 - \vec{r}_2|} d\vec{r}_2 \qquad \hat{v}_{XC}(\vec{r}) = \frac{\partial E_{XC}(\rho)}{\partial\rho(\vec{r})} \qquad \hat{v}_{eff}(\vec{r}) = \hat{v}_C(\vec{r}) + \hat{v}_{XC}(\vec{r}) \tag{3.2.40}$$

The first one is the sum of the nuclear-electron potential energy and the electron repulsion term. Both appear due to Coulomb forces, and the potential is known as the Coulomb potential. The second one is called exchange correlation potential.
Finally, the compact equation we obtain is:

$$\frac{\partial \hat{T}_r(\rho)}{\partial\rho(\vec{r})} + \hat{v}_{eff}(\vec{r}) = \mu$$

(3.2.41)

This result only differs from the result for the non-interacting system in the expression for the potential. Therefore, we will have a very similar equation for the Hamiltonian which will be solved through very similar HF equations:

$$\hat{h}_{KS} = -\frac{1}{2}\nabla^2 + \hat{v}_{eff}(\vec{r}) \tag{3.2.42}$$

A set of Kohn-Sham orbitals can be written to define a Slater determinant that allows obtaining the electron density, and are solutions to the Schrödinger equation:

$$\rho(\vec{r}) = \sum_{i=1}^{N_{oc}} |\chi_i(\vec{r})|^2 \tag{3.2.43}$$

$$\hat{h}_{KS}\chi_i = \varepsilon_i \chi_i \tag{3.2.44}$$

Them the most precise solution for the energy and wave function of the system is obtained through an iterative procedure until convergence. The exact procedure of the method is as follows:

1. An initial guess for the Kohn-Sham molecular orbitals χ_i is selected.
2. The electron density is calculated from them (equation (3.2.43))
3. The exchange-correlation potential is calculated with equation (3.2.40b) with the expression given by a previously selected exchange-correlation functional.
4. With the density and the exchange correlation potential the effective potential is calculated (equation (3.2.43c) and (3.2.43a)).
5. The Hamiltonian is now known (equation (3.2.42)) and the KS equations (equation (3.2.44)) can be written and solved. A new set of KS orbitals are obtained.
6. The electron density is calculated again with the new orbitals. If the result is the same as the one obtained in step 2, then the convergence is reached and the orbitals and energy obtained in this cycle are the most precise ones this method can give. If the results differ, the cycle is repeated from step 3 until convergence.

It is important to point out the main differences of DFT with respect to HF.
In HF the energy is minimized with respect to the coefficients of the basis set expansion, while in DFT the energy is minimized with respect to the density. Also, in HF the molecular orbitals and its energies have physical meaning, but KS orbitals and its energies do not. The KS wave function is an approximation to the exact wave function, and using it to calculate values of observables is not correct. However the KS

orbitals have the same shape, symmetry and energetic order as the HF ones, and due to this they can be correctly used for reactivity studies. Besides, unlike HF, DFT is able to take into account all correlation energy if the exchange-correlation functional is appropriate. Finally, although an approximate Hamiltonian is used, it is important to notice that in DFT the electron density is exact for as long as the exchange-correlation is, for it is the only source of error in the method.

Therefore, in DFT the exchange-correlation functional chosen is the key to obtain the most precise results. However, one of the main disadvantages of the method is that there is no systematic way of improving the results because it is impossible to know in advance which exchange-correlation functional is going to give better results for a given system.

3.2.3. EXCHANGE-CORRELATION POTENTIAL TYPES

There are lots of different exchange-correlation potential types. In the present work only a brief description of the main ones is provided.

3.2.3.1. Local Density Approximation (LDA) and Local Spin Density Approximation (LSDA)

In this approximation the exchange-correlation effects are considered just local, and its energy depends only on the density. The energy is usually divided into exchange and correlation energy, with the homogeneous gas constant density taken as a model for the exchange part:

$$E_{XC}^{LDA}(\rho) = E_X^{LDA}(\rho) + E_C^{LDA}(\rho) \tag{3.2.46}$$

Thus, this approximation works very well in systems in which the density doesn't change much. If it does, though, it is still possible to obtain good approximations by applying it to infinitesimal volumes.
One of the most known functional of this type is the VWN of Vosko, Wilk and Nusair[9]
If we have an open shell system instead of a closed one, and therefore we have different α and β densities, this method is used instead of just LDA. It follows the same concepts but the densities must be calculated separately. This method is also known as the unrestricted Kohn-Sham (UKS) method. In this method the kinetic and exchange energy depend only on one of the spins, α, while the Coulomb repulsion and the correlation energy depend on both.

$$E_{XC}^{LSDA}(\rho^{\alpha}, \rho^{\beta}) = E_X^{LSDA}(\rho^{\alpha}) + E_C^{LSDA}(\rho^{\alpha}, \rho^{\beta}) \tag{3.2.47}$$

The energies in the end are minimized separately but not independently, because for the energy of the α electrons we need the β density and vice versa.

Since both methods are based in a uniform electron gas, the results are not very good for real molecules. The overall results for geometries are similar to HF ones, but the distances are underestimated, overestimating the strength of the bonds (the bond energy). They are not good for systems with weak bonds but they have been used to study extended systems like metals where the description of a constant electron density can be valid.

3.2.3.2. Generalized Gradient Approximations (GGA) and Meta-GGA functionals (meta-GGA).

This approximation is semi-local and the exchange-correlation energy is described in terms of the density and density gradients, i.e., considering the value of the density and its variation around the point.

$$E_{XC}^{GGA} = E_X^{GGA} + E_C^{GGA} \tag{3.2.48}$$

$$E_{XC}^{GGA}(\rho) = \int f(\rho, \nabla\rho) d\vec{r} \tag{3.2.49}$$

This method modifies the LDA exchange correlation energy in order to have correct scaling properties and correct asymptotic behavior, i.e. to behave correctly in the limits of Fermi and Coulomb holes, which have to be -1 and 0 respectively. There are empirical and non-empirical approaches to this problem.

In 1988 Becke proposed the B88 or B GGA functional[7], from an empirical approach. It was based in adding a correction term to the LDA exchange energy, because it was the term with more error in LDA:

$$E_X^{GGA}(\rho) = E_X^{LDA}(\rho) + E_X^{NLDA}(\rho) \tag{3.2.50}$$

The correction term is a function of the density and of a parameter x, which at the same time depends on the density gradient. However, the expression of x is such that it remains dimensionless for the integral to maintain its energy units:

$$E_X^{NLDA}(\rho) = \int \rho^{4/3}(\vec{r}) f^{NLDA}(x) \qquad x = -\frac{|\nabla\rho|}{\rho^{4/3}} \tag{3.2.51}$$

With these conditions, the asymptotic behavior of the density could be corrected using any of two mathematical functions. Becke found that one of them, that had a parameter β, fitted better than the other one, for a series of atoms, when β=0.0042:

$$f^{NLDA}(x) = -\frac{\beta x^2}{1+6\beta x \sinh^{-1} x} \tag{3.2.52}$$

As to the correlation functionals, more complex analytic expressions were developed. One of the most famous is the one of Lee, Yang and Parr correlation[8]:

$$f^{LYP} = a\int \frac{\rho}{1+d\rho^{-1/3}}dr - ab\int \omega\rho^2\left[C_F\rho^{8/3} + |\nabla|^2\left(\frac{5}{12}-\delta\frac{7}{72}\right)\right] - \frac{11}{24}\rho^2|\nabla\rho|^2 dr \tag{3.2.53}$$

Where a, b, c and d are parameters that are fitted to the data of the helium atom.

These two constitute one of the most used functionals, the BLYP, but there are many other possibilities due to the fact that all exchange and correlation functionals can be combined.

The GGA functionals successfully improve the values for the geometries, frequencies and charge densities with respect to the LDA functional and even work well for hydrogen bonds, but they still fail to describe weaker interactions and therefore they are not good to describe van der Waals complexes.

The meta-GGA functionals improve GGA functionals by adding higher order derivatives of the density. Therefore, the exchange-correlation energy does not only contain the density and its gradient but also the Laplacian of the density. Since the orbital kinetic energy density and the Laplacian are related by the effective potential they contain, both magnitudes can be used, and since the calculation of the orbital kinetic energy is numerically more stable than the one of the Laplacian, the orbital kinetic energy is preferred:

$$\tau(\vec{r}) = \frac{1}{2}\sum_{i=1}^{N_{oc}}|\nabla\chi_i(\vec{r})|^2 \tag{3.2.54}$$

$$E_{XC}^{meta-GGA}(\rho) = \int f(\rho, \nabla\rho, \tau, \nabla^2\rho)d\vec{r} \tag{3.2.55}$$

3.2.3.3. Hybrid Functionals.

Hybrid functionals include part of the exact exchange energy from a HF calculation. The adiabatic connection justifies the existence of this type of methods:

Given a system with a two-electron interaction λ/r_{12}, an external potential $v_s^{\lambda}(r)$ can be fitted so that for any value of λ one obtains the same density $\rho(r)$: the one that corresponds to λ=1. λ is called coupling constant because its value depends on the interaction between electrons, so that it is 0 for a system without electron-electron interactions and is 1 for a system with Coulomb electron-electron interactions.
This parameter is continuous, and therefore it gradually connects the model system without electron-electron interactions with the real system.
For the system with the two-electron interaction λ/r_{12}, we have:

$$\hat{H}^{\lambda} = \sum_{i=1}^{N} -\frac{1}{2}\nabla^2(i) + \sum_{i=1}^{N} \hat{v}_s^{\lambda}(i) + \sum_{i=1}^{N}\sum_{j>i}^{N} \frac{\lambda}{r_{ij}} \tag{3.2.56}$$

$$E^{\lambda} = \left\langle \Psi^{\lambda} \middle| \hat{H}^{\lambda} \middle| \Psi^{\lambda} \right\rangle \tag{3.2.57}$$

The energies of the systems with λ=0 and λ=1 are given by:

$$E^0 = \hat{T}_r(\rho) + \int \rho(\vec{r}) v_r(\vec{r}) d\vec{r} \tag{3.7.3}$$

$$E^1 = \hat{T}_r(\rho) + \int \rho(\vec{r}) v_n(\vec{r}) d\vec{r} + \frac{1}{2}\iint \frac{\rho(\vec{r}_1)\rho(\vec{r}_2)}{|\vec{r}_1 - \vec{r}_2|} d\vec{r}_1 d\vec{r}_2 + E_{XC}(\rho) \tag{3.2.58}$$

Therefore:

$$E_{XC}(\rho) = E^1 - E^0 + \int \rho(\vec{r})(v_s(\vec{r}) - v_n(\vec{r}))d\vec{r} - \frac{1}{2}\iint \frac{\rho(\vec{r}_1)\rho(\vec{r}_2)}{|\vec{r}_1 - \vec{r}_2|} d\vec{r}_1 d\vec{r}_2 \tag{3.2.59}$$

The Hellmann-Feynman theorem says that the derivative of the total energy with respect to a parameter is equal to the expectation value of the derivative of the Hamiltonian with respect to the same parameter:

$$\frac{dE^{\lambda}}{d\lambda} = \left\langle \Psi^{\lambda} \middle| \frac{d\hat{H}^{\lambda}}{d\lambda} \middle| \Psi^{\lambda} \right\rangle = \left\langle \Psi^{\lambda} \middle| \sum_{i}^{N} \frac{dv_r^{\lambda}}{d\lambda} + \sum_{i}^{N}\sum_{j>i}^{N} \frac{1}{r_{ij}} \middle| \Psi^{\lambda} \right\rangle \tag{3.2.60}$$

Since $\int_0^1 \frac{dE^{\lambda}}{d\lambda} = E^1 - E^0$, then:

$$E^1 - E^0 = \int_0^1 \frac{dE^{\lambda}}{d\lambda} = \int_0^1 \left\langle \Psi^{\lambda} \middle| \sum_{i}^{N} \frac{dv_r^{\lambda}}{d\lambda} \middle| \Psi^{\lambda} \right\rangle d\lambda + \frac{1}{2}\iint\int_0^1 \frac{\rho^{\lambda}(\vec{r}_1, \vec{r}_2)}{r_{12}} d\vec{r}_1 d\vec{r}_2 d\lambda \tag{3.2.61}$$

$$E^1 - E^0 = \int_0^1 \int \rho(\vec{r}) \frac{dv_r^\lambda}{d\lambda} d\vec{r} d\lambda + \frac{1}{2} \int \int \int_0^1 \frac{\rho(\vec{r}_1)\rho(\vec{r}_2)}{r_{12}} d\vec{r}_1 d\vec{r}_2 d\lambda + \frac{1}{2} \int \int \int_0^1 \frac{\rho(\vec{r}_1)\rho_{XC}^\lambda(\vec{r}_1, \vec{r}_2)}{r_{12}} d\vec{r}_1 d\vec{r}_2 d\lambda \quad (3.2.62)$$

Integrating the two first terms with respect to λ:

$$E^1 - E^0 = \int \rho(\vec{r})(v_s(\vec{r}) - v_n(\vec{r}))d\vec{r} + \frac{1}{2} \int \int \frac{\rho(\vec{r}_1)\rho(\vec{r}_2)}{|\vec{r}_1 - \vec{r}_2|} d\vec{r}_1 d\vec{r}_2 + \frac{1}{2} \int \int \int_0^1 \frac{\rho(\vec{r}_1)\rho_{XC}^\lambda(\vec{r}_1, \vec{r}_2)}{r_{12}} d\vec{r}_1 d\vec{r}_2 d\lambda \quad (3.2.63)$$

Therefore:

$$E_{XC}(\rho) = E^1 - E^0 + \int \rho(\vec{r})(v_s(\vec{r}) - v_n(\vec{r}))d\vec{r} - \frac{1}{2} \int \int \frac{\rho(\vec{r}_1)\rho(\vec{r}_2)}{|\vec{r}_1 - \vec{r}_2|} d\vec{r}_1 d\vec{r}_2 \quad (3.2.64)$$

$$E_{XC}(\rho) = \frac{1}{2} \int \int \int_0^1 \frac{\rho(\vec{r}_1)\rho_{XC}^\lambda(\vec{r}_1, \vec{r}_2)}{r_{12}} d\vec{r}_1 d\vec{r}_2 d\lambda = \frac{1}{2} \int \int_0^1 \rho(\vec{r}) v_{XC}^\lambda(\vec{r}) d\vec{r} d\lambda \quad (3.2.65)$$

And this equation can be written as a function of the interaction of ρ with its exchange correlation hole ρ_{XC} :

$$E_{XC}(\rho) = \int_0^1 W_{XC}^\lambda(\rho) d\lambda \quad (3.2.68)$$

Where $W_{XC}(\rho)$ is the electronic part of the exchange-correlation energy for a system with electron-electron interaction λ / r_{12} and is mathematically defined as:

$$W_{XC}(\rho) = \frac{1}{2} \int \rho(\vec{r}_1) d\vec{r}_1 \int \frac{\rho_{XC}^\lambda(\vec{r}_1, \vec{r}_2)}{|\vec{r}_1 - \vec{r}_2|} d\vec{r}_2 = \int \rho(\vec{r}_1) v_{XC}^{hole}(\vec{r}_1) d\vec{r}_1 \quad (3.2.69)$$

The equation (3.2.68) is the adiabatic connection formula for the exchange-correlation energy. Since for the exchange correlation energy of a system with electron-electron interactions we obtain an integral between λ=1 and λ=0 for $W_{XC}(\rho)$, a term of $W_{XC}(\rho)$ for λ=0 in the exchange correlation energy of that system is granted. This means that since that $W_{XC}^0(\rho)$ corresponds to systems where there are no electron-electron interactions, i.e. to the exchange HF energy, the existence of hybrid methods, that include part of this exchange HF energy to describe systems with electron-electron interactions (λ=1), is clearly possible. It is important to remark that $W_{XC}^0(\rho)$ is therefore exact while $W_{XC}^1(\rho)$ is approximated.

The first approximation for these hybrid functionals was made by Becke, who proposed the Half & Half method in which $W_{XC}(\rho)$ depends linearly on λ. Another famous method he proposed was the three parameters method B3PW91[41, 42], in which the exchange-correlation energy followed the expression:

$$E_{XC}^{B3PW91} = E_{XC}^{LSDA} + a_0\left(E_X^{HF} - E_X^{LSDA}\right) + a_x\left(E_X^{B88} - E_X^{LSDA}\right) + a_c\left(E_C^{P3PW91} - E_C^{LSDA}\right) \quad (3.2.70)$$

a_0, a_x and a_c are parameters fitted to experimental thermochemical data, and the best fitted values for them are 0.20, 0.72 and 0.81 respectively.

Many others functionals were developed with this same procedure, varying the amount of HF exchange energy included, but the most famous hybrid functional is B3LYP, due to the surprisingly good results it provides. It this hybrid functional the exchange correlation energy has the following expression:

$$E_{XC}^{B3LYP} = E_{XC}^{LSDA} + a\left(E_X^{HF} - E_X^{LSDA}\right) + b\left(E_X^{B88} - E_X^{LSDA}\right) + c\left(E_C^{LYP} - E_C^{LSDA}\right) \quad (3.2.71)$$

The only difference between B3PW91 and B3LYP is in the correlation functional used, and the parameters a, b and c are not fitted to B3LYP but simply directly taken from those of B3PW91, i.e. $a = 0.20$, $b = 0.72$ and $c = 0.81$. This functional, however, usually gives good results with these default parameters. However, the parameters can be modified in Gaussian, not only for this particular one but for any hybrid method, for Gaussian has a general equation for hybrid methods:

$$E_{XC} = P_2 E_{XC}^{HF} + P_1\left(P_4 E_X^{LSDA} + P_3 \Delta E_X^{non-local}\right) + P_6 E_C^{local} + P_5 \Delta E_C^{non-local} \quad (3.2.72)$$

Therefore we would only need to adapt the values of P_i to result in the values we want for the parameters of our hybrid functional and set the values of P_i in Gaussian with the keyword IOp.

3.2.3.4. The hybrid-meta-GGA functionals.

These functionals are based in including HF exchange energy to some extent in meta-GGA functionals. To this type of functionals belongs the M06 series family.
They are, as GGA functionals, functionals with parameters that are fitted empirically.

The M06 series are, in addition, constrained to the uniform electron gas. We have tried M06 and M06-2X because they are known to be good for non-covalent interactions, specially the first one. M06 has a 27% of HF exchange energy, while M06-2X doubles that quantity to a total of 54% of HF exchange energy.

The main problem of DFT for our case of interest is that the correlation-exchange functionals in a weakly bonded system are not able to treat properly the dispersion energy. The failure lies in the impossibility of the local or semilocal functionals to describe an interaction whose nature is non-local. In fact, for weakly bonded systems it is generally necessary to correct the correlation-exchange functionals. However, for systems that are not strictly dispersive such as hydrogen bonds, which we already are similar to beryllium bonds, the GGA and meta-GGA functionals give quite reasonable results, and that is why M06 and M06-2X were chosen, along with B3LYP, for the early study of the molecules of the present work.

3.3. MØLLER PLESSET PERTUBATION THEORY.

Moller-Plesset perturbation theory is a post-Hartree-Fock method. Post-Hartree-Fock methods try to solve one of the main issues of the Hartree-Fock method, which is the inclusion of the electron correlation. The Hartree-Fock motion averages the field where electrons move and therefore only considers one electron and a field at a time, being imposible then to consider the correlation in the movement of the electrons. It is, then, the only amount of energy that the Hartree-Fock method doesn't account for, and the correlation energy can be therefore defined as the difference between the exact energy and the Hartree-Fock method's one:

$$E_{corr} = E_{exact} - E_{HF} \tag{3.3.1}$$

Moller-Plesset perturbation theory tries then to add the electron correlation effects by means of the Rayleigh-Schrödinger perturbation theory (RS-PT), which is one of the best and more common approaches and has the advantage of being size-consistent.
It can be applied to any order, but the most used ones are to second order (MP2), third (MP3) and fourth (MP4).

Perturbation theory is based on supposing that the Hamiltonian of a system, whose eigenvalues and eigenfunctions cannot be exactly calculated, is similar to the Hamiltionian of a system whose eigenvalues and eigenfunctions are known exactly, so that the first Hamiltonian can be considered as a slightly perturbed self of the second one. The idea behind it is that, as a consequence, the wavefunctions and energies associated with the exact Hamitonian will also be similar to the ones of the real system, and therefore one could use them to obtain good approximations to the wavefunctions and energies of the real system. The Hamiltonian can thus be separated in two terms:

$$\hat{H} = \hat{H}^0 + \hat{V} \tag{3.3.2}$$

where $\hat{V}$ is the perturbation and $\hat{H}^0$ is the Hamiltonian of the known system. It is possible to demonstrate that this separability of the Hamiltonian is correct and exact. The system with $\hat{H}^0$ has known zero-order solutions:

$$\hat{H}^0\Psi_k^{(0)} = E_k^{(0)}\Psi_k^{(0)} \tag{3.3.3}$$

From here, when applying the perturbation theory one has to choose the form of the known Hamiltonian. Moller and Plesset method considers this zero order as the sum of the one particle Fock operators:

$$\hat{H}^0 = \sum_i \hat{f}(i) \tag{3.3.4}$$

Therefore the eigenfunctions of $\hat{f}$ are the occupied and virtual Hartree-Fock orbitals of the system and the eigenvalues are the associated one electron energies:

$$\hat{f}\varphi_i = \varepsilon_i\varphi_i \tag{3.3.5}$$

And the corresponding Hartree-Fock wavefunction would be:

$$\Psi^{(0)}(1,2,...,N) = \hat{A}\varphi_1(1)\varphi_2(2)...\varphi_N(N) \tag{3.3.6}$$

where $\hat{A}$ is the corresponding anti-symmetric operator. This wave function is an eigenfunction of $\hat{H}_0$ with an eigenvalue equal to the sum of the one electron energies of the occupied spin orbitals:

$$E^{(0)} = \sum_{i=1}^{N} \varepsilon_i \tag{3.3.7}$$

Besides, a key idea of Moller-Plesset perturbation theory is that all Slater determinants for electron excitations are also eigenfunctions of $\hat{H}_0$ with an eigenvalue equal to the sum of the one electron energies of the occupied spin orbitals, so that the determinant formed by exciting the electron of spin orbital i to spin orbital a is:

$$\Psi_i^a = \hat{A}\varphi_1(1)\varphi_2(2)...\varphi_{i-1}(i-1)\varphi_a(i)\varphi_{i+1}(i+1)...\varphi_N(N) \tag{3.3.8}$$

And it has the eigenvalue:

$$E_i^a = E^{(0)} + \varepsilon_a - \varepsilon_i \tag{3.3.9}$$

Similarly, a double excitation in which one electron goes from spin orbital i to spin orbital a and another from spin orbital j to spin orbital b would have the eigenvalue:

$$E_{ij}^{ab} = E^{(0)} + \varepsilon_a - \varepsilon_i + \varepsilon_b - \varepsilon_j \tag{3.3.10}$$

With N electrons we have N ground state spin orbitals ($i = 1,2,...,N$), but the number of virtual orbitals depends on the number of functions in the expansion basis.

Since all the eigenvalues and eigenfunctions of $\hat{H}_0$ are known, perturbation theory can be used with them in order to find the energies and eigenfunctions of $\hat{H}$.

From the definition of the Fock operator for an electron i, we have:

$$\hat{f}(i) = \hat{h}(i) + \sum_{i<j}^{N} \left(\hat{J}_j(i) - \hat{K}_j(i) \right) \tag{3.3.11}$$

Therefore:

$$\hat{V} = \hat{H} - \hat{H}^0 = \sum_i \left(\hat{h}(i) + \sum_{i<j}^{N} \left(\hat{J}_j(i) - \hat{K}_j(i) \right) \right) - \sum_i \left(\hat{h}(i) + \hat{V}_{HF}(i) \right) = \sum_i \sum_{i<j}^{N} \left(\left(\hat{J}_j(i) - \hat{K}_j(i) \right) - \frac{1}{r_{ij}} \right)$$

(3.3.12)

Thus, the perturbation is the difference between the electron-electron interaction between each electron pair and the average electron-electron interaction. Due to this, this perturbation is sometimes called 'fluctuation potential', for it can be seen as a measure of the deviation from the mean of the electron-electron interaction.

To find the relation between perturbed and unperturbed systems, a parameter λ is introduced in the range [0, 1], so that it is equal to zero when the system is unperturbed and as it increases towards 1 the system is more and more perturbed:

$$\hat{H} = \hat{H}^0 + \lambda \hat{V} \tag{3.3.13}$$

As this Hamiltonian depends now on λ, its eigenfunctions and eigenvalues also depend on it, and they can be written as Taylor's expansions:

$$\Psi_n = \Psi_n^{(0)} + \lambda \Psi_n^{(1)} + \lambda^2 \Psi_n^{(2)} + ... \tag{3.3.14}$$

$$E_n = E_n^{(0)} + \lambda E_n^{(1)} + \lambda^2 E_n^{(2)} + \ldots \tag{3.3.15}$$

Substituting in the Schrödinger equation:

$$\left(\hat{H}^0 + \lambda\hat{V}\right)\left(\Psi_n^{(0)} + \lambda\Psi_n^{(1)} + \lambda^2\Psi_n^{(2)} + \ldots\right) = \left(E_n^{(0)} + \lambda E_n^{(1)} + \lambda^2 E_n^{(2)} + \ldots\right)\left(\Psi_n^{(0)} + \lambda\Psi_n^{(1)} + \lambda^2\Psi_n^{(2)} + \ldots\right)$$

$$\hat{H}^0\Psi_n^{(0)} + \lambda\left(\hat{H}^0\Psi_n^{(1)} + \hat{V}\Psi_n^{(0)}\right) + \ldots = E_n^{(0)}\Psi_n^{(0)} + \lambda\left(E_n^{(1)}\Psi_n^{(0)} + E_n^{(0)}\Psi_n^{(1)}\right) + \ldots \tag{3.3.16}$$

Identifying terms with the same power of λ one obtains:

For λ^0: $\hat{H}^0\Psi_n^{(0)} = E_n^{(0)}\Psi_n^{(0)}$ (3.3.17)

For λ^1: $\hat{V}\Psi_n^{(0)} + \hat{H}^0\Psi_n^{(1)} = E_n^{(1)}\Psi_n^{(0)} + E_n^{(0)}\Psi_n^{(1)}$ (3.3.18)

For λ^2: $\hat{V}\Psi_n^{(1)} + \hat{H}^0\Psi_n^{(2)} = E_n^{(1)}\Psi_n^{(1)} + E_n^{(0)}\Psi_n^{(2)} + E_n^{(2)}\Psi_n^{(0)}$ (3.3.19)

The first equation is easily recognized as the Schrodinger equation of the unperturbed system, while the other two provide a link between perturbed and unperturbed quantities. In fact, projecting the second equation into the $\left\langle\Psi_n^{(0)}\right|$ states, one finds:

$$\left\langle\Psi_n^{(0)}\middle|\hat{V}\middle|\Psi_n^{(0)}\right\rangle + \left\langle\Psi_n^{(0)}\middle|\hat{H}^0\middle|\Psi_n^{(1)}\right\rangle = E_n^{(1)}\left\langle\Psi_n^{(0)}\middle|\Psi_n^{(0)}\right\rangle + E_n^{(0)}\left\langle\Psi_n^{(0)}\middle|\Psi_n^{(1)}\right\rangle \tag{3.3.20}$$

Since $\hat{H}^0$ is hermitian, it is fulfilled that $\left\langle\Psi_n^{(0)}\middle|\hat{H}^0\middle|\Psi_n^{(1)}\right\rangle = \left\langle\Psi_n^{(1)}\middle|\hat{H}^0\middle|\Psi_n^{(0)}\right\rangle$, and thus $\left\langle\Psi_n^{(0)}\middle|\hat{H}^0\middle|\Psi_n^{(1)}\right\rangle = E_n^{(0)}\left\langle\Psi_n^{(1)}\middle|\Psi_n^{(0)}\right\rangle = E_n^{(0)}\left\langle\Psi_n^{(0)}\middle|\Psi_n^{(1)}\right\rangle$. Finally, since the wavefunctions $\Psi_n^{(0)}$ are normalized to unity, $\left\langle\Psi_n^{(0)}\middle|\Psi_n^{(0)}\right\rangle = 1$, and therefore equation (3.3.20) transforms into:

$$E_n^{(1)} = \left\langle\Psi_n^{(0)}\middle|\hat{V}\middle|\Psi_n^{(0)}\right\rangle \tag{3.3.21}$$

This equation allows evaluating the first order correction to the energy as the mean value of the perturbation potential but, and this is the most important fact, using the known wavefunctions of the unperturbed system.

Similarly, by projecting the third equation (3.3.19) into the $\left\langle\Psi_n^{(0)}\right|$ states, establishing that $\left\langle\Psi_n^{(0)}\middle|\Psi_n^{(m)}\right\rangle = \delta_{m0}$ and noticing that we have intermediate normalization $\left\langle\Psi_n^{(0)}\middle|\Psi_n\right\rangle = 1$, one finally obtains:

$$E_n^{(2)} = \left\langle \Psi_n^{(0)} \middle| \hat{V} \middle| \Psi_n^{(1)} \right\rangle \tag{3.3.22}$$

And in general, for a k-order correction:

$$E_n^{(k)} = \left\langle \Psi_n^{(0)} \middle| \hat{V} \middle| \Psi_n^{(k-1)} \right\rangle \tag{3.3.23}$$

If the potential is substituted in the equation (3.3.21), and taking into account the Slater-Condon rules one obtains:

$$E_n^{(1)} = \left\langle \Psi_n^{(0)} \middle| \hat{V} \middle| \Psi_n^{(0)} \right\rangle = \left\langle \Psi_n^{(0)} \middle| \sum_{j>i} \left(\hat{J}_j(i) - \hat{K}_j(i) \right) \middle| \Psi_n^{(0)} \right\rangle - \left\langle \Psi_n^{(0)} \middle| \sum_i \hat{V}_{HF}(i) \middle| \Psi_n^{(0)} \right\rangle; \tag{3.3.24}$$

$$E_n^{(1)} = \hat{V}_{el-el} - 2\hat{V}_{el-el} = \frac{1}{2}\sum_{a,b} \langle ab \| ba \rangle - \sum_{a,b} \langle ab \| ba \rangle = -\frac{1}{2}\sum_{a,b} \langle ab \| ba \rangle = -\hat{V}_{el-el} \tag{3.3.25}$$

$$E_n^{(0)} + E_n^{(1)} = \sum_{i=1}^{N} \varepsilon_i - \frac{1}{2}\sum_{a,b} \langle ab \| ba \rangle = E_{HF} \tag{3.3.26}$$

This result means that the first-order correction to the energy is already included in the Hartree-Fock energy of the real system. The first correction of the perturbation theory to the HF energy comes after first order.

The second order correction to the energy depends on the first order correction to the wavefunction, and this is obtained by projecting the equation (3.3.18) into the $\left\langle \Psi_i^{(0)} \right|$ states and using the expressions $\left\langle \Psi_i^{(0)} \middle| \Psi_j^{(0)} \right\rangle = \delta_{ij}$, which is 0 when $i \neq j$ and 1 otherwise, and $\left\langle \Psi_i^{(0)} \middle| \Psi_j^{(1)} \right\rangle = c_i^{(1)}$:

$$c_i^{(1)} = \left\langle \Psi_i^{(0)} \middle| \Psi_n^{(1)} \right\rangle = \frac{\left\langle \Psi_i^{(0)} \middle| \hat{V} \middle| \Psi_n^{(0)} \right\rangle}{E_n^{(0)} - E_i^{(0)}} \Rightarrow \left| \Psi_n^{(1)} \right\rangle = c_i^{(1)} \left| \Psi_i^{(0)} \right\rangle = \frac{\left\langle \Psi_i^{(0)} \middle| \hat{V} \middle| \Psi_n^{(0)} \right\rangle}{E_n^{(0)} - E_i^{(0)}} \left| \Psi_i^{(0)} \right\rangle \tag{3.3.27}$$

That expression is for the correction of one single state. To account for all:

$$\left| \Psi_n^{(1)} \right\rangle = \sum_{i \neq n} \frac{\left\langle \Psi_i^{(0)} \middle| \hat{V} \middle| \Psi_n^{(0)} \right\rangle}{E_n^{(0)} - E_i^{(0)}} \left| \Psi_i^{(0)} \right\rangle \tag{3.3.28}$$

And by substituting in the equation above (3.3.22):

$$E_n^{(2)} = \left\langle \Psi_n^{(0)} \middle| \hat{V} \sum_{i \neq n} \frac{\left\langle \Psi_i^{(0)} \middle| \hat{V} \middle| \Psi_n^{(0)} \right\rangle}{E_n^{(0)} - E_i^{(0)}} \middle| \Psi_i^{(0)} \right\rangle = \sum_{i \neq n} \frac{\left| \left\langle \Psi_i^{(0)} \middle| \hat{V} \middle| \Psi_n^{(0)} \right\rangle \right|^2}{E_n^{(0)} - E_i^{(0)}} \tag{3.3.29}$$

While the first order correction term was very easy to calculate, these two last expressions contain an infinite number of terms (the summation is over any state different from the ground state i), and the summation has to be cut at a point in order to allow its calculation. That is why the perturbation potential V must be weak, so that the convergence is achieved, preferably, at first order. Another thing to consider is that since the denominator contains energy differences between unperturbed states, the unperturbed system must not be degenerate, for it would make the equation lead to divergencies.

It is important to notice that these equations are reached by granting the intermediate normalization between the higher order wavefunctions corrections and the wavefunctions of the unperturbed system, and therefore they must be orthogonal. A set of wavefunctions which fulfills this constrain is the set that represent the excitations from the occupied φ_a in $\Psi_n^{(0)}$ to spin orbitals which are unoccupied in it. As we saw before, its wavefunctions are also eigenfunctions of the Hamiltonian of the unperturbed system and this if very convenient for that way it provides easy expressions for the energy. Moller-Plesset perturbation theory is based on this last idea, and specifically the second order Moller-Plesset perturbation theory is the method most commonly used because higher order perturbation expansions become more computationally expensive and do not perform as well as other methods which have more or less the same computational cost.

The Slater rules applied to the second order energy correction expression states that only doubly excited determinants will have non-zero contributions to the MP2 energy. The first order wavefunction correction can be expressed as:

$$\Psi_n^{(1)} = \sum_{a>b;r>s} C_{n,abrs}^{(1)} \Psi_{ab}^{rs} \tag{3.3.30}$$

Where the coefficients are determined by:

$$C_{n,abrs}^{(1)} = \left\langle \Psi_{ab}^{rs} \middle| \Psi_n^{(1)} \right\rangle = \sum_{a>b;r>s} \frac{\left\langle \Psi_{ab}^{rs} \middle| \Psi_n^{(1)} \right\rangle}{\varepsilon_a + \varepsilon_b - \varepsilon_r - \varepsilon_s} \tag{3.3.31}$$

Substituting this in the expression for the second order energy correction (3.3.29) one obtains:

$$E_0^{(2)} = \sum_{a>b;r>s} \frac{\left\langle \Psi_0^{(0)} \middle| \frac{1}{r_{12}} \middle| \Psi_{ab}^{rs} \right\rangle}{\varepsilon_a + \varepsilon_b - \varepsilon_r - \varepsilon_s} = \sum_{a>b;r>s} \frac{\left| \langle ab \| rs \rangle \right|^2}{\varepsilon_a + \varepsilon_b - \varepsilon_r - \varepsilon_s} = \frac{1}{4} \sum_{abrs} \frac{\left| \langle ab \| rs \rangle \right|^2}{\varepsilon_a + \varepsilon_b - \varepsilon_r - \varepsilon_s} \tag{3.3.32}$$

The same issue with degenerate states the perturbation theory has appears in Moller-Plesset perturbation theory as well, and it is easily identified with the degeneration between occupied (a,b) and virtual (r,s) orbitals. When the separation between them is too small, the method gives wrong results. This turns especially evident when studying a dissociation process, for this orbital separation decreases at long distances, and the second order correction to the energy would increase more and more as the atomic distance increases and the occupied and virtual orbitals get closer, therefore giving overestimated energy results. This effect can be so acute that it may give rise to a negative dissociation energy. It is important therefore to grant that the system does not have such degenerations, and if it has, one may find the solution is applying multireference methods instead. There is also evidence that the use of large basis sets can give rise to this unwanted effect of divergence[43].

Although MP2 is quite inexpensive, has a correct separability (is size consistent) and accounts for 80-90% of the correlation energy, it is a non-variational method and, as such, it is not possible to know the sign of the error of the estimated energy.

3.4. COUPLED CLUSTER.

Coupled cluster is another post-Hartree-Fock method, and as such it tries to improve the HF method by accounting for electron correlation.

In CC theory, as in perturbation theory, the wavefunction Ψ of the system is expressed in terms of the reference wavefunction Ψ^0, but this methods does so through an exponential expression:

$$\Psi = e^{\hat{T}}\Psi^0 \tag{3.4.1}$$

Where $\hat{T}$ is the cluster operator and can be expanded as a sum of cluster operators:

$$\hat{T} = \hat{T}_1 + \hat{T}_2 + \hat{T}_3 + \ldots \tag{3.4.2}$$

The indexes of the operators indicate the excitation degree they account for:

$$\hat{T}_1 = \sum_{a,r} t_a^r \hat{a}_r^* \hat{a}_a \tag{3.4.3}$$

$$\hat{T}_2 = \sum_{a<b;r<s} t_{ab}^{rs} \hat{a}_r^* \hat{a}_s^* \hat{a}_b \hat{a}_a \tag{3.4.4}$$

$$\hat{T}_3 = \sum_{a<b<c;r<s<t} t_{abc}^{rst} \hat{a}_r^* \hat{a}_s^* \hat{a}_t^* \hat{a}_c \hat{a}_b \hat{a}_a \tag{3.4.5}$$

where $t_a^r, t_{ab}^{rs}, t_{abc}^{rst}, \ldots$ are the cluster amplitudes, $\hat{a}_i$ are the annihilation operators and $\hat{a}_i^*$ are the creation operators. These operators belong to the language of second quantization, in which the quantum states are expressed in terms of the number of particles that occupy each eigenstate. The annihilation operator lowers by one the number of particles in a given state, while the creation operator increases by one the number of particles, and the latter is the adjoint of the former. The particle removed or added comes from or goes to the eigenstate indicated by the operator subscript.

The exponential of the cluster operator can be expanded in a Taylor series:

$$e^{\hat{T}} = \hat{1} + \hat{T} + \frac{1}{2!}\hat{T}^2 + \frac{1}{3!}\hat{T}^3 + \ldots \tag{3.4.6}$$

From equation (3.4.2) and (3.4.6) it can be written:

$$e^{\hat{T}} = \hat{1} + \hat{T}_1 + \hat{T}_2 + \hat{T}_3 + \ldots + \frac{1}{2!}\left(\hat{T}_1 + \hat{T}_2 + \hat{T}_3 + \ldots\right)^2 + \frac{1}{3!}\left(\hat{T}_1 + \hat{T}_2 + \hat{T}_3 + \ldots\right)^3 + \ldots \tag{3.4.7}$$

$$e^{\hat{T}} = \hat{1} + \hat{T}_1 + \left(\frac{1}{2}\hat{T}_1^2 + \hat{T}_2\right) + \left(\frac{1}{6}\hat{T}_1^3 + \hat{T}_2\hat{T}_1 + \hat{T}_3\right)^3 + \left(\frac{1}{24}\hat{T}_1^4 + \frac{1}{2}\hat{T}_2^2 + \frac{1}{2}\hat{T}_2\hat{T}_1^2 + \hat{T}_3\hat{T}_1 + \hat{T}_4\right) + \ldots \tag{3.4.8}$$

It can be seen from this equation that there is only a way of having a single excitation, $\hat{T}_1$, but two ways of having double excitations: a pure double excitation $\hat{T}_2$ or two consecutive single excitations $\hat{T}_1$, which then fulfill $\hat{T}_1\hat{T}_1 = \hat{T}_1^2$. Similarly there are three ways of generating a triple excitation: a pure triple excitation $\hat{T}_3$, a single and a double consecutive excitations $\hat{T}_1\hat{T}_2$ or three successive single excitations $\hat{T}_1\hat{T}_1\hat{T}_1 = \hat{T}_1^3$ and so on.

These pure excitations are known as connected cluster components, while the excitations whose excitation degree is achieved by the product of two or more operators of lower excitation are called disconnected components.

An operator can be defined to group these types of excitations:

For single excitations: $\hat{C}_1 = \hat{T}_1$ (3.4.9)

For double excitations: $\hat{C}_2 = \hat{T}_2 + \frac{1}{2}\hat{T}_1^2$ (3.4.10)

For triple excitations: $\hat{C}_3 = \hat{T}_3 + \hat{T}_1\hat{T}_2 + \frac{1}{3!}\hat{T}_1^3$ (3.4.11)

For quadruple excitations: $\hat{C}_4 = \hat{T}_4 + \frac{1}{2}\hat{T}_2^2 + \frac{1}{2}\hat{T}_1^2\hat{T}_2 + \hat{T}_1\hat{T}_3 + \frac{1}{4!}\hat{T}_1^4$ (3.4.12)

And so on.

One can then rewrite the exponential operator in a simpler form:

$$e^{\hat{T}} = \hat{1} + \hat{C}_1 + \hat{C}_2 + \hat{C}_3 + \ldots \quad (3.4.13)$$

If one substitutes in the Schrödinger equation:

$$\hat{H}\Psi = E\Psi \Rightarrow \hat{H}e^{\hat{T}}\Psi^0 = E_{CC}e^{\hat{T}}\Psi^0 \Rightarrow \left(\hat{H} - E^0\right)e^{\hat{T}}\Psi^0 = \left(E_{CC} - E^0\right)e^{\hat{T}}\Psi^0 \Rightarrow \left(\hat{H} - E^0\right)e^{\hat{T}}\Psi^0 = \left(E_{CCcorr}\right)e^{\hat{T}}\Psi^0 \quad (3.4.14)$$

To obtain the equation for evaluating the correlation energy one has to multiply on the left by Ψ^{0^*} and integrate over all space:

$$\left\langle \Psi^{0^*} \middle| \hat{H} - E^0 \middle| \left(\hat{1} + \hat{C}_1 + \hat{C}_2 + \hat{C}_3 + \ldots\right)\Psi^0 \right\rangle = E_{CCcorr}\left\langle \Psi^{0^*} \middle| \left(\hat{1} + \hat{C}_1 + \hat{C}_2 + \hat{C}_3 + \ldots\right)\Psi^0 \right\rangle \quad (3.4.15)$$

By definition, $\left\langle \Psi^{0^*} \middle| \hat{H} - E^0 \middle| \Psi^0 \right\rangle = -E^0 + E^0 = 0$, and since Ψ^0 is the HF eigenfunction, Brillouins theorem states that $\left\langle \Psi^{0^*} \middle| \hat{H} - E^0 \middle| \hat{C}_1\Psi^0 \right\rangle = 0$. Also, Slater Condon rules dictate that only the double excitation term on the left and the zero excitation term on the right survive. Therefore one obtains:

$$\left\langle \Psi^{0^*} \middle| \hat{H} - E^0 \middle| \hat{C}_2\Psi^0 \right\rangle = E_{CCcorr} \quad (3.4.16)$$

$$E_{CCcorr} = \left\langle \Psi^{0^*} \middle| \hat{H} - E^0 \middle| \left(\hat{T}_2 + \frac{1}{2}\hat{T}_1^2\right)\Psi^0 \right\rangle = \left\langle \Psi^{0^*} \middle| \hat{H}\hat{T}_2 \middle| \Psi^0 \right\rangle + \frac{1}{2}\left\langle \Psi^{0^*} \middle| \hat{H}\hat{T}_1^2 \middle| \Psi^0 \right\rangle \quad (3.4.17)$$

$$E_{CCcorr} = E_0 + \sum_{a<b}^{occ}\sum_{r<s}^{vir}\left(t_{ab}^{rs} + t_a^r t_b^s - t_a^s t_b^r\right)\left\langle \Psi^{0^*} \middle| \hat{H} \middle| \Psi_{ab}^{rs} \right\rangle \quad (3.4.18)$$

The second term corresponds to two electron integrals over molecular orbitals:

$$E_{CCcorr} = E_0 + \sum_{a<b}^{occ}\sum_{r<s}^{vir}\left(t_{ab}^{rs} + t_a^r t_b^s - t_a^s t_b^r\right)\left(\left\langle \varphi_a\varphi_b \middle| \varphi_s\varphi_r \right\rangle - \left\langle \varphi_a\varphi_b \middle| \varphi_r\varphi_s \right\rangle\right) \quad (3.4.19)$$

This result shows that the coupled cluster correlation energy is determined just by the amplitudes of single and double excitations and only two electron integrals are needed.

To obtain the equations to evaluate these amplitudes one has to multiply the Schrödinger equation (3.4.14) on the left by a single excitation Ψ_a^r:

$$\left\langle \Psi_a^r \left| \left(\hat{H} - E^0\right) e^{\hat{T}} \right| \Psi^0 \right\rangle = E_{CCcorr} \left\langle \Psi_a^r \left| e^{\hat{T}} \right| \Psi^0 \right\rangle \tag{3.4.20}$$

And substituting the exponential operator:

$$\left\langle \Psi_a^r \left| \hat{H} - E^0 \right| \left(\hat{1} + \hat{C}_1 + \hat{C}_2 + \hat{C}_3 + ...\right) \Psi^0 \right\rangle = E_{CCcorr} \left\langle \Psi_a^r \left| \left(\hat{1} + \hat{C}_1 + \hat{C}_2 + \hat{C}_3 + ...\right) \Psi^0 \right\rangle \right. \tag{3.4.21}$$

Here the Slater-Condon rules state that only up to triple excitations contribute to the term on the left and only the single excitation Ψ_a^r contributes to the term on the right:

$$\left\langle \Psi_a^r \left| \hat{H} - E^0 \right| \left(\hat{1} + \hat{C}_1 + \hat{C}_2 + \hat{C}_3\right) \Psi^0 \right\rangle = E_{CCcorr} t_a^r \tag{3.4.22}$$

And from that expression, once the correlation energy is known, the single excitation amplitude can be obtained. Similarly, the double excitation amplitude can be obtained by multiplying the Schrödinger equation (3.4.14) on the left by a double excitation Ψ_{ab}^{rs} and so on.

The first approximation of CC methods truncates this expansion at the double excitations $\hat{T} = \hat{T}_1 + \hat{T}_2$, which leads to the CCSD approximation:

$$\Psi = e^{\hat{T}} \Psi^0 = e^{\left(\hat{T}_1 + \hat{T}_2\right)} \Psi^0 = \left(\hat{1} + \hat{T}_1 + \hat{T}_2 + \frac{1}{2}\left(\hat{T}_1 + \hat{T}_2\right)^2 + \frac{1}{3!}\left(\hat{T}_1 + \hat{T}_2\right)^3 + ... \right) \Psi^0 \tag{3.4.23}$$

The equations for the energy and the amplitudes are obtained following the same procedure described for the general CC, by successively projecting into $\Psi^0, \Psi_a^r, \Psi_{ab}^{rs}$,... the corresponding Schrödinger equation:

$$\left(\hat{H} - E^0\right) e^{\left(\hat{T}_1 + \hat{T}_2\right)} \Psi^0 = E_{corr,CC} e^{\left(\hat{T}_1 + \hat{T}_2\right)} \Psi^0 \tag{3.4.24}$$

The resulting equation for the energy is:

$$\left\langle \Psi_a^r \left| \hat{H} - E^0 \right| \left(\hat{1} + \hat{T}_1 + \hat{T}_2 + \frac{1}{2}\hat{T}_1^2 \right) \Psi^0 \right\rangle = E_{CCcorr} \tag{3.4.25}$$

And for the amplitudes:

$$\left\langle \Psi_a^r \left| \hat{H} - E^0 \right| \left(\hat{T}_1 + \hat{T}_2 + \frac{1}{2}\left(\hat{T}_1^2 + 2\hat{T}_1\hat{T}_2\right) + \frac{1}{3!}\hat{T}_1^3 \right) \Psi^0 \right\rangle = E_{CCcorr} t_a^r \tag{3.4.26}$$

$$\left\langle \Psi_{ab}^{rs} \left| \hat{H} - E^0 \right| \left(\hat{T}_1 + \hat{T}_2 + \frac{1}{2}\left(\hat{T}_1^{\,2} + \hat{T}_2^{\,2} + 2\hat{T}_1\hat{T}_2\right) + \frac{1}{3!}\left(\hat{T}_1^{\,3} + 3\hat{T}_1^{\,2}\hat{T}_2\right) + \frac{1}{4!}\hat{T}_1^{\,4} \right) \Psi^0 \right\rangle = E_{CCcorr} t_{ab}^{rs} \tag{3.4.27}$$

Notice that the expression of the exponential operator for the energy is equal to $\hat{1} + \hat{C}_1 + \hat{C}_2$ and thus the expression for the correlation energy will be the same as the one for the general CC (3.4.19), while the expressions for the amplitudes do change.

In both sides of the equations for the amplitudes there are disconnected contributions that therefore cancel out, and this ensures the size-consistency of the method.

Triple excitations are also included in different CC methods, being the most common CCSDT, the method that includes them exactly $\left(\hat{T} = \hat{T}_1 + \hat{T}_2 + \hat{T}_3\right)$, and CCSD(T), in which singles and doubles are treated with coupled cluster theory, as CCSD, and an estimate to the connected triples $\hat{T}_3$ is calculated non-iteratively by means of perturbation theory[21].

The main drawback of this method is that the equation to solve is not linear anymore and algorithms to solve non-linear equations are needed. Also, as the perturbational method, CC methods need the HF wavefunction to give a qualitatively correct description of the system. Multirreference CC methods exist but they are complex and are not normally used.

3.5. ATOMS IN MOLECULES.

The Quantum Theory of Atoms in Molecules (QTAIM), developed by Professor Richard F. W. Bader and coworkers[27, 28], is based on the supposition that, since atoms and bonds are concepts that have been proved to be very useful in the understanding of chemistry and its predictions, there should be a physical explanation to that fact.

According to this theory, the electron density, together with the gradient paths of the electron density, reveals the structure of the system through its stationary points.

QTAIM is able to define atoms and chemical bonding from the topology of the electron density, justifying the concept of functional groups of atoms with certain characteristic properties that is so commonly used in chemistry. In addition, the theory allows the calculation of some physical properties in terms of atoms basis, dividing it into terms containing exactly one nucleus, justifying the additive characteristic of those properties.

Besides, as it was seen for density functional theory, the density is directly derived from the wavefunction of the system (see equation 3.2.6) and therefore there is no lost information in taking this approach.

At those points where the first derivative of the density, i.e. its gradient $\nabla\rho$, is equal to zero, we have what it is called a critical point CP, and the density surface accordingly presents a minimum, maximum or saddle point at the point with the coordinates given by r_c.

$$\nabla\rho(r_c) = i\frac{d\rho}{dx} + j\frac{d\rho}{dy} + k\frac{d\rho}{dz} = 0 \tag{3.5.1}$$

The gradient at this point must be zero in all directions of space and therefore each individual derivative must be zero and not just their sum. It also goes to zero as r goes to infinity, where there is no molecule and therefore there is no electronic density.

The gradient of a scalar function, as is the density, in a point of space, is a vector which points towards the direction in which the increase of the density is greatest, and has a magnitude equal to the rate of increase in that direction.

To determine if at a certain critical point we have a local minimum, maximum or saddle point mathematics states the second derivative $\nabla^2\rho$ must be calculated. $\nabla^2\rho$, as the derivative of a vector, constitutes then a tensor, and each second derivative of the density is written in the matrix called 'Hessian matrix':

$$\nabla^2\rho(r_c) = \begin{pmatrix} \frac{\partial^2\rho}{\partial x^2} & \frac{\partial^2\rho}{\partial x\partial y} & \frac{\partial^2\rho}{\partial x\partial z} \\ \frac{\partial^2\rho}{\partial y\partial x} & \frac{\partial^2\rho}{\partial y^2} & \frac{\partial^2\rho}{\partial y\partial z} \\ \frac{\partial^2\rho}{\partial z\partial x} & \frac{\partial^2\rho}{\partial z\partial y} & \frac{\partial^2\rho}{\partial z^2} \end{pmatrix}_{r=r_c} \tag{3.5.2}$$

This matrix is real and symmetric and thus diagonalizable.

Its diagonalization, naturally, gives a series of eigenvalues $\lambda_1, \lambda_2, \lambda_3$ with their associated eigenvectors. The final shape for the diagonal form of the Hessian matrix is as follows:

$$\begin{pmatrix} \frac{\partial^2\rho}{\partial x^2} & 0 & 0 \\ 0 & \frac{\partial^2\rho}{\partial y^2} & 0 \\ 0 & 0 & \frac{\partial^2\rho}{\partial z^2} \end{pmatrix}_{r=r_c} = \begin{pmatrix} \lambda_1 & 0 & 0 \\ 0 & \lambda_2 & 0 \\ 0 & 0 & \lambda_3 \end{pmatrix} \tag{3.5.3}$$

Therefore the eigenvalues are the second derivatives of the density with respect to the three principal axes x, y, z, i.e., are the curvatures of the density at the critical point, while the eigenvectors are their associated directions in space. Thus, a negative sign on any of the eigenvectors indicates that the density decreases from the critical point in the direction of its eigenvector and a positive sign indicates that the density increases from the critical point. As a result, a local maximum will be the critical point that has the three curvatures with a negative sign, while a local minimum would have the three of them with positive sign. A saddle-point, similarly, would have two negative curvatures and only a positive one.

In order to indicate this more easily, a critical point is labeled with two values. The first one is called rank ω, the second one is called signature σ, and the label is written as (ω,σ). The rank is the number of non-zero curvatures of the density and the signature is the sum of the algebraic signs of the three curvatures. A critical point of rank less than three indicates a change in the topology of the density, i.e. a change in the molecular structure, and therefore they are not commonly found in equilibrium distributions. As to the signature, the way it is defined allows it having just the values -3,-1,1,3 in equilibrium charge distributions. Therefore, there are four types of stable critical points having non-zero eigenvalues:

(3, -3) Three negative curvatures, the density decreases in every direction from the critical point: local maximum.

(3, -1) Two negative curvatures and a positive one, the density decreases in two directions from the critical point and increases in just one direction.

(3, +1) Two positive curvatures and a negative one, the density increases in two directions from the critical point and decreases in just one direction.

(3, +3) Three positive curvatures, the density increases in every direction from the critical point: local minimum.

Each type of critical point is identified with a concept of the chemical structure:

(3, -3) Local maximum: Nuclear critical point (NCP).

(3, -1) Saddle point: Bond critical point (BCP).

(3, +1) Reverse saddle point: Ring critical point (RCP).

(3, +3) Local minimum: Cage critical point (CCP).

A ring critical point appears in a plane space closed by bond paths, while a cage critical point appears in a volume closed by several ring surfaces. The gradient of the density function is discontinuous at a NCP, and therefore these are not true critical points, but they are considered as such because in practice they behave as a NCP would do.

The gradient path is the trajectory the gradient follows considering the maximum increase in the density. This path starts at an arbitrary point, the derivatives of the density are calculated and the vector points to the maximum increase of the density. The next point of the gradient path is selected by moving in that direction a small distance, and then the derivatives are calculated again, a new direction chosen, a new point and so on. When the gradient paths of the whole molecule are calculated, the gradient vector field is obtained, and it can be seen that every trajectory starts and ends at a critical point where the derivative of the density is zero, as NCP do. As a result, NCP are referred to as point attractors of the gradient vector field.

The basin of the attractor is defined as the region that contains all the trajectories of the gradient that end into the attractor. As a result of this, the space the molecular density is distributed in can be separated into atomic basins, separated regions that contain only one point attractor or nucleus. Thus, in this theory an atom is defined as a point attractor and the associated gradient paths that constitute its atomic basin.

Between an atom and a bonded other there is an interatomic surface, and that makes possible another definition of an atom in terms of the limits of its basin with the other atom's basins, i.e. delimited by one or more interatomic surface. Since the trajectories of the gradient of the density never cross and terminate at a critical point, in this interatomic surface the flux of the gradient of the density is zero, i.e. no gradient path crosses it or exists within it.

Usually (3, -3) critical points only appear in the center of a nucleus, but in some cases a local maximum of the density can be found at different positions, and behave as those point attractors. These are known as non-nuclear attractors (NNA) and are topologically undistinguishable from nuclear attractors, for they also have an associated basin and are bounded by a zero-flux surface. They are also called pseudo-atoms and can be bonded to other atoms and pseudo-atoms. In some cases the density of a BCP behaves as a NNA and artificial bonds between atoms and BCP or between BCPs are found.

The gradient path that links two neighboring atoms with the maximum electron density is called 'atomic interaction line'. The accumulation of density in this line is showed by the fact of presenting a (3, -1) critical point. This is a necessary condition for two atoms to be bonded[44] but is also sufficient when the system possess the minimum energy, which is the case of the equilibrium geometry. Therefore in those cases the atomic interaction line is called bond path and the (3, -1) critical point is called bond critical point.

With these bond paths and BCPs a molecular graph can be drawn for a given geometry of the system, showing its bondings. The bond paths of this molecular graph are usually found to coincide with the ones determined chemically, regardless of the character of the bond and including weak interactions such as van der Waals's. This fact is an indication that the topology of the electron density can account for the physics of atomic interactions and its corresponding chemical properties.

The molecular graph provides then a good definition of the molecular structure and can be used to locate changes in the mentioned structure along a reaction path.

Besides, the value of the density at the BCP is usually correlated with the bond energy, and from it one could define the bond order n of the bond. For instance:

$$n = e^{[A(\rho_{BCP} - B)]} \tag{3.5.4}$$

Where A and B are constants that depend on the nature of the bonded atoms.

It is important to remark, though, that although it is the general case, not every bond path is a bond[45]. In addition, unless dictated by symmetry, the length of the bond path will be greater than the interatomic distance due to the bond path being slightly bent. This bending can be quantified by means of the bond path angle and is more acute on cases of strain in which the deformation is needed to maximize the binding.

The Hessian eigenvalues of the density can also provide information about the characteristics of the bond. The two negative curvatures at a BCP indicate if there is a preferential direction of the density in the bonding, as happens in π bonds. If their magnitude is similar, then there is no preference, otherwise it is said that the density is preferentially accumulated in the plane associated to the smallest curvature, for a smaller curvature means a smaller decrease of the density along its axis, which determines the mentioned plane.

The elipticity is defined as:

$$\varepsilon = \frac{\lambda_1}{\lambda_2} - 1 \tag{3.5.5}$$

And it is used to give this measure of the preferential accumulation of the density on a plane. When there is no preference, $\lambda_1 = \lambda_2$ and $\varepsilon = 0$. If there is preferential accumulation on the plane associated to λ_2 then the ellipticity is positive, while if the accumulation is preferential on the perpendicular plane, associated to λ_1, then the ellipticity is negative.

If the negative curvatures determine the preferential concentration along the bond path, in either of the planes, the positive remaining curvature determines the depletion of charge in the region and the distribution of that density towards the atomic basins. The Laplacian, as the sum of the three curvatures, can then be used to know where the density is locally depleted or concentrated, providing important information about the character of the bond. If the Laplacian is greater than zero it means that in the surroundings of r_c the average density is greater and the density at r_c is locally depleted, while if the Laplacian is lower than zero there is a local concentration of the density in the surrounding of r_c.

It is useful to define a function $L(r)$ as the negative of the Laplacian, so that a positive value of $L(r)$ indicates a local concrentation of density and a negative value of $L(r)$ indicates a density depletion.

This local depletion on the density is characteristic of closed shell systems, especially of ionic character or with ionic character predominancy, such as hydrogen bonds and van der Waals interactions. Due to this the density at the bond critical point usually is very low, of about 0.10 and below, in this type of bonds. It is worth noting, though, that QTAIM has been found to overestimate the atomic charge or electron density in the atoms[46], giving rise to bonds that are more ionic than they should.

A local concentration, on the contrary, is characteristic of a shared interaction, being the covalent bonds the most common type of bonds that present this character. They usually have a high density, of about 0.2 and up.

Of course, there are intermediate unclassified types of bonding which have a value of $L(r)$ close to zero and may have any density.

All in all, AIM theory is a useful tool in determining the structure and bonds of chemical species, being able to characterize even conjugation and hyperconjugation, but it is not exempt of flaws, and therefore it should be used with caution.

3.6. NATURAL BOND ORBITALS.

Mathematically, the Natural Orbitals (NO) Θ_k of a wavefunction Ψ can be defined as the orbitals that are eigenfunctions of the first-order reduced density matrix that was seen in the DFT method (see equation 3.2.12), also called first-order reduced density operator:

$$\rho_1(\vec{x}_1';\vec{x}_1) = \hat{O} \Rightarrow \hat{O}\Theta_k = p_k\Theta_k \qquad (3.6.1)$$

Where the eigenvalue p_k represents the population i.e. the occupancy of the eigenfunction Θ_k. From the expression of the first-order reduced density matrix it can be seen that the wavefunction Ψ is the only variable that participates in the definition of the NOs, and therefore natural orbitals are like the eigenfunctions of the eigenfunctions of the system. That is why they are called Ψ own eigenorbitals or natural orbitals, and they are seen as the orbitals chosen by the wavefunction as being optimal for its own description of the electron density and other single-electron properties. Since this in an Hermitian eigenvalue problem, the NOs form a complete orthonormal set.

The NOs can be characterized as maximum occupancy orbitals, and they can be calculated by a variational maximization of the occupancy of each orbital, starting with a trial orbital ϕ . The electronic occupancy of the trial orbital, p_ϕ, is evaluated as the expectation value of the density operator:

$$p_\phi = \left\langle \phi^* \left| \hat{O} \right| \phi \right\rangle \tag{3.6.2}$$

And the variational equations are:

$$p_{\Theta_1} = \max \left\langle \phi^* \left| \hat{O} \right| \phi \right\rangle \tag{3.6.3}$$

$$p_{\Theta_2} = \max \left\langle \phi'^* \left| \hat{O} \right| \phi' \right\rangle \tag{3.6.4}$$

$$p_{\Theta_3} = \max \left\langle \phi''^* \left| \hat{O} \right| \phi'' \right\rangle \tag{3.6.5}$$

And so on. Each of the equations follows a variational procedure, starting by the trial orbital, obtaining the value of the population, finding another set of orbitals by equation (3.6.1) and recalculating the population until convergence. Each of the equations leads to optimal populations and orbitals. The populations, according to Pauli exclusion principle, fulfill $0 \le p_\phi \le 2$.

The wavefunction of a system is commonly described with basis orbitals that form a basis set, and it is important to know that, in spite of this, the natural orbitals are in principle independent of the particular basis orbitals chosen.

Natural orbitals are intrinsic and unique to the wavefunction of the system, while the basis orbitals are general fitting functions numerically convenient.

Natural Bond Orbitals (NBO) are localized natural orbitals whose N/2 leading members give the most accurate Lewis-like description of the total N-electron density. The program search all possibilities of drawing the bonds and lone pairs of the system to reproduce the variationally optimal bonding pattern which places the electron density precisely in the leading N/2 Lewis type NBOs. These Lewis-type NBOs are the ones that determine the Natural Lewis Structure (NLS) representation of the wavefunction, and the rest of the NBOs, the non-Lewis type, complete the basis and account for residual delocalization effects. Lewis is at the core of valence bond theory, and in this way NBOs provide a valence bond-like description of the wavefunction, linking it to classical Lewis structure concepts.

The NBOs have a unique association to the wavefunction of the system, and are practically insensitive to the variation of the basis set and method. Besides, its occupancies are generally non-degenerate, and its variations indicate a variation on the idealized Lewis structure, which may then indicate that for a more appropriate description of the system additional resonance delocalization corrections are needed. In

general, however, each NBO is uniquely determined by its local properties as eigenorbital.

NBOs are composed of Natural Hybrid Orbitals (NHO) h_A, and each of them is an optimized linear combination of Natural Atomic Orbitals (NAO) in a given center:

$$h_A = \sum_k a_k \Theta_k \tag{3.6.6}$$

Natural Atomic Orbitals are localized 1-center orbitals and are defined as the effective natural orbitals of a certain atom in the molecular environment. They differ from isolated atom orbitals (and standard basis orbitals) in two important features.

The first one is that they are optimized to the effective atomic charge, and adapts to the molecular environment contracted if the atom is more cationic of diffusing if the atom is more anionic, in what is called breathing. This effect commonly requires several basis functions of variable range (DZ, TZ…) in other basis sets, as it has seen in section 3.1.

The second one is that NAOs also adapt their oscillatory features and kinetic energy as neighboring NAOs overlap, preserving the nodal behavior with respect to both its inner core and the filled orbitals of other atoms, fulfilling thus the interatomic orthogonality required by the Pauli exclusion principle. This effect is commonly ignored in standard basis orbitals.

The NHOs form a complete orthonormal basis set that spans the full basis space, just as NAOs do.

Core NBOs are commonly of nearly pure NAO character, and are labeled as CR in NBO outputs.

A 1-center lone pair n_A of atom A that does not participate in any bond is labeled LP and is composed of a single normalized NHO:

$$n_A = h_A \tag{3.6.7}$$

A two center bond between atoms A and B is labeled BD and is a normalized linear combination of two normalized NHOs:

$$\Omega_{AB} = a_A h_A + a_B h_B \tag{3.6.8}$$

Where a_A, a_B are polarization coefficients that fulfill $a_A{}^2 + a_B{}^2 = 1$. These coefficients are a measure of the covalent $(a_A = a_B)$ and ionic $(a_A >> a_B)$ character of the bond. The problem is that it is not possible to distinguish a highly polar bond from a 1-center NBO $(a_A = 1; a_B = 0)$. In an attempt to avoid this error as much as possible, a value of 95% is set in the NBO program for the amount of density that has to be in a single center A with respect to B, as a minimum, for the program to identify a highly polarized

bond as a lone-pair. Two center bonds are often classified as sigma (σ_A) or pi (π_A) according to the local diatomic symmetry, but it is important to remark that the NBO procedure has no constraints regarding the shape of the orbitals.

Each of these two center bonds must have its orthogonal antibonding NBO, labeled as BD*:

$$\Omega^*_{AB} = a_B h_A - a_A h_B \tag{3.6.9}$$

These orbitals are of non-Lewis type and don't participate in the ground-state natural Lewis structure description, but as we can see in the equation, they are derived from the same unfilled valence hybrids orbitals that give rise to the bonding NBOs, and therefore they represent the unused valence shell capacity of atoms A and B. These orbitals are usually the most important non-Lewis acceptor orbitals due to its participation in intermolecular donor-acceptor processes. To know the shapes and energies of the available antibonding NBOs is usually very important in understanding species which present delocalization or non-covalent interactions that result in structures different to the idealized Lewis strcutre.

Finally, a set of Rydberg-type 1-center NBOs, labeled RY, are used to complete the span of the NBO basis. These orbitals are commonly ignored due to its usually negligible occupancy.

There are more NBO types, especially in excited states, but the ones reviewed are the most common ones.

Natural orbitals are important because they concentrate in one-electron functions the multiconfigurational character of the wavefunction, including electron correlation. In fact, this inclusion of the electron correlation is what causes the populations to not being integers anymore: some virtual orbitals participate in the wavefunction, obtaining some occupation, and some occupied orbitals participate in excitations to virtual orbitals, losing some occupation. Furthermore, the one-electron functions are actually orbitals, and as such they result to be qualitatively easier to understand.

4. RESULTS AND DISCUSSION

4.1. COMPLEXES BETWEEN BeX_2 (X = H, F, CL) AND ACETYLENE.

As said in the methodology, several calculations with the DFT method were carried out in order to establish which of the two geometries is preferred by each pair of molecules when interacting together in the complex.

The calculations with acetylene were made first, and 3 different functionals were used, namely B3LYP, M06 and M06-2X, all with the same 6-311+G(d,p) basis set.
For the three functionals the first of the structures of Figure 2 was preferred by all complexes:

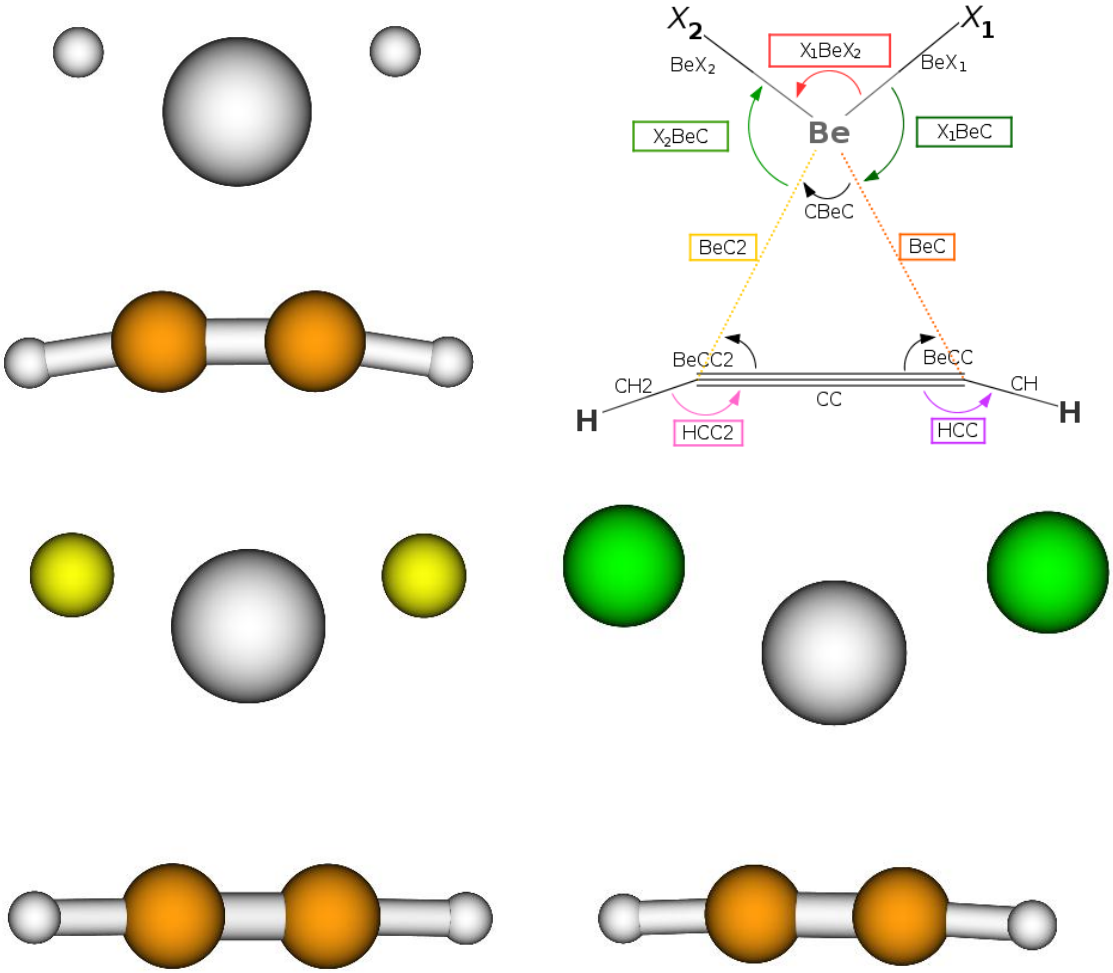

Figure 4. MOLDEN visualization of the optimized structures at the B3LYP/6-311+G(d,p) level for the complexes between acetylene and BeH_2 (white), BeF_2 (yellow) and $BeCl_2$ (green).

The optimizations with the other geometry either didn't converge or converged with an imaginary frequency that, as a matter of fact, corresponded to the one in which the complex moved towards a more planar structure.

At the same levels of theory, the corresponding calculations for each isolated molecule were carried out in order to provide the dissociation energy. Of course, in all of them an additional calculation of frequencies was carried out to obtain the zero-point vibrational energies that contribute to the total energy.
The results for the energy of the three complexes are:

Complex	B3LYP/6-311+G(d,p)	M06/6-311+G(d,p)	M06-2X/6-311+G(d,p)
C_2H_2-BeH_2	26.8	27.2	39.8
C_2H_2-BeF_2	22.0	34.2	43.5
C_2H_2-$BeCl_2$	7.8	21.6	31.6

Table 1. Dissociation energies (D_0 or ΔH_{int}, kJ mol^{-1}) of DFT methods.

The rest of the energy values used to obtain these dissociation energies, including the values of the energy of the isolated molecules, along with the frequencies and the rest of the spectroscopic data that these calculations provide can be found in the Appendix section (I-III, VII-X).

The energy for M06-2X/6-311+G(d,p) calculations is considerably higher than for the other two functionals. This could mean that the interactions are too weak for general DFT methods to describe them correctly, and since M06-2X includes more HF exchange energy it describes them more precisely, or could mean just the opposite. The same applies when comparing M06 with B3LYP results. Due to the nature of DFT methods, as seen in the methodology, it isn't easy to know which the most reliable results are without comparing them with the values given by either more precise methods or experimental data.
However, the next step of the methodology will allow us to know, for, once we know what the preferential geometry is, optimization calculations with more precise methods are used on it. In this case, MP2/6-311+G(d,p) and CCSD/6-311+G(d,p) optimization calculations were carried out. If we add the results of these methods to those of Table 1:

Complex	B3LYP	M06	M06-2X	MP2	CCSD
C_2H_2-BeH_2	26.8	27.2	39.8	24.7	19.5
C_2H_2-BeF_2	22.0	34.2	43.5	29.0	28.4
C_2H_2-$BeCl_2$	7.8	21.6	31.6	20.9	14.5

Table 2. Dissociation energies (D_0 or ΔH_{int}, kJ mol^{-1}) of DFT methods (with functionals B3LYP, M06 and M06-2X), MP2 and CCSD methods, all of them with the 6-311+G(d,p) basis.

As with the DFT calculations, the rest of the energy values of MP2 and CCSD calculations used to obtain these dissociation energies, including the values of the energy of the isolated molecules, along with the frequencies and the remaining spectroscopic data can be found in the Appendix section (I-III, VII-X).

Comparing with the DFT methods, we can now see that the M06-2X functional provides a very different result. Furthermore, M06-2X gives a much higher result than the other DFT methods, while M06 method was already overestimating the results, according to the lower values obtained at the CCSD level of theory. The M06-2X method practically doubles the CCSD results. Consequently, the M06-2X functional was discarded for the calculations with ethylene.

It is worth noting, though, that both M06 and M06-2X qualitatively reproduce the series behavior, in the sense that the energy increases from the complex with X = H to the complex with X = F and then decreases to the complex with X = Cl. B3LYP, on the contrary, doesn't.

However, both trends are different to what was expected according to bibliography, for Yañez, M., et al., recently studied these interactions between the same beryllium molecules and different bases and found that the dissociation energy, concerning the beryllium derivatives, followed the trend: $F_2Be > Cl_2Be > H_2Be$.[1]

The different relaxation of the isolated molecules in each complex has a strong influence on this dissociation energy, and therefore it might be the cause to these discrepancies. In order to make further and proper method comparisons, the vertical dissociation energy must be calculated.

Besides, in order to give the most accurate values of the energy for the complexes and at the same time to compare the methods, MP2 and CCSD(T) single-point calculations were carried out with the aug-cc-pVTZ basis on the MP2/6-311+G(d,p) and CCSD/6-311+G(d,p) optimized geometries, respectively.

The vertical dissociation energy was calculated at all the levels of theory with 6-311+G(d,p) basis and also at the MP2/aug-cc-pVTZ and CCSD(T)/aug-cc-pVTZ levels of theory. The corresponding calculations for the isolated molecules in both geometries were carried out, and can be found in the Appendix section (XII-XXI).

As it was indicated in the section 3.3, MP2 can give rise to wrong results when dealing with an equilibrium state that is close in energy to another. As it will be discussed later on, with the results from AIM theory, we also find mathematical instabilities which may point to this idea of an energetically nearby different unstable geometry. Also, this type of issue with MP2 was favored when using large basis sets[43]. Therefore, this is likely the reason why for the calculation of the C_2H_2-$BeCl_2$ complex at the MP2/aug-cc-pVTZ

the result provides an unstable structure with a negative dissociation energy, while MP2 with a smaller basis showed a perfectly stable geometry. The dissociation energy and the vertical dissociation energy results for each complex and method are:

Complex	B3LYP	M06	MP2	CCSD	MP2*	CCSD(T)*
C_2H_2-BeH_2	26.8	27.2	24.7	19.5	28.5	29.5
C_2H_2-BeF_2	22.0	34.2	29.0	28.4	30.2	33.0[b]
C_2H_2-$BeCl_2$	7.8	21.6	20.9	14.5	-[a]	27.1[b]

Complex	B3LYP	M06	MP2	CCSD	MP2*	CCSD(T)*
C_2H_2-BeH_2	61.3	57.6	47.9	41.8	51.5	49.9
C_2H_2-BeF_2	41.7	52.3	48.8	48.8	48.7	50.0[b]
C_2H_2-$BeCl_2$	48.3	56.5	58.8	52.6	-[a]	59.7[b]

Table 3. Dissociation energies (upper table, D_0 or ΔH_{int}, kJ mol^{-1}) and vertical dissociation energies (lower table, E_{int} or ΔH_{ver}, kJ mol^{-1}) of DFT methods (with functionals B3LYP and M06), MP2 and CCSD methods with the 6-311+G(d,p) basis, and MP2 and CCSD(T) methods with the aug-cc-pVTZ basis. (*)aug-cc-pVTZ basis set used. ([a])the structure was not stable. ([b])due to lack of time this data was calculated with the ZPVE from CCSD/6-311+G(d,p).

What is immediately seen is that the values for the vertical dissociation energy or interaction energy are more than twice the value of the hydrogen bond in water molecules, which is of about 20 kJ mol^{-1} [47]. Therefore, these are significantly strong non-covalent interactions.

In addition, another thing that is clear is that when we take into account the energy of relaxation of the subunits of the complex, i.e. when we consider the interaction energy, the general trend observed before for the dissociation energy is not maintained. In fact, if we take a look at the relaxation energies:

Complex	B3LYP	M06	MP2	CCSD	MP2*	CCSD(T)*
C_2H_2-BeH_2	34.5	30.3	23.3	22.3	22.9	20.4
C_2H_2-BeF_2	19.7	18.1	19.9	20.4	18.5	17.0
C_2H_2-$BeCl_2$	40.5	34.9	38.0	38.1	-	32.3

Table 4. Relaxation energies (ΔH_{relax}, kJ mol^{-1}) for all methods with the 6-311+g(d,p) basis. (*)aug-cc-pVTZ basis set used.

The values vary, but the general trend is that this relaxation energy is much lower for X = F than for X = Cl, while X = H gives higher values than the former and lower than the latter. Due to this, the vertical dissociation energy for X = Cl increases dramatically, and though its complex gave the lowest dissociation energy of the three, in turns out to give

the highest vertical dissociation energy.Besides, the complex with BeH_2, which had lower dissociation energy than the complex of BeF_2 for all methods but B3LYP, also turns out to give higher vertical dissociation energy than the complex with fluoride.

These values of the relaxation energies mean that the subunits of the complex with $BeCl_2$ are the more unstable ones when they keep the geometry they have within the complex, and this likely indicates that they are the most deformed and therefore the beryllium bond between them is the strongest, for much energy was needed to compensate this effect and make the complex stable. Following the same reasoning, the complex with H should be the second more bent or the second in the strength of its beryllium bond, and the complex with F should be the last one in both terms.

If we now see the values of distances and angles of the optimized geometries for each complex and we compare them with the ones of the isolated molecules for each method:

Property	B3LYP	M06	MP2	CCSD
HBeH	137.787	138.723	141.059	142.090
HBeC	92.971	92.674	91.739	92.014
BeC	1.954	1.967	2.070	2.091
HCC	170.930	172.722	174.988	175.406
BeH	1.347	1.347	1.347	1.349
CC	1.216	1.213	1.227	1.219
CBeC	36.272	35.929	34.462	33.883
BeCC	71.864	72.036	72.769	73.059
CH	1.065	1.066	1.066	1.068

Table 5. Distances and angles for the optimized geometries of the complex BeH_2-C_2H_2 for each method, all of them with the 6-311+G(d,p) basis.

Property	B3LYP	M06	MP2	CCSD
FBeF	148.200	148.197	148.194	148.009
FBeC	90.722	90.600	90.488	90.658
BeC	2.298	2.277	2.295	2.293
HCC	179.314	179.806	179.554	179.499
BeF	1.415	1.408	1.418	1.414
CC	1.203	1.202	1.220	1.213
CBeC	30.355	30.602	30.829	30.674
BeCC	74.822	74.699	74.585	74.663
CH	1.065	1.067	1.067	1.068

Table 6. Distances and angles for the optimized geometries of the complex BeF_2-C_2H_2 for each method, all of them with the 6-311+G(d,p) basis.

Property	B3LYP	M06	MP2	CCSD
ClBeCl	136.764	138.241	137.987	138.075
ClBeC	95.965	95.323	95.191	95.391
BeC	2.234	2.244	2.241	2.262
HCC	177.152	177.811	176.866	177.035
BeCl	1.858	1.851	1.844	1.847
CC	1.205	1.204	1.221	1.214
CBeC	31.307	31.112	31.632	31.143
BeCC	74.347	74.444	74.184	74.429
CH	1.065	1.067	1.067	1.068

Table 7. Distances and angles for the optimized geometries of the complex $BeCl_2$-C_2H_2 for each method, all of them with the 6-311+G(d,p) basis.

Bond	B3LYP	M06	MP2	CCSD
CH	1.063	1.064	1.065	1.066
CC	1.199	1.197	1.216	1.210
BeH	1.327	1.327	1.329	1.330
BeF	1.387	1.380	1.293	1.387
BeCl	1.799	1.797	1.792	1.794

Table 8. Bond distances for acetylene and BeX_2 molecules in their isolated equilibrium geometries optimized by the indicated methods and the 6-311+G(d,p) basis set.

At any level of theory it can be seen that, as expected, there is a bending of both BeX_2 and acetylene molecules, as a consequence to the adaptation of the orbitals to the new electronic distribution due to the new beryllium bond.

In fact, since B3LYP and M06 overestimated the relaxation energy of the complex with BeH_2, in the optimized geometries for that complex the BeH_2 molecule is almost as bent as $BeCl_2$ in $BeCl_2$ complexes, while for MP2 and CCSD the angle ClBeCl of the $BeCl_2$ complexes is clearly the lowest and therefore its $BeCl_2$ molecule is the most bent. This result follows the relaxation energy trend: C_2H_2-$BeCl_2$ > C_2H_2-BeH_2 > C_2H_2-BeF_2.

The angle HCC of acetylene may not change so much because it is measured as the angle between CC and CH bonds, and since the two carbons share the interaction, with the displaced charge more probably being between them, the hydrogen atoms may not feel the interaction as much as the atoms directly bonded to the beryllium atom. It is worth noting that the HCC angle changes much more in the BeH_2 complex when changing the method, from the almost 171º and 173º of B3LYP and M06 to the 175º of MP2 and CCSD, while the same angle for the other two complexes only varies in one degree at the most. The fact that the angle is significantly lower at B3LYP and M06

levels than at the rest is probably one of the causes for the relaxation energy to increase. However, even small, a lengthening of the CC bond can be observed, what constitutes an additional indication of the small hybridization of the carbons, which share now some electronic density in a new direction and therefore lose a bit of their strict sp hybridization.

Besides, in these values the second effect of beryllium bonding can also be seen: as a consequence of the charge transfer to the antibonding orbitals σ_{BeX*} of Be-X bonds, these bonds weaken and they become longer. This effect is very clear in the case of the Be-Cl bond for which the change is of about 0.05 Å, but it is also still clear for Be-F and Be-H bonds, for which the change is of about 0.03 Å and 0.02 Å, respectively. This means that more electronic density is going into the antibonding orbital of Be-Cl than on the one of Be-F or Be-H, contributing to reinforce the strength of the beryllium bond for the C_2H_2- $BeCl_2$ complex. This result agrees with the vertical dissociation energy trend: C_2H_4-$BeCl_2$ > C_2H_4-BeF_2 ~ C_2H_4-BeH_2.

In order to study in depth the bonding between the interacting molecules, an AIM study was performed for the optimized geometries of all methods. The qualitative results were practically the same for all methods when X = Cl, but when X = H and X = F we obtained a different result depending on the methods.

For X = H we obtained:

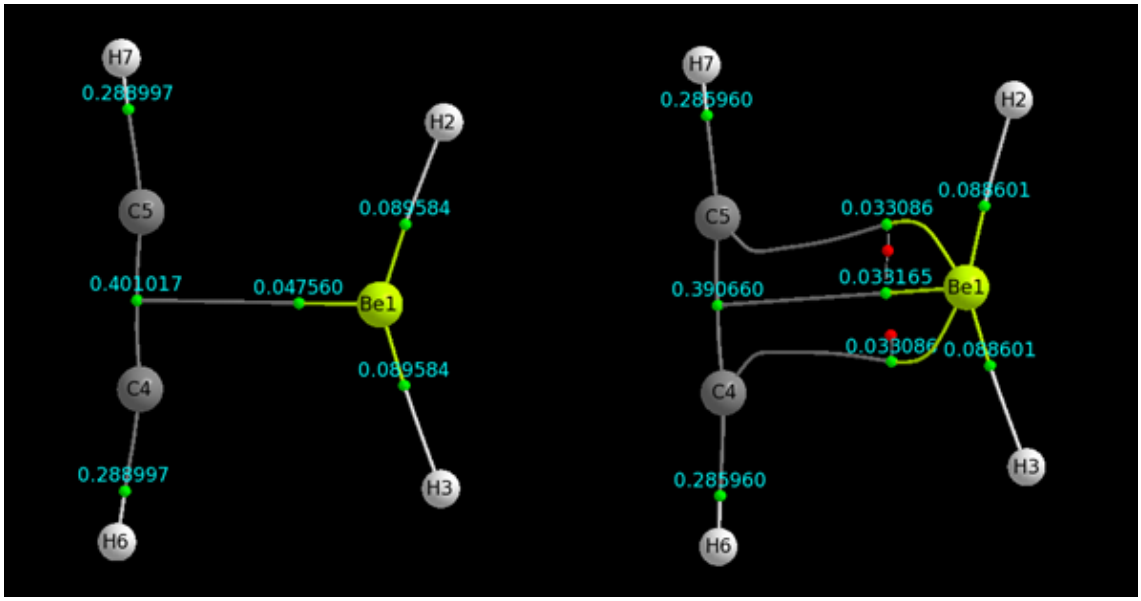

Figure 5. Density plots for the complex BeH_2-C_2H_2 at B3LYP/6-311+G(d,p) (left) and at CCSD/6-311+G(d,p) (right) from aimstudio.

The green points are what are called bond critical points, which mathematically states the existence of a bond between the linked atoms, and the line they fall into are the so-called bond paths, which have not to be misjudged as bonds.

With X = H, both B3LYP and M06 give the same qualitative result, as so do MP2 and CCSD methods, but they are different between them, as shown in Figure 5.

The positive result is that, in fact, a critical point is found for all the methods between the molecules, granting some kind of bonding between them. However, the plots are not as conventional as expected.

Firstly, it is important to notice that in both cases the bond path ends into the critical point for the CC bond, instead of into an atom. This constitutes an example of what has been called the conflict catastrophe. It is caused by the competition of the two carbons for the line of maximum charge density which links the beryllium. It is mathematically unstable, for the gradient of the density defines one and only one direction for each point r, and therefore there should be no intersection of both paths. This effect usually occurs when the structure under study is an unstable one in the limits of a change between stable structures, but, as it was briefly explained in the theory section, it can also happen for weak bonds in equilibrium structures[48] and therefore the QTAIM plots are to be considered carefully. In these cases, the two-dimensional manifold of CC acts as an attractor of the bond path of the beryllium, and in fact this kind of issue is now being studied regarding the possibility of having an 'atomic basin' with more than a single nucleus in an equilibrium geometry, which can therefore act together[49].

As to the difference between the plots, it seems to be another catastrophe issue, but of bifurcation. Mathematically, a bifurcation appears when a small change in the parameter values of a system -the gradient in our case- produces a sudden change in the qualitative behavior of its solutions –a topological change in our case-. More specifically, in this case we seem to have a supercritical pitchfork bifurcation, which is a local bifurcation that generally occurs in systems with symmetry, and consists in the separation of a point where the gradient is zero into three, where the one that follows the previous direction is unstable and the other two remain stable. Indeed these situations arise when the electron density is very flat and depending on the threshold value used to locate the bond critical points, the code sometimes finds three or only one. This is evident when looking at the values of the density in Figure 5. In the molecular graph at the right three critical points are located, but clearly they have practically the same electron density. In the molecular graph on the left, only one critical point is found because the differences in the electron densities are marginal.

If we take a look at the following table that collects all the AIM data for the complex at the CCSD/6-311+G(d,p) level:

BCP	$\rho(r)$	$-\nabla^2\rho(r)$	ε	λ_1	λ_2	λ_3
Be1 - C5	0.033086	+0.038472	2.223705	-0.034550	-0.010717	+0.083739
Be1 - H2	0.088601	+0.202039	0.085841	-0.181113	-0.166795	+0.549946
Be1 - C4	0.033086	+0.038472	2.223705	-0.034550	-0.010717	+0.083739
Be1 - H3	0.088601	+0.202039	0.085841	-0.181113	-0.166795	+0.549946
Be1 - C4	0.033165	+0.176881	13.749168	-0.050304	-0.003411	+0.230596
C4 - C5	0.390660	-1.115323	0.021235	-0.619322	-0.606444	+0.110442
C4 - H6	0.285960	-1.047795	0.002813	-0.803327	-0.801073	+0.556605
C5 - H7	0.285960	-1.047795	0.002813	-0.803327	-0.801073	+0.556605

Table 9. AIM data at the CCSD/6-311+G(d,p) level for the BeH_2-C_2H_2 complex.

The data for the rest of the methods can be found in the Appendix section (XXII).

By looking at the density and its second derivative, the Laplacian, we can see that the character of the bonds is well described for the bonds within the acetylene, which shows the big density values and negative Laplacian values characteristic of covalent bonds, while for the Be-H bonds the character appears as slightly ionic, for they have a small density and, though small, they also have a positive value for the Laplacian. This positive value of the Laplacian is characteristic of Lewis acids, as we expected the BeH_2 to be in the complex[3]. Therefore we have more like a $Be^{+\delta}$-$H^{-\delta}$ bond.

Similarly, for the beryllium bond (Be1-C5) we obtain an even smaller density, although not so small recalling that it constitutes a non-covalent interaction, and a more positive value for the Laplacian. This agrees with what has been said about the beryllium bonds having an important ionic character, such as hydrogen bonds do.

Regarding the ellipticity, the high value it has for the beryllium bond shows the strong preferential accumulation in the plane of λ_2, which agrees with the fact that the bonding is made through an orbital p of beryllium. However, such a high value of the ellipticity also indicates the presence of an approaching instability and a change in structure, which could also explain the bifurcation catastrophe mentioned before.

If we take a look at the plot when X=F:

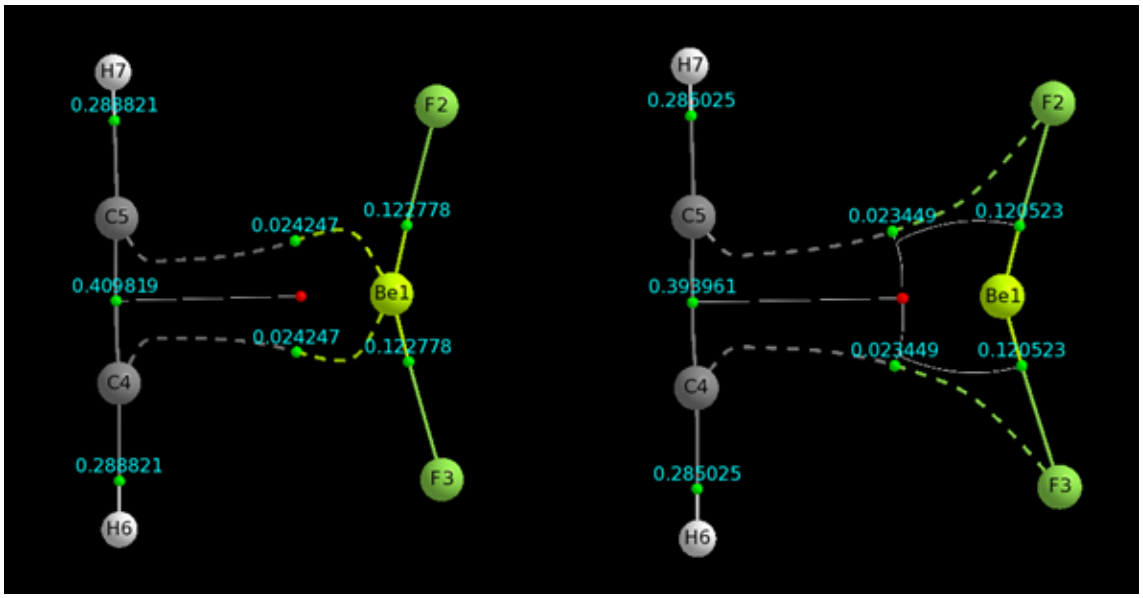

Figure 6. Density plots for the complex BeF_2-C_2H_2 at B3LYP/6-311+G(d,p) (left) and at CCSD/6-311+G(d,p) (right) from aimstudio.

In this case only the B3LYP/6-311+G(d,p) method gave a different result, while the rest gave qualitatively the same topological structure.

The first thing to notice here is that the paths for the beryllium bond are also split and we have again the pitchfork bifurcation catastrophe –with the central unstable line not completely described-, although the overall plot is a bit more complicated to study, as it seems that we don't have the conflict catastrophe but for most of the methods the bond path links the carbon atoms with the fluoride atoms, instead of beryllium. This could be due to the flatness of the density in this region or could mean that the fluoride atoms -or BeF orbitals- significantly participate in the bond, trying to retain more electron density, which could be due to the electronegativity of its nature, or giving away charge due to the lone pairs of fluoride, which is a good π-donor. This would also explain why the BeF_2 molecule doesn't bend as much as expected: if the fluoride is participating in the bond in some way the distance towards it should shorten. Should this be the cause, we would have two opposed effects: the bending and lengthening of Be-F bonds from the beryllium bond alone and the unbending and shortening from the fluoride participation in the beryllium bond. Since the participation of fluoride is not as much as the one of beryllium, the BeF_2 molecule ends up bent and the Be-F lengthens, but not as much as was expected, and the general trend changes. We will discuss this possibility later when we check the results of the NBO calculations.

The second thing is that the bond path is drawn with a dashed line. The program has a default value of 0.025 for the density to consider that there is a bond and draw it in a continued line. It is clear then that there is less density between the molecules of this complex than in the previous one. If we look at the AIM data:

BCP	ρ(r)	$-\nabla^2\rho(r)$	ε	λ_1	λ_2	λ_3
Be1 - F2	0.120523	+1.118560	0.009020	-0.338810	-0.335781	+1.793151
Be1 - F3	0.120523	+1.118560	0.009020	-0.338810	-0.335781	+1.793151
F3 - C4	0.023449	+0.037247	1.066192	-0.020441	-0.009893	+0.067580
F2 - C5	0.023449	+0.037247	1.066192	-0.020441	-0.009893	+0.067580
C4 - C5	0.393961	-1.128493	0.022376	-0.621270	-0.607673	+0.100450
C4 - H6	0.285025	-1.042295	0.004915	-0.800797	-0.796881	+0.555383
C5 - H7	0.285025	-1.042295	0.004915	-0.800797	-0.796881	+0.555383

Table ¡Error! No hay texto con el estilo especificado en el documento.**10. AIM data at the CCSD/6-311+G(d,p) level for the BeF_2-C_2H_2 complex.**

The data for the rest of the methods can be found in the Appendix section (XXIII).

We can see that the character of the bonds is, as in the previous complex, correctly described for the bonds within the acetylene, and for the Be-F bonds we find a quite big positive value of the Laplacian and a small density having thus a stronger ionic character than Be-H bonds in the previous complex. This effect is probably produced for the much greater electronegativity of fluoride with respect to hydrogen. As to the beryllium bond, we obtain a very small density, in the edge of AIMAll limit, and a very small positive value for the Laplacian. Therefore, the beryllium bond still has a predominant ionic character.
Regarding the ellipticity, the beryllium bond still has a high value, which shows the same strong preferential accumulation in the plane of λ_2, and could also explain the bifurcation catastrophe mentioned before.

Finally, if we look at the plot when X=Cl:

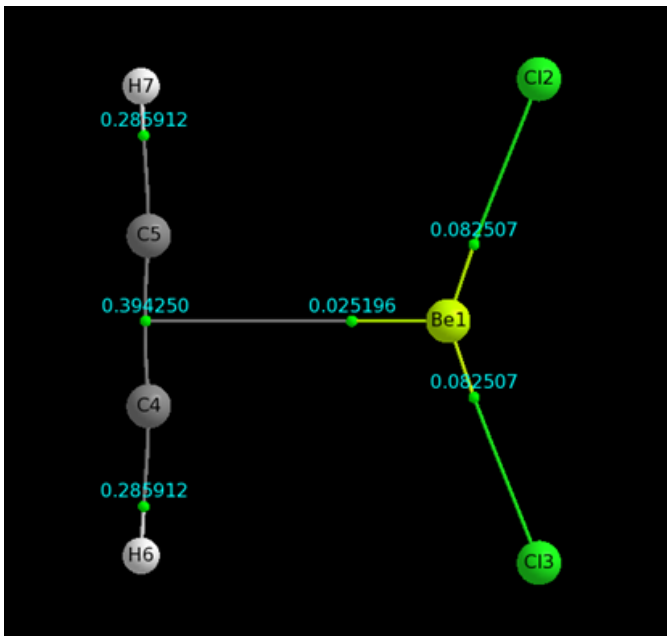

Figure 7. Density plot for the complex $BeCl_2$-C_2H_2 at the CCSD/6-311+G(d,p) level of theory from aimstudio.

In this case the result is qualitatively the same for all the methods.

The only strange thing here is that, as for the BeH_2 complex, the beryllium bond path ends in a bond critical point instead of on the carbon atoms, due to the conflict catastrophe. If we look at the AIM data:

BCP	ρ(r)	$-\nabla^2\rho(r)$	ε	λ_1	λ_2	λ_3
Be1 - Cl2	0.082507	+0.324241	0.020538	-0.144598	-0.141688	+0.610527
Be1 - Cl3	0.082507	+0.324241	0.020538	-0.144598	-0.141688	+0.610527
Be1 - C5	0.025196	+0.095569	8.439991	-0.028389	-0.003007	+0.126965
C4 - C5	0.394250	-1.139970	0.041338	-0.634903	-0.609699	+0.104631
C4 - H6	0.285912	-1.051170	0.005778	-0.807456	-0.802818	+0.559104
C5 - H7	0.285912	-1.051170	0.005778	-0.807456	-0.802818	+0.559104

Table 11. AIM data at the CCSD/6-311+G(d,p) level for the $BeCl_2$-C_2H_2 complex.

The data for the rest of the methods can be found in the Appendix section (XXIV).

We can see that the character of the bonds is, as in the previous complexes, correctly described for the bonds within the acetylene, and for the Be-Cl bonds we find a positive value of the Laplacian, greater than that of Be-H bonds but smaller than that of Be-F bonds, and a small density, even a bit smaller than that of Be-H bonds. Thus, Be-Cl bonds have more ionic character than the Be-H bonds but less than the Be-F bonds. This is just natural since the electronegativity of chloride is also greater than that of hydrogen but lower than that of fluoride.

As to the beryllium bond, we obtain a very small density, higher than the one of BeF_2 complex but still much lower than the BeH_2 one, and a very small positive value for the Laplacian, higher than the one of BeF_2 complex but still much lower than the BeH_2 one. Therefore, the beryllium bond still has a predominant ionic character, a bit more than the one of BeF_2 complex but still much lower than the BeH_2 one.

Regarding the ellipticity, the beryllium bond of the complex has the highest value of the three –and it is even bigger for the other methods-, which shows the same strong preferential accumulation of density in the plane of λ_2, but it seems that it is not enough to produce any bifurcation catastrophe, as it happens in other complexes, which had to have a larger ellipticity at the critical point.

All in all, what we have is that, regarding the beryllium bond under study, both the value of the density, that serves as an indication of the strength of the bond, and the positive value of the Laplacian, that serves as an indication of the ionic character of the bond due to the density being small, follow the trend: $BeH_2 > BeCl_2 > BeF_2$. This result disagrees with the values of the vertical dissociation energies, which follow the trend $BeCl_2 > BeF_2 \approx BeH_2$. Therefore, some other effect must be affecting these bonds.

The NBO analysis were firstly made with B3LYP and M06 methods, but given the results obtained for the energy and densities of these methods, an additional calculation at the CCSD level was carried out, in order to try to justify the trends observed all under the same approach.

From what has being explained, in the NBO analysis a beryllium bond is expected to present population in orbitals p of Be, labeled LP*(Be) and initially empty, due to the charge transfer from the triple CC bond that constitutes the main contribution to the beryllium bond. Also, some population should be found in the antibonding orbitals of the Be-X bond, labeled BD*(BeX), due to the charge transfer that comes also from the CC bond to these orbitals. As a consequence, the bonding orbitals of the CC bond, labeled BD(CC), should have less population. Accordingly, there hybridization of C and Be should also be seen in the different bonds as a consequence of the beryllium bonding. Finally, important contributions to the energy should be found corresponding to the charge transfer processes.
If we take a look at the following tables:

Complex	BD*(BeX)	BD (CC)	LP*(Be)
C_2H_2-BeH_2	0.003	1.989; 1.979; 1.868	0.149; 0.021
C_2H_2-BeF_2	0.011	1.990; 1.993; 1.918	0.136; 0.102
C_2H_2-$BeCl_2$	0.020	1.990; 1.985; 1.859	0.222; 0.174

Table 12. NBO populations obtained at the CCSD/6-311+G(d,p) level of theory.

Complex	BD(CC) → LP*(Be)	BD(CC) → BD*(Be-X)
C_2H_2-BeH_2	467.08	0.25
C_2H_2-BeF_2	222.32	2.93
C_2H_2-$BeCl_2$	416.38	8.04

Table 13. NBO second order perturbational correction energies at the CCSD/6-311+G(d,p) level of theory, in kJ/mol.

Complex	BD (CC)	BD (CH)	LP* (Be)	BD* (BeX)
C_2H_2-BeH_2	sp1.22; p100%; p94%	sp1.04	sp7.29(p87%); p97%	sp1.27
C_2H_2-BeF_2	sp1.00; p100%; p98%	sp1.06	sp7.86(p88%); p100%	sp1.26
C_2H_2-$BeCl_2$	sp1.11; p100%; p96%	sp1.04	sp6.72(p87%); p99%	sp1.31

Table 14. NBO hybridization of C and Be atoms in certain bonds, at the CCSD/6-311+G(d,p) level of theory.

As a matter of fact, it is indeed found everything just said: there is population in BD*(BeX) and LP*(Be), there is less population in the BD(CC), the C and Be atoms show different hybridization and there are contributions to the energy for the two main processes of the Beryllium bond.

On the one hand, the trend for the charge transfer BD(CC) → BD*(Be-X) is Cl > F > H. This agrees with the observed trend for the elongation of the Be-X bond, with the population of the BD*(BeX) orbital and, more importantly, with the interaction energy trend.

On the other hand, the trend observed for the charge transfer BD(CC) → LP*(Be) is H > Cl > F, that is the same trend that was followed by the density at the BCP of the beryllium bond.

In addition, it can be seen that Wiberg bond order (BO) follows the same trend too:

Complex	**Wiberg BO (BeC)[a]**	**Density ρ(r)**
C_2H_2-BeH_2	0,174	0,033
C_2H_2-BeF_2	0,086	0,023[b]
C_2H_2-$BeCl_2$	0,148	0,025

Table 15. Density at the BCP of the beryllium bond of each complex at the CCSD/6-311+G(d,p) level of theory and its corresponding Wiberg bond order. (a) For one carbon only, the other one has the same value. (b) The density is that of a bifurcation point, not exactly at the BCP.

Therefore, as we saw with AIM results, we find again that the trend of the density of the beryllium bond and the trend of the interaction energy are not the same. Since both indicate the strength of the beryllium bond, they should, and therefore there must be some effect that we are not considering.

Studying further the NBO analysis, additional contributions to the energy for other charge transfers which are not expected are found:

Complex	**BD(BeX) → BD*(CC)**	**LP(X) → BD*(CC)**
C_2H_2-BeH_2	35.55	-
C_2H_2-BeF_2	2.60	0.000; 6.531; 0.544
C_2H_2-$BeCl_2$	4.65	0.502; 6.113; 0.921

Table 16. Other important contributions to the energy from the NBO analysis at the CCSD/6-311+G(d,p) level of theory, in kJ/mol. The contributions are per bond/atom.

If there is such a great contribution from the BD(BeH) of the C_2H_2-BeH_2 complex to the antibonding orbital of the BD*(CC) that participates in the bond, the density at the BCP of the beryllium bond increases. Besides, since Wiberg BO depends on the square of the density[50], it is only natural that it increases even if the electronic density is accommodated in the antibonding orbitals of the bond, decreasing its strength.
In other words, the fact that a significant amount of electronic density is placed on an antibonding orbital would explain why, despite the fact that the C_2H_2-BeH_2 complex has more density at the BCP than the other complexes, its interaction energy turns out to be the lowest one.

If we look for the populations of these BD(BeX), BD*(CC) and LP(X) orbitals we find:

Complex	**BD(BeX)**	**BD*(CC)**	**LP(X)**
C_2H_2-BeH_2	1.967	0.016; 0.000; 0.057	-
C_2H_2-BeF_2	1.998	0.013; 0.001; 0.010	1.991; 1.960; 1.950
C_2H_2-$BeCl_2$	1.996	0.012; 0.002; 0.018	1.983; 1.940; 1.917

Table 17. Population of indicated orbitals from the NBO analysis at the CCSD/6-311+G(d,p) level of theory.

The population of the BD(BeH) of the complex where X = H clearly shows a loss that is also reflected in the increase of the BD*(CC) orbital. For X = F, Cl the populations do not show much of a difference because the contribution to the energy for this process was not as much. In any case, the observed trend for this sort of retrodonation is H > Cl > F, a trend that is also reflected in the small elongation of the CC bond of acetylene observed in Table 5.

Even though there is a significant LP(X) → BD*(CC) charge transfer, the influence of it over the populations of LP(X) are not easily determined because within the BeX_2 molecule these orbitals participate in the bonds, and charge transfers from the LP(X) orbitals to Be are also found that indeed follow the corresponding inverse trend, being the greatest the one of the third lone pair, then the second and lastly the first lone pair.

There are flaws to this reasoning, however, mainly in the elongation of the Be-H, which should be larger due to the loss of density of its bonding orbital. Besides, similar strange behaviors were found to happen in literature with similar systems[51], and it was found that the deformation undergone by the moieties were the cause. Further researches are needed, though, to confirm and understand this point.

4.2. COMPLEXES BETWEEN BeX_2 (X=H, F, Cl) AND ETHYLENE.

In this case the DFT functionals used in the calculations made in order to establish which of the two geometries is preferred were B3LYP and M06, both with the same 6-311+G(d,p) basis set.

For the two of them the complex BeH_2-C_2H_4 preferred the first of the structures of Figure 3 while the second was preferred by the other two complexes:

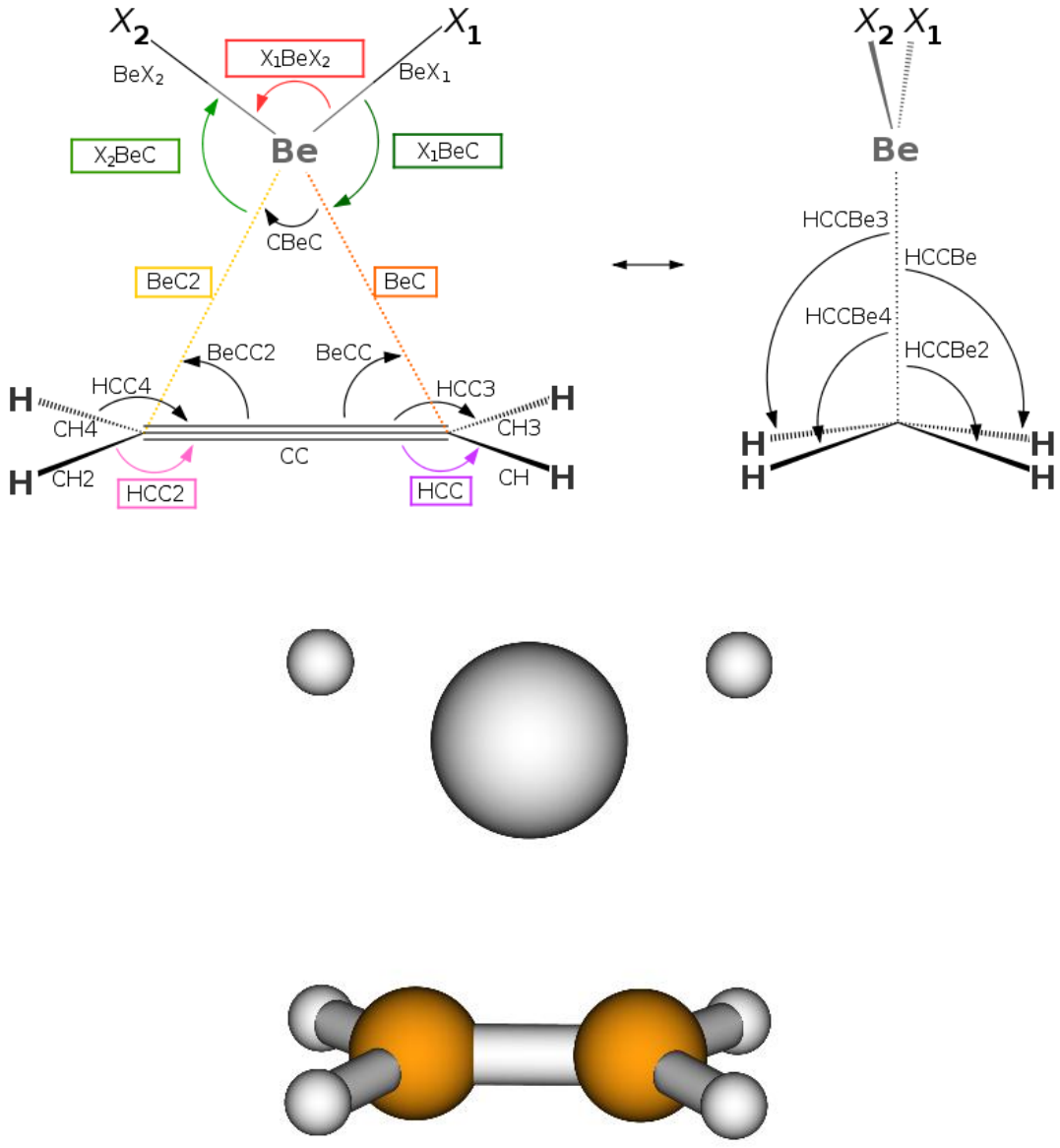

Figure 8. MOLDEN visualization of the optimized structure at the B3LYP/6-311+G(d,p) level for the complex between ethylene and BeH_2.

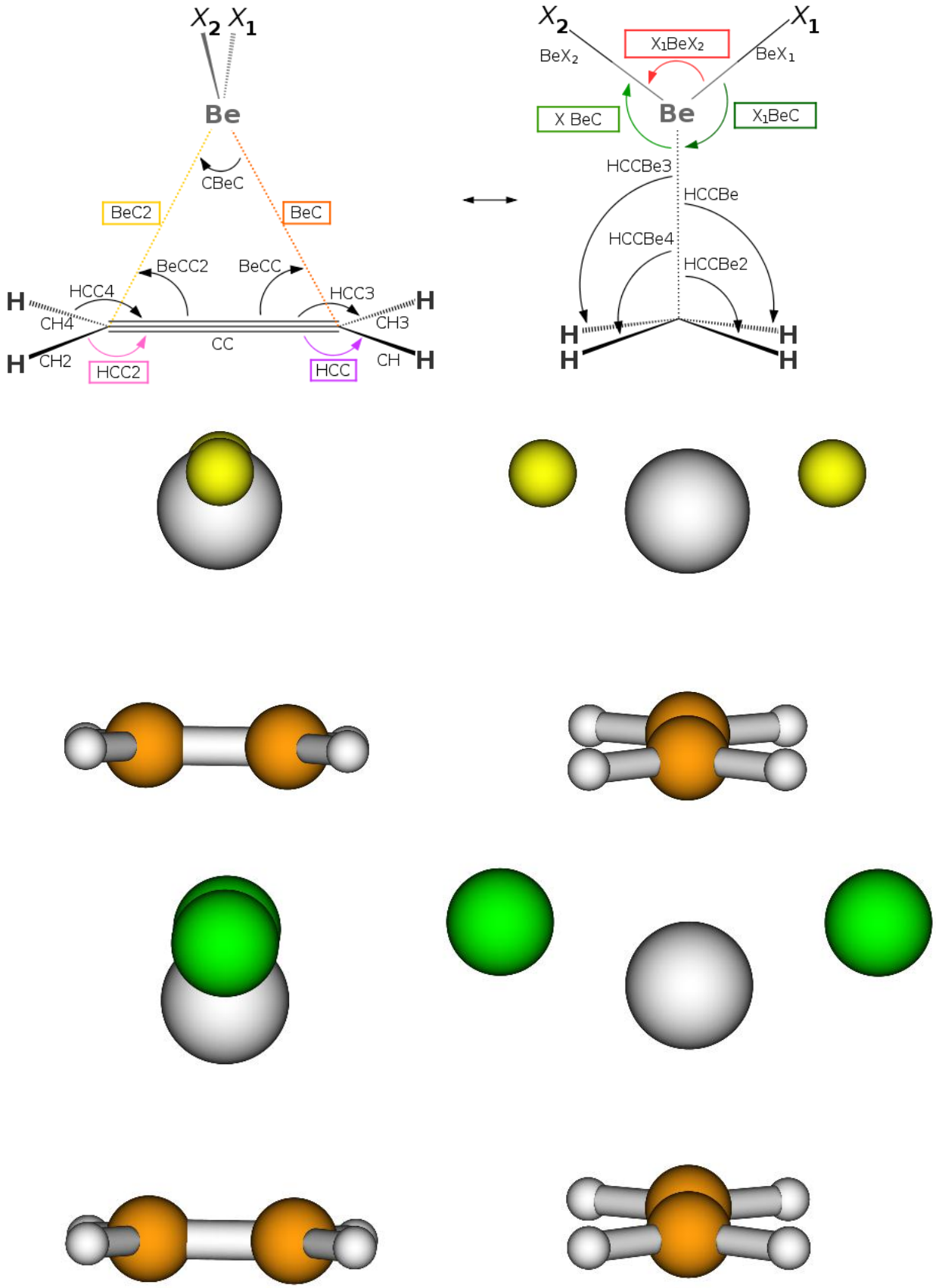

Figure 9. MOLDEN visualization of the optimized structures at the B3LYP/6-311+G(d,p) level for the complexes between ethylene and BeF_2 (yellow) or $BeCl_2$ (green).

The optimizations with the other geometries either didn't converge or converged with an imaginary frequency that, as happened for the acetylene complexes, corresponded to the one in which the complex moved towards a more planar structure.

At the same levels of theory, the corresponding calculations for each isolated molecule were carried out in order to provide the dissociation energy, as well as an additional calculation of frequencies to obtain the zero-point vibrational energies that contribute to the total energy.

The results for the energy of the three complexes are:

Complex	B3LYP/6-311+G(d,p)	M06/6-311+G(d,p)
C_2H_4-BeH_2	13.0	15.7
C_2H_4-BeF_2	18.0	30.3
C_2H_4-$BeCl_2$	7.7	23.4

Table 18. Dissociation energies (D_0 or ΔH_{int}, kJ mol^{-1}) of DFT methods.

The rest of the energy values used to obtain these dissociation energies, including the values of the energy of the isolated molecules, along with the frequencies and the rest of the spectroscopic data that these calculations provide can be found in the Appendix section (IV-VI, VII-IX, XI).

The energy for the C_2H_4-BeH_2 complex is similar for both methods but when dealing with the C_2H_4-BeF_2 and C_2H_4-$BeCl_2$ complexes the energy varies a lot from one functional to the other. With the preferential geometry, additional optimization calculations at MP2/6-311+G(d,p) and CCSD/6-311+G(d,p) levels were carried out. If we add the results of these methods to those of Table 1:

Complex	B3LYP	M06	MP2	CCSD
C_2H_4-BeH_2	13.0	15.7	15.5	9.2
C_2H_4-BeF_2	18.0	30.3	28.4	26.4
C_2H_4-$BeCl_2$	7.7	23.4	27.1	19.0

Table 19. Dissociation energies (D_0 or ΔH_{int}, kJ mol^{-1}) of DFT methods (with functionals B3LYP, M06 and M06-2X), MP2 and CCSD methods, all of them with the 6-311+G(d,p) basis.

As with the DFT calculations, the rest of the energy values of MP2 and CCSD calculations used to obtain these dissociation energies, including the values of the energy of the isolated molecules, along with the frequencies and the remaining spectroscopic data can be found in the Appendix section (IV-VI, VII-IX, XI).

All the methods qualitatively follows the same trend, in the sense that the energy increases from the complex with X = H to the complex with X = F and then decreases to the complex with X = Cl. B3LYP provides very low results of the complex where X = F and X = Cl, to a point that its trend changes, and for this method the trend is X = F > X= H > X= Cl. With the exception of B3LYP, the methods follow the expected trend F_2Be > Cl_2Be > H_2Be.[1] It is important to remark that the complex with X = H has a different geometry from the other two and therefore it may not follow any trend.

Since the different relaxation of the isolated molecules in each complex has a strong influence on this dissociation energy, the vertical dissociation energy must be calculated in order to allow a proper comparison. Besides, as we did for the series of complexes with the acetylene, MP2 and CCSD(T) single-point calculations were carried out with the aug-cc-pVTZ basis on the MP2/6-311+G(d,p) and CCSD/6-311+G(d,p) optimized geometries, respectively, in order to give the most accurate values of the energy for the complexes and at the same time to compare the methods.

The vertical dissociation energy was calculated at all the levels of theory with 6-311+G(d,p) basis and also at the MP2/aug-cc-pVTZ and CCSD(T)/aug-cc-pVTZ levels of theory. The corresponding calculations for the isolated molecules in both geometries were carried out, and can be found in the Appendix section (IV-VI, VII-IX, XI, XV-XVII).

The dissociation energy and the vertical dissociation energy results for each complex and method are:

Complex	B3LYP	M06	MP2	CCSD	MP2*	CCSD(T)*
C_2H_4-BeH_2	13.0	15.7	15.5	9.2	20.0	18.4
C_2H_4-BeF_2	18.0	30.3	28.4	26.4	28.7	29.0[a]
C_2H_4-$BeCl_2$	7.7	23.4	27.1	19.0	33.8	27.1[a]

Complex	B3LYP	M06	MP2	CCSD	MP2*	CCSD(T)*
C_2H_4-BeH_2	47.4	44.7	41.2	33.5	45.6	42.1
C_2H_4-BeF_2	38.9	49.0	50.8	49.3	50.1	49.6[a]
C_2H_4-$BeCl_2$	40.0	51.7	59.1	51.6	62.7	56.2[a]

Table 20. Dissociation energies (upper table, D_0 or ΔH_{int}, kJ mol^{-1}) and vertical dissociation energies (lower table, E_{int} or ΔH_{ver}, kJ mol^{-1}) of DFT methods (with functionals B3LYP, M06 and M06-2X), MP2 and CCSD methods with the 6-311+G(d,p) basis, and MP2 and CCSD(T) methods with the aug-cc-pVTZ basis. (*)aug-cc-pVTZ basis set used. ([a])due to lack of time this data was calculated with the ZPVE from CCSD/6-311+G(d,p).

As was pointed out for acetylene, in this case it is also clear that the values for the vertical dissociation energy or interaction energy are also more than twice the value of the hydrogen bond in water molecules, which, as said before, is of about 20 kJ mol^{-1} [47]. Therefore, these are significantly strong non-covalent interactions too.

Again, although the dissociation energy at the MP2/aug-cc-pVTZ level already gave a different trend, it is clear that the general trend observed for the dissociation energy does not hold when the relaxation energies of the subunits of the complex are taken into account, as the interaction energy trend regarding the beryllium molecule of the complex is $BeCl_2 > BeF_2 > BeH_2$. If we take a look at the relaxation energies:

Complex	B3LYP	M06	MP2	CCSD	MP2*	CCSD(T)*
C_2H_4-BeH_2	34.4	29.0	25.7	24.3	25.6	23.7
C_2H_4-BeF_2	20.9	18.7	22.4	22.9	21.3	20.7
C_2H_4-$BeCl_2$	32.3	28.2	32.0	32.7	28.9	29.1

Table 21. Relaxation energies (ΔH_{relax}, kJ mol^{-1}) for all methods with the 6-311+g(d,p) basis. (*)aug-cc-pVTZ basis set used.

With the exception of DFT methods, which give a similar value for the complexes where X = H and X = Cl, being slightly higher for the complex with X = H, and similarly to what was found above for acetylene complexes, the relaxation energy has a much lower value for X = F than for X = Cl, while X = H gives higher values than the former and lower than the latter, which results in the general trend: C_2H_4-$BeCl_2 \geq C_2H_4$-$BeH_2 > C_2H_4$-BeF_2. Due to this, the vertical dissociation energy for X = Cl increases and though its complex gave the lowest dissociation energy of the three, it turns out to give the highest vertical dissociation energy. Besides, as it happened in the previous complex series with acetylene, the relaxation energy of the C_2H_4-BeH_2 complex is overestimated by the B3LYP and M06 functionals. The overestimation is not as much as in that case, though, and the M06 values almost follow the general trend. However, this overestimation causes the B3LYP method to give a much higher value for the C_2H_4-BeH_2 complex, to the point that it no longer follows the trend for the interaction energy stated by the rest of the methods, which is: C_2H_4-$BeCl_2 > C_2H_4$-$BeF_2 > C_2H_4$-BeH_2.
This result is the same that we obtained for the energies with the acetylene complexes, although the difference between F and H is larger in this case. As explained before, these values of the relaxation energies means that the subunits of the complex with Cl are the more unstable ones when they keep the geometry they have within the complex, which may mean the $BeCl_2$ molecule the most bent and its beryllium bond is the strongest. Following the same reasoning, the complex with F should be the second more bent or the second in the strength of its beryllium bond, and the complex with H should be the last one in both terms.

If we now see the values of distances and angles of the optimized geometries for each complex and compare them with the ones of the isolated molecules for each method:

Property	B3LYP	M06	MP2	CCSD
HBeH	138,309	140,670	142,787	143,180
HBeC	91,869	91,008	90,358	90,486
BeC	2,077	2,100	2,163	2,197
HCC	121,940	122,048	121,610	121,746
BeH	1,347	1,347	1,347	1,348
CC	1,351	1,344	1,355	1,352
HCH	115.891	115.759	116.700	116.436
CBeC	37,953	37,315	36,497	35,848
BeCC	71,024	71,343	71,752	72,076
CH	1,084	1,085	1,085	1,086
HCCBe	92,861	92,292	91,671	91,598

Table 22. Distances and angles for the optimized geometries of the complex BeH_2-C_2H_4 for each method, all of them with the 6-311+G(d,p) basis.

Property	B3LYP	M06	MP2	CCSD
FBeF	150,329	150,819	149,545	149,189
FBeC	104,205	103,958	104,537	104,709
BeC	2,344	2,311	2,291	2,293
HCC	121,348	121,328	120,901	121,129
BeF	1,411	1,405	1,418	1,412
CC	1,338	1,333	1,349	1,348
HCH	117.280	117.333	118.184	117.721
CBeC	33,166	33,524	34,243	34,199
BeCC	73,417	73,238	72,879	72,901
CH	1,085	1,087	1,086	1,087
HCCBe	90,934	90,627	90,687	90,859

Table 23. Distances and angles for the optimized geometries of the complex BeF_2-C_2H_4 for each method, all of them with the 6-311+G(d,p) basis.

Property	B3LYP	M06	MP2	CCSD
ClBeCl	142,674	144,318	142,924	142,795
ClBeC	107,839	107,045	107,674	107,750
BeC	2,32	2,294	2,276	2,293
HCC	121,337	121,334	120,971	121,151
BeCl	1,848	1,844	1,837	1,840
CC	1,341	1,335	1,351	1,350
HCH	117.284	117.310	118.008	117.643
CBeC	33,597	33,829	34,535	34,249
BeCC	73,201	73,085	72,732	72,875
CH	1,085	1,087	1,086	1,087
HCCBe	91,221	90,854	91,307	91,362

Table 24. Distances and angles for the optimized geometries of the complex $BeCl_2$-C_2H_4 for each method, all of them with the 6-311+G(d,p) basis.

Bond	B3LYP	M06	MP2	CCSD
CH	1.085	1.086	1.085	1.087
CC	1.329	1.323	1.339	1.340
HCC	121.759	121.810	121.409	121.568
HCH	116.482	116.379	117.182	116.865
BeH	1.327	1.327	1.329	1.330
BeF	1.387	1.380	1.293	1.387
BeCl	1.799	1.797	1.792	1.794

Table 25. Bond distances and angles for ethylene and BeX_2 molecules in their isolated equilibrium geometries optimized by the indicated methods and the 6-311+G(d,p) basis set.

At any level of theory it can be seen that, as expected, there is a bending of the BeX_2 molecules. Since B3LYP and M06 overestimated the relaxation energy of the complex with BeH_2, in the optimized geometries for that complex the BeH_2 molecule is almost as bent as $BeCl_2$ in $BeCl_2$ complexes, while for MP2 the difference is just of 0.2 Å and finally for CCSD the angle ClBeCl of the $BeCl_2$ complex is clearly the lowest and therefore its $BeCl_2$ molecule is the most bent. This result follows the relaxation energy trend for each of the methods.

The ethylene molecule has a small but significant bending that can be seen through the sum of the HCH and the two HCC angles. When ethylene is planar, this value is, obviously, of 360º.

If we take a look at the following table containing these angle sums:

C_2H_4-BeH_2	B3LYP	M06	MP2	CCSD
Angle sum	359.771	359.855	359.920	359.928
Difference	-0.229	-0.145	-0.080	-0.072

C_2H_4-BeF_2	B3LYP	M06	MP2	CCSD
Angle sum	359.976	359.989	359.986	359.979
Difference	-0.024	-0.011	-0.014	-0.021

C_2H_4-$BeCl_2$	B3LYP	M06	MP2	CCSD
Angle sum	359.958	359.978	359.950	359.945
Difference	-0.042	-0.022	-0.050	-0.055

Table 26. Sum of the HCH and HCC angles of ethylene in each complex and method, all with the 6-311+G(d,p) basis set, and difference with respect to the 360° of a planar ethylene.

Similarly to what happened in acetylene, the deformation over the angles with the C-H bonds is not so much because since the two carbons share the interaction with the displaced charge more probably being between them, the hydrogen atoms don't feel the interaction as much as the atoms directly bonded to the beryllium atom.

Here we see again that the deformation changes much more in the BeH_2 complex when changing the method, while the same angle for the $BeCl_2$ complex varies slightly with the methods and the one of BeF_2 complex practically does not vary. These variations, however, are in agreement with the variations of the relaxation energy.

In addition to that, a small lengthening of the CC bond can be observed, what constitutes an additional indication of the light hybridization of the carbons, which in this case lose a bit of their strict sp2 hybridization.

The angle HCH does also vary slightly, and it is easy to see that since the structures of the complexes with X = F, Cl and the complex with X = H are different these angles vary accordingly. Therefore, hydrogen atoms of the ethylene move to avoid some electronic repulsion tension, and therefore in the case of the transversal BeH_2 they move slightly towards the edges of the ethylene, making the HCC angle bigger and the HCH smaller, while in the case of BeF_2 and $BeCl_2$ they move laterally, making the HCC angle smaller and the HCH bigger.

Besides, as it was seen for acetylene complexes, it can also be seen in these values the second effect of beryllium bonding: as a consequence to the charge transfer to the antibonding orbitals σ_{BeX^*} of Be-X bonds, these bonds weaken and they become longer. This effect is very clear in the case of the Be-Cl bond for which the change is of about 0.05 Å, but it is also still clear for Be-F and Be-H bonds, for which the change is of

about 0.025 Å and 0.015 Å, respectively. This means that more electronic density is participating in the antibonding orbital of Be-F than of Be-H, i.e. the strength of the beryllium bond should be higher for the C_2H_4-BeF_2 complex, in spite of the FBeF being less bent.

This result follows the vertical dissociation energy trend of each method, and as a general trend we find: C_2H_4-$BeCl_2$ > C_2H_4-BeF_2 > C_2H_4-BeH_2, and therefore we expect the beryllium bond in the $BeCl_2$ complex to be the strongest one, followed by the one in the BeF_2 complex and finally the one in the BeH_2 complex.

In order to study in depth the bonding between the interacting molecules, an AIM study was performed for the optimized geometries of all methods. The qualitative results were practically the same for all methods when X = Cl and X = F but when X = H we obtained a different result depending on the methods.

For X = H we obtained:

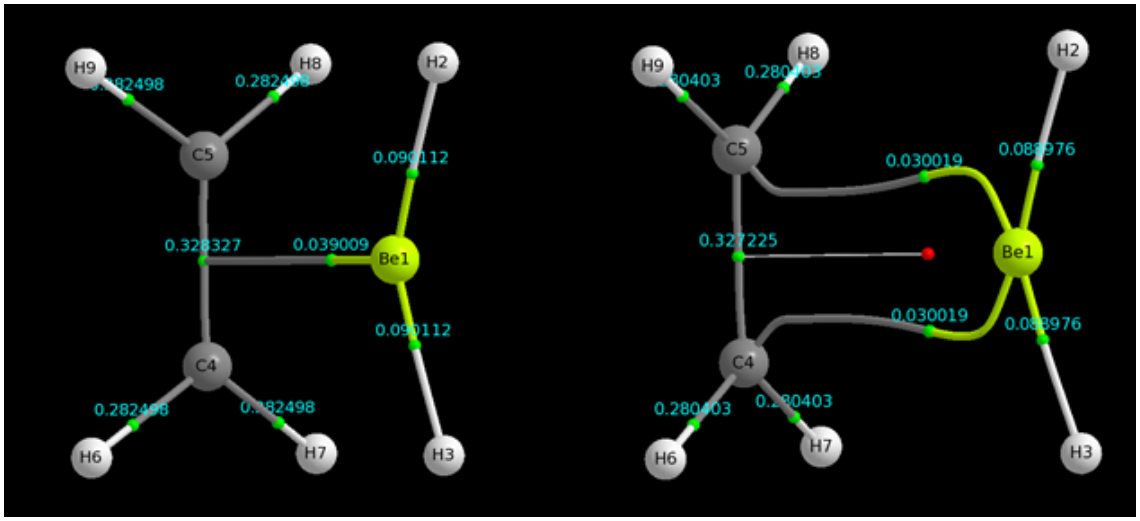

Figure 10. Density plots for the complex BeH_2-C_2H_4 at B3LYP/6-311+G(d,p) (left) and at CCSD/6-311+G(d,p) (right) from aimstudio.

With X = H, both B3LYP and M06 give the same qualitative result, as so do MP2 and CCSD methods, but they are different between them, as shown in Figure 10.
Again, in fact, a critical point is found for all the methods between the molecules, granting some kind of bonding between them. However, the plots are as unconventional as the ones of acetylene complexes.

We find again the conflict catastrophe that causes the bond path to end into the critical point for the CC bond, instead of into an atom, already discussed above. As to the difference between the plots, we also have the same bifurcation catastrophe when passing from DFT methods to MP2 and CCSD, with the third unstable part of the

bifurcation not completely drawn by the program as in the BeF_2-C_2H_2 complex. Therefore, a high value of the ellipticity is expected for the beryllium bond.

If we take a look at the following table, that collects all the AIM data for the complex at the CCSD/6-311+G(d,p) level:

BCP	ρ(r)	$-\nabla^2\rho(r)$	ε	λ_1	λ_2	λ_3
Be1 - C4	0.030019	+0.021129	0.979185	-0.030142	-0.015229	+0.066500
Be1 - C5	0.030019	+0.021129	0.979185	-0.030142	-0.015229	+0.066500
Be1 - H2	0.088976	+0.200081	0.078837	-0.182214	-0.168899	+0.551194
Be1 - H3	0.088976	+0.200081	0.078837	-0.182214	-0.168899	+0.551194
C4 - C5	0.327225	-0.944279	0.365209	-0.692804	-0.507471	+0.255996
C4 - H6	0.280403	-0.971200	0.013244	-0.741946	-0.732248	+0.502994
C4 - H7	0.280403	-0.971200	0.013244	-0.741946	-0.732248	+0.502994
C5 - H8	0.280403	-0.971200	0.013244	-0.741946	-0.732248	+0.502994
C5 - H9	0.280403	-0.971200	0.013244	-0.741946	-0.732248	+0.502994

Table 27. AIM data at the CCSD/6-311+G(d,p) level for the BeH_2-C_2H_4 complex.

The data for the rest of the methods can be found in the Appendix section (XXV).

By looking at the density and its second derivative, the Laplacian, we can see that the character of the bonds is well described for the bonds within the ethylene, which show the big density values and negative Laplacian values characteristic of covalent bonds, while for the Be-H bonds the character appears as slightly ionic, for they have a small density and, though small, they also have a positive value for the Laplacian. As it was said before, this positive value of the Laplacian is also a characteristic of Lewis acids, and we have a $Be^{+\delta}$-$H^{-\delta}$ bond[3]. Similarly, for the beryllium bond (Be1-C4 and Be1-C5) we obtain a relatively small density, although not so small for a non-covalent interaction, and a more positive value for the Laplacian. This agrees with the fact that beryllium bonds have an important ionic character, such as hydrogen bonds do.

Regarding the ellipticity, it has a high value in BCP of Be1-C4 and Be1-C5 which, as said before, indicates an approaching instability and a change in structure, but when the BCP stays –without pitchfork bifurcation- unsplit, for other methods, this value is even higher, up to 16, which explains the appearance of the bifurcation catastrophe. Also, the densities at those points are very similar to the density at the unsplit BCP, which indicates a flat density that reinforces the explanation of the bifurcation catastrophe appearance.

If we now take a look at the plot when X=F:

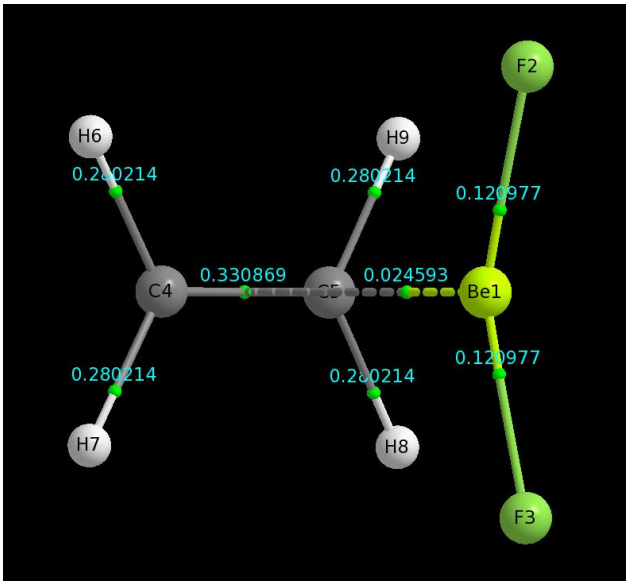

Figure 11. Density plot for the complex BeF_2-C_2H_4 at the CCSD/6-311+G(d,p) level of theory from aimstudio.

In this case all methods gave the same qualitative result.
Here, as for most of the complexes, the beryllium bond path ends in a bond critical point instead of on the carbon atoms, due to the conflict catastrophe. In addition, the bond path is drawn with a dashed line, since the electronic density at the BCP of the beryllium bond does not reach the default minimum value of 0.025 of the program to be drawn in a continuous line. It is clear then that there is less density between the molecules of this complex than in the previous one.

If we look at the AIM data:

BCP	ρ(r)	$-\nabla^2\rho(r)$	ε	λ_1	λ_2	λ_3
Be1 - C5	0.024593	+0.080526	2.287989	-0.019619	-0.005967	+0.106111
Be1 - F2	0.120977	+1.131909	0.006764	-0.340070	-0.337785	+1.809764
Be1 - F3	0.120977	+1.131909	0.006764	-0.340070	-0.337785	+1.809764
C4 - C5	0.330869	-0.969917	0.349859	-0.703457	-0.521134	+0.254675
C4 - H6	0.280214	-0.970596	0.015309	-0.743525	-0.732314	+0.505242
C4 - H7	0.280214	-0.970596	0.015309	-0.743525	-0.732314	+0.505242
C5 - H8	0.280214	-0.970596	0.015309	-0.743525	-0.732314	+0.505242
C5 - H9	0.280214	-0.970596	0.015309	-0.743525	-0.732314	+0.505242

Table 28. AIM data at the CCSD/6-311+G(d,p) level for the BeF_2-C_2H_4 complex.

The data for the rest of the methods can be found in the appendix section (XXVI).

We see that in fact the BCP of the beryllium bond has a value of 0.0246 that is much lower to the value found for the BCP of the same bond of the previous complex, which was, in total, of 0.06. It can also be seen that it has a very low positive value for the Laplacian, which means its character is less ionic but with still has ionic predominance.
With respect to the rest of the bonds, we can see that their character is correctly described within the ethylene, and for the Be-F bonds we find again a quite big positive value of the Laplacian and a small density, having thus a stronger ionic character than Be-H bonds in the previous complex, as it should due to the much greater electronegativity of fluoride with respect to hydrogen.

Regarding the ellipticity, the beryllium bond still has a high value, which shows the same strong preferential accumulation in the plane of λ_2, but it is not enough to produce any bifurcation catastrophe, as it happens in other complexes.

Finally, if we look at the plot when X=Cl:

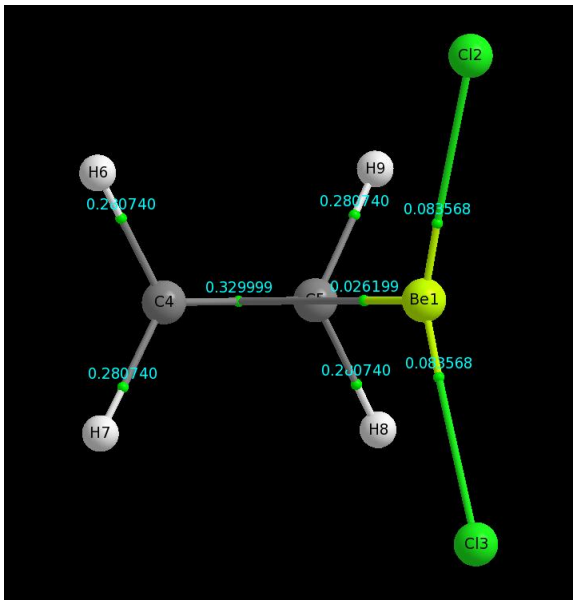

Figure 12. Density plot for the complex $BeCl_2$-C_2H_4 at the CCSD/6-311+G(d,p) level of theory from aimstudio.

In this case the result is qualitatively the same for all the methods.

The only strange thing here is that, as for the BeH_2 complex, the beryllium bond path ends in a bond critical point instead of on the carbon atoms, due to the conflict catastrophe.

If we look at the AIM data:

BCP	ρ(r)	$-\nabla^2\rho(r)$	ε	λ_1	λ_2	λ_3
Be1 - C5	0.026199	+0.077499	1.136194	-0.020875	-0.009772	+0.108146
Be1 - Cl2	0.083568	+0.332620	0.011042	-0.146854	-0.145251	+0.624725
Be1 - Cl3	0.083568	+0.332620	0.011042	-0.146854	-0.145251	+0.624725
C4 - C5	0.329999	-0.966765	0.339055	-0.699959	-0.522726	+0.255921
C4 - H6	0.280740	-0.974603	0.014440	-0.747154	-0.736518	+0.509069
C4 - H7	0.280740	-0.974603	0.014440	-0.747154	-0.736518	+0.509069
C5 - H8	0.280740	-0.974603	0.014440	-0.747154	-0.736518	+0.509069
C5 - H9	0.280740	-0.974603	0.014440	-0.747154	-0.736518	+0.509069

Table 29. AIM data at the CCSD/6-311+G(d,p) level for the $BeCl_2$-C_2H_4 complex.

The data for the rest of the methods can be found in the appendix section (XXVII).
We can see that the character of the bonds is, as in the previous complexes, correctly described for the bonds within the ethylene, and for the Be-Cl bonds we find a small density, even a bit smaller than that of Be-H bonds, and a positive value of the Laplacian, greater than that of Be-H bonds but smaller than that of Be-F bonds. Thus, Be-Cl bonds have more ionic character than the Be-H bonds but less than the Be-F bonds, which is just natural since the electronegativity of chloride is also greater than that of hydrogen but lower than that of fluoride. It also confirms the acidity order: BeF_2 > $BeCl_2$ > BeH_2.
As to the beryllium bond, we obtain a very small density, slightly higher than the one of BeF_2 complex but still much lower than the BeH_2 one, and a very small positive value for the Laplacian, higher than the one of BeF_2 complex but still much lower than the BeH_2 one. Therefore, the beryllium bond still has a predominant ionic character, a bit more than the one of BeF_2 complex but still much lower than the BeH_2 one.

Regarding the ellipticity, the beryllium bond of the complex has the lowest value of the three but it is still quite large, which shows the same strong preferential accumulation of density in the plane of λ_2, but it is not enough to produce any bifurcation catastrophe, as it happens in other complexes.

All in all, what we have is that, regarding the beryllium bond under study, both the value of the density, that serves as an indication of the strength of the bond, and the positive value of the Laplacian, that serves as an indication of the ionic character of the bond due to the density being small, follow the trend: BeH_2 > $BeCl_2$ > BeF_2.
It is worth noting that once more there is not a clear correlation between the electron density at the Beryllium bond critical point and the interaction energies. We have already shown that the interaction energies vary as Cl > F > H whereas de electron densities follow a different trend, H > Cl ≥ F. This likely indicates that, as it has been found previously in the literature, the deformation undergone by the Lewis acid may affect its intrinsic acidity.[52] The investigation of this particular point is the main goal of our future work regarding these complexes.

As to the NBO calculations, at the CCSD/6-311+G(d,p) level of theory the NNBO analysis separates the atoms of the $BeCl_2$ molecule and treats them as separate units, making impossible to see the interactions properly. As explained in section 3.4 of Theoretical Foundations this indicates that the bonds are highly polar, to a point where the program separates them. Anyhow, the following discussion is based then in the NBO calculations obtained at the M06/6-311+G(d,p) level of theory.

Again, what is expected in the NBO analysis are populations in the initially empty orbitals p of Be, labeled LP*(Be), and in the antibonding orbitals of the Be-X bond, labeled BD*(BeX). As a consequence, the bonding orbitals of the CC bond, labeled BD(CC), should have less population. Also, these charge transfers should be reflected in the hybridization of C and Be in the different bonds and, finally, important contributions to the energy should be found corresponding to the charge transfer processes.

If we take a look at the following tables:

Complex	BD*(BeX)	BD (CC)	LP*(Be)
C_2H_4-BeH_2	0.003	1.996; 1.858	0.159; 0.006
C_2H_4-BeF_2	0.015	1.996; 1.908	0.165; 0.134
C_2H_4-$BeCl_2$	0.023	1.996; 1.871	0.244; 0.220

Table 30. NBO populations obtained at the M06/6-311+G(d,p) level of theory.

Complex	BD(CC) → LP*(Be)	BD(CC) → BD*(Be-X)
C_2H_4-BeH_2	315.48	2.55
C_2H_4-BeF_2	150.35	5.36
C_2H_4-$BeCl_2$	228.01	6.80

Table 31. NBO second order perturbational correction energies at the M06/6-311+G(d,p) level of theory, in kJ/mol.

Complex	BD (CC)	BD (CH)	LP* (Be)	BD* (BeX)
C_2H_4-BeH_2	sp1.71; p96%	sp2.35	sp7.02(p89%); p97%	sp1.28
C_2H_4-BeF_2	sp1.51; p99%	sp2.37	sp8.96(p90%); p100%	sp1.23
C_2H_4-$BeCl_2$	sp1.61; p98%	sp2.35	sp8.99(p90%); p100%	sp1.23

Table 32. NBO hybridization of C and Be atoms in certain bonds, at the M06/6-311+G(d,p) level of theory.

As a matter of fact, it is indeed found that there is population in BD*(BeX) and LP*(Be), there is less population in the BD(CC), the C and Be atoms show different

hybridization and there are contributions to the energy for the two main processes of the Beryllium bond.

Again, we find two opposed trends:
On the one hand, the trend for the charge transfer BD(CC) → BD*(Be-X) is Cl > F > H, as it was for acetylene complexes. This also agrees with the observed trend for the elongation of the Be-X bond, with the population of the BD*(BeX) orbital and, more importantly, with the interaction energy trend.

On the other hand, and again as obtained for acetylene complexes, the trend observed for the charge transfer BD(CC) → LP*(Be) is H > Cl > F, that is the same trend the density at the BCP of the beryllium bond follows.

Additionally, the Wiberg bond order (BO) follows the same trend too:

Complex	**Wiberg BO (BeC)[a]**	**Density ρ(r)**
C_2H_4-BeH_2	0,186	0,036
C_2H_4-BeF_2	0,089	0,024
C_2H_4-$BeCl_2$	0,127	0,027

Table 33. Density at the BCP of the beryllium bond of each complex at the CCSD/6-311+G(d,p) level of theory and its corresponding Wiberg bond order. (a) For one carbon only, the other one has the same value.

Therefore, the trend of the density at the beryllium bond and the trend of the interaction energy are not the same. Here again, he find that there must be some effect that we are not considering.

Studying further the NBO analysis, checking the additional contributions to the energy for other charge transfers which were found for acetylene complexes, one finds:

Complex	**BD(BeX) → BD*(CC)**	**LP(X) → BD*(CC)**
C_2H_4-BeH_2	36.47	-
C_2H_4-BeF_2	-	0.000; 0.000; 0.251
C_2H_4-$BeCl_2$	-	-

Table 34. Other important contributions to the energy from the NBO analysis at the M06/6-311+G(d,p) level of theory, in kJ/mol. The contributions are per bond/atom.

It is here more evident that the different relative disposition of the BeH_2 molecule with respect to the ethylene allows the orbital overlap necessary for the charge transfer BD(BeX) → BD*(CC) to be possible. The change in this disposition prevents the other two complexes to present this process. It is also clear that this change also mostly prevents the charge transfer from lone pairs of the X atoms to the CC bond, probably because they are too far to overlap.

As it was explained before, such a great contribution from the BD(BeH) of the C_2H_2-BeH_2 complex to the antibonding orbital of the BD*(CC) increases the density at the BCP of the beryllium bond and also the Wiberg BO, for it depends on the square of the density[50]. As a result, the fact that a significant amount of electronic density is placed on an antibonding orbital would explain why, despite the fact that the C_2H_2-BeH_2 complex has more density at the BCP than the other complexes, its interaction energy is the lowest one.

If we look for the populations of these BD(BeX), BD*(CC) and LP(X) orbitals we find:

Complex	**BD(BeX)**	**BD*(CC)**	**LP(X)**
C_2H_4-BeH_2	1.935	0.009; 0.119	-
C_2H_4-BeF_2	1.999	0.003; 0.007	1.989; 1.950; 1.929
C_2H_4-$BeCl_2$	1.999	0.004; 0.012	1.983; 1.927; 1.884

Table 35. Population of indicated orbitals from the NBO analysis at the CCSD/6-311+G(d,p) level of theory.

The population of the BD(BeH) of the complex where X = H shows an even higher loss than in the case of C_2H_2-BeH_2 and, correspondingly, there is an even higer increase in the population of the BD*(CC) orbital. For X = F, Cl the populations show no evidence of any transfer. We can see here that in spite of this, the population of the lone pairs of F or Cl are lower, due to the fact that they partially give it away to beryllium, as we explained before. In any case, this sort of retrodonation observed for the C_2H_2-BeH_2 complex may be the cause that increases the elongation of CC with respect to the elongation achieved for the other complexes, which can be seen in Table 5, even when the C_2H_2-BeH_2 complex is the less stable of the three.

There are here the same flaws to this reasoning, as explained for the acetylene series, and only further researches will clarify the cause for this behavior.

REFERENCES

1. Yáñez, M., et al., *Beryllium Bonds, Do They Exist?* Journal of Chemical Theory and Computation, 2009. **5**(10): p. 2763-2771.
2. P. Hobza, R.Z.a.K.M.-D., Collect. Czech. Chem. Commun. , 2006. **71**: p. 443-531.
3. Housecroft, C.S., A.G., *Inorganic Chemistry*. 3rd ed. 2008: Prentice Hall: New York.
4. Scott Bl Fau - McCleskey, T.M., et al., *The bioinorganic chemistry and associated immunology of chronic beryllium disease.* (1359-7345 (Print)).
5. Mó, O., et al., *Modulating the Strength of Hydrogen Bonds through Beryllium Bonds.* Journal of Chemical Theory and Computation, 2012. **8**(7): p. 2293-2300.
6. M. J. Frisch, G.W.T., H. B. Schlegel, G. E. Scuseria, M. A. Robb, J. R. Cheeseman, G. Scalmani, V. Barone, B. Mennucci, G. A. Petersson, H. Nakatsuji, M. Caricato, X. Li, H. P. Hratchian, A. F. Izmaylov, J. Bloino, G. Zheng, J. L. Sonnenberg, M. Hada, M. Ehara, K. Toyota, R. Fukuda, J. Hasegawa, M. Ishida, T. Nakajima, Y. Honda, O. Kitao, H. Nakai, T. Vreven, J. A. Montgomery, Jr., J. E. Peralta, F. Ogliaro, M. Bearpark, J. J. Heyd, E. Brothers, K. N. Kudin, V. N. Staroverov, R. Kobayashi, J. Normand, K. Raghavachari, A. Rendell, J. C. Burant, S. S. Iyengar, J. Tomasi, M. Cossi, N. Rega, J. M. Millam, M. Klene, J. E. Knox, J. B. Cross, V. Bakken, C. Adamo, J. Jaramillo, R. Gomperts, R. E. Stratmann, O. Yazyev, A. J. Austin, R. Cammi, C. Pomelli, J. W. Ochterski, R. L. Martin, K. Morokuma, V. G. Zakrzewski, G. A. Voth, P. Salvador, J. J. Dannenberg, S. Dapprich, A. D. Daniels, Ö. Farkas, J. B. Foresman, J. V. Ortiz, J. Cioslowski, and D. J. Fox,, *Gaussian 09*. 2009, Gaussian, Inc.: Wallingford CT.
7. Becke, A.D., J. Chem. Phys., 1993. **98**: p. 5648-5652.
8. C. Lee, W.Y., R.G. Parr, Phys. Rev. B, 1988. **37**: p. 785-789.
9. S.H. Vosko, L.W., M. Nusair, Can. J. Phys., 1980. **58**: p. 1200-1211.
10. P. J. Stephens, F.J.D., C.F. Chabalowski, M. J. Frisch, J. Phys. Chem., 1994. **98**: p. 11623-11627.
11. Hertwig, R.H. and W. Koch, *On the parameterization of the local correlation functional. What is Becke-3-LYP?* Chemical Physics Letters, 1997. **268**(5–6): p. 345-351.
12. Zhao, Y. and D. Truhlar, *The M06 suite of density functionals for main group thermochemistry, thermochemical kinetics, noncovalent interactions, excited states, and transition elements: two new functionals and systematic testing of four M06-class functionals and 12 other functionals.* Theoretical Chemistry Accounts, 2008. **120**(1-3): p. 215-241.
13. Hehre, W.J., R.F. Stewart, and J.A. Pople, *Self-Consistent Molecular-Orbital Methods: I. Use of Gaussian Expansions of Slater-Type Atomic Orbitals.* J. Chem. Phys., 1969: p. 2657-2664.
14. Møller, C. and M.S. Plesset, *Note on an Approximation Treatment for Many-Electron Systems.* Physical Review, 1934. **46**(7): p. 618-622.
15. Head-Gordon, M., J.A. Pople, and M.J. Frisch, *MP2 energy evaluation by direct methods.* Chemical Physics Letters, 1988. **153**(6): p. 503-506.

16. Sæbø, S. and J. Almlöf, *Avoiding the integral storage bottleneck in LCAO calculations of electron correlation.* Chemical Physics Letters, 1989. **154**(1): p. 83-89.
17. Frisch, M.J., M. Head-Gordon, and J.A. Pople, *Semi-direct algorithms for the MP2 energy and gradient.* Chemical Physics Letters, 1990. **166**(3): p. 281-289.
18. Bartlett, R.J., *Many-Body Perturbation Theory and Coupled Cluster Theory for Electron Correlation in Molecules.* Annual Review of Physical Chemistry, 1981. **32**(1): p. 359-401.
19. J. A. Pople, R.K., H. B. Schlegel, and J. S. Binkley,, *Electron Correlation Theories and Their Application to the Study of Simple Reaction Potential Surfaces.* Int. J. Quantum Chem., 1978. **14**.
20. Cížek, J., *Advances in Chemical Physics*. Vol. 14. 1969: P. C. Hariharan.
21. Bartlett, G.D.P.I.a.R.J., *A full coupled-cluster singles and doubles model - the inclusion of disconnected triples.* J. Chem. Phys., 1982. **76**: p. 1910-18.
22. G. E. Scuseria, C.L.J., and H. F. Schaefer III, *An efficient reformulation of the closed-shell coupled cluster single and double excitation (CCSD) equations.* J. Chem. Phys., 1988. **89**: p. 7382-87.
23. G. E. Scuseria and H. F. Schaefer III, *Is coupled cluster singles and doubles (CCSD) more computationally intensive than quadratic configuration-interaction (QCISD)?* J. Chem. Phys., 1989. **90**: p. 3700-03.
24. LANDIS, F.W.a.C.R., *NATURAL BOND ORBITALS AND EXTENSIONS OF LOCALIZED BON.* CERP, 2001. **2**: p. 91-104.
25. Foster, J.P. and F. Weinhold, *Natural hybrid orbitals.* Journal of the American Chemical Society, 1980. **102**(24): p. 7211-7218.
26. E. D. Glendening, J., K. Badenhoop, A. E. Reed, J. E. Carpenter, J. A. Bohmann, C. M. Morales, and F. Weinhold, *NBO 5.0*. 2001, Theoretical Chemistry Insitute: University of Wisconsin, Madison.
27. Bader, R.F.W., *Atoms in Molecules: A Quantum Theory*. 1990, Oxford: Oxford University Press.
28. Bader, R.F., *Atoms in Molecules.* Acounts of Chemical Research, 1985. **18**: p. 9-15.
29. Nguyen-Dang, R.F.W.B.a.T.T., *Quantum Theory of Atoms in Molecules: Dalton Revisited.* Advances in Quantum Chemistry. **14**: p. 63-124.
30. Keith, T.A., *AIMAll (Version 13.01.27)*. 2013, TK Gristmill Software: Overland Park KS, USA.
31. Jr, T.H.D., *Gaussian basis sets for use in correlated molecular calculations. I. The atoms boron through neon and hydrogen.* J. Chem. Phys., 1989. **90**: p. 1007-23.
32. R. A. Kendall, T.H.D.J., and R. J. Harrison, *Electron affinities of the first-row atoms revisited. Systematic basis sets and wave functions.* J. Chem. Phys., 1992. **96**: p. 6796-806.
33. Noordik, G.S.a.J.H., *Molden: a pre- and post-processing program for molecular and electronic structures.* J. Comput.-Aided Mol. Design, 2000. **14**: p. 123-134.
34. Slater, J.C., Phys. Rev. , 1930. **36**: p. 57.
35. Boys, S.F., Proc. royal Soc. London, 1950. **258**: p. 402.
36. W. J. Hehre, R.F.S., J. A. Pople, J. Chem. Phys., 1969. **51**: p. 2657.
37. Ditchfield, R., W.J. Hehre, and J.A. Pople, *Self-Consistent Molecular-Orbital Methods. IX. An Extended Gaussian-Type Basis for Molecular-Orbital Studies*

of Organic Molecules. The Journal of Chemical Physics, 1971. **54**(2): p. 724-728.
38. Hohenberg, P.a.K., W., *Inhomogeneous Electron Gas.* Phys. Rev. B, 1964. **136**: p. 864-971.
39. Coleman, A.J., Rev. Mod. Phys., 1963. **35**: p. 668.
40. Kohn, W.a.S., L. J., *Self-consistent equations including exchange and correlation effects.* Phys. Rev. A, 1965. **140**: p. 1133-1138.
41. J. P. Perdew, J.A.C., S. H. Vosko, K. A. Jackson, M. R. Pederson, D. J. Singh, and C. Fiolhais, *Atoms, molecules, solids, and surfaces: Applications of the generalized gradient approximation for exchange and correlation.* Phys. Rev. B, 1992. **46**: p. 6671-87.
42. Becke, A.D., *Density-functional thermochemistry III The role of the exact exchange.* J. Chem. Phys., 1993. **98**: p. 5648-5652.
43. O. Christiansen, J.O., P. Jorgensen, H. Koch, P. A. Malmqvist,, Chem. Phys. Lett., 1996. **261**: p. 369.
44. Bader, R.F.W., J. Phys. Chem. A, 1998. **102**: p. 7314-7323.
45. Bader, R.F.W., *Bond Paths Are Not Chemical Bonds.* The Journal of Physical Chemistry A, 2009. **113**(38): p. 10391-10396.
46. Matito E Fau - Sola, M., et al., *Electron sharing indexes at the correlated level. Application to aromaticity calculations.* (1359-6640 (Print)).
47. Fiadzomor, P.A.Y., et al., *Interaction energy of water dimers from pressure broadening of near-IR absorption lines.* Chemical Physics Letters, 2008. **462**(4–6): p. 188-191.
48. Farrugia Lj Fau - Senn, H.M. and H.M. Senn, *Metal-metal and metal-ligand bonding at a QTAIM catastrophe: a combined experimental and theoretical charge density study on the alkylidyne cluster Fe3(mu-H)(mu-COMe)(CO)10.* (1520-5215 (Electronic)).
49. Foroutan-Nejad, C. and S. Shahbazian, *Atomic basins with more than a single nucleus: A computational fact or a mathematical artifact?* Journal of Molecular Structure: THEOCHEM, 2009. **894**(1–3): p. 20-22.
50. DICK, et al., *Analysis of bonding properties in molecular ground and excited states by a Cohen-type bond order*. Vol. 24. 1983, New York, NY, ETATS-UNIS: John Wiley & Sons.
51. Goar Sánchez-Sanz, I.A., Jose Elguero, Manuel Yañez and Otilia Mo, Phys. Chem. Chem. Phys., 2012. **14**: p. 11468-11477.
52. Sanchez-Sanz, G., et al., *Strong interactions between copper halides and unsaturated systems: new metallocycles? Or the importance of deformation.* Physical Chemistry Chemical Physics, 2012. **14**(32): p. 11468-11477.

APPENDIX

I. Energies and structural data for C_2H_2-BeH_2

Method/6-311+G(d,p)	B3LYP	M06	MP2	CCSD
μ /D	3,577	3,465	3,917	3,902
ZPVE /kcal/mol	27,24	27,18	27,27	27,30
-E /H/P	93,3	93,2	92,9	93,0
-E /Kcal/mol	58541,3	58.489,8	58325,9	58344,0
$-E_t$ (E+ZPVE) /Kcal/mol	58514,0	58.462,6	58298,6	58316,7
ΔH_{int} /Kcal/mol	6,4	6,5	5,9	4,7
ΔH_{int} /KJ/mol	26,8	27,2	24,7	19,5
ΔH_{vert} /Kcal/mol	14,6	13,8	11,4	10,0
ΔH_{vert} /KJ/mol	61,3	57,6	47,9	41,8
ν_1 (a_2, a_1, a_2, a_2)	365	307	298	281
ν_2 (a_1, a_2, a_1, a_1)	366	335	300	291
ν_3 (b_2)	448	461	407	399
ν_4 (b_2)	486	490	577	576
ν_5 (b_1, b_1, a_2, a_2)	660	671	629	640
ν_6 (b_2)	712	710	660	677
ν_7 (a_2, a_2, b_1, b_1)	720	727	693	694
ν_8 (a_1)	779	780	795	804
ν_9 (b_1)	791	797	796	814
ν_{10} (a_1)	825	848	883	881
ν_{11} (a_1)	1952	1961	1917	1977
ν_{12} (a_1)	1981	1988	2005	1995
ν_{13} (b_2)	2082	2098	2140	2118
ν_{14} (b_2)	3399	3372	3445	3428
ν_{15} (a_1)	3488	3468	3530	3522
A /GHz	28,700	28,697	28,143	28,342
B /GHz	16,769	16,626	15,157	14,840
C /GHz	10,585	10,527	9,851	9,740
HBeH /°	137,787	138,723	141,059	142,090
HBeC /°	92,971	92,674	91,739	92,014
BeC /Å	1,954	1,967	2,070	2,091
HCC /°	170,930	172,722	174,988	175,406
BeH /Å	1,347	1,347	1,347	1,349
CC /Å	1,216	1,213	1,227	1,219
CBeC /°	36,272	35,929	34,462	33,883
BeCC /°	71,864	72,036	72,769	73,059
CH /Å	1,065	1,066	1,066	1,068

II. Energies and structural data for C_2H_2-BeF_2

Method/6-311+G(d,p)	B3LYP	M06	MP2	CCSD
μ /D	3,608	3,601	3,863	3,861
ZPVE /kcal/mol	22,11	22,12	21,93	22,10
-E /H/P	292,0	291,9	291,3	291,3
-E /Kcal/mol	183255,8	183.166,3	182810,0	182817,2
$-E_t$ (E+ZPVE) /Kcal/mol	183233,7	183.144,2	182788,1	182795,1
ΔH_{int} /Kcal/mol	5,3	8,2	6,9	6,8
ΔH_{int} /KJ/mol	22,0	34,2	29,0	28,4
ΔH_{vert} /Kcal/mol	10,0	12,5	11,7	11,6
ΔH_{vert} /KJ/mol	41,7	52,3	48,8	48,8
ν_1 (a_2)	74	72	59	59
ν_2 (b_2)	174	176	186	185
ν_3 (a_1)	188	182	206	208
ν_4 (b_2)	245	258	259	261
ν_5 (a_1)	315	322	332	334
ν_6 (b_1)	395	398	403	408
ν_7 (a_2)	695	716	596	604
ν_8 (b_2)	709	721	648	666
ν_9 (a_1)	737	743	740	750
ν_{10} (b_1)	800	805	795	802
ν_{11} (a_1)	813	810	818	830
ν_{12} (b_2)	1367	1382	1377	1392
ν_{13} (a_1)	2046	2042	1955	2019
ν_{14} (b_2)	3401	3368	3437	3419
ν_{15} (a_1)	3505	3477	3525	3520
A /GHz	5,974	6,019	5,924	5,969
B /GHz	4,659	4,747	4,678	4,679
C /GHz	2,618	2,654	2,614	2,623
FBeF /°	148,200	148,197	148,194	148,009
FBeC /°	90,722	90,600	90,488	90,658
BeC /Å	2,298	2,277	2,295	2,293
HCC /°	179,314	179,806	179,554	179,499
BeF /Å	1,415	1,408	1,418	1,414
CC /Å	1,203	1,202	1,220	1,213
CBeC /°	30,355	30,602	30,829	30,674
BeCC /°	74,822	74,699	74,585	74,663
CH /Å	1,065	1,067	1,067	1,068

III. Energies and structural data for C_2H_2-$BeCl_2$

Method/6-311+G(d,p)	B3LYP	M06	MP2	CCSD
μ /D	4,585	4,297	4,908	4,873
ZPVE /kcal/mol	20,85	20,90	20,75	20,85
-E /H/P	1012,7	1.012,6	1011,3	1011,3
-E /Kcal/mol	635482,3	635.393,0	634561,9	634585,3
$-E_t$ (E+ZPVE) /Kcal/mol	635461,5	635.372,1	634541,1	634564,5
ΔH_{int} /Kcal/mol	1,9	5,1	5,0	3,5
ΔH_{int} /KJ/mol	7,8	21,6	20,9	14,5
ΔH_{vert} /Kcal/mol	11,5	13,5	14,1	12,6
ΔH_{vert} /KJ/mol	48,3	56,5	58,8	52,6
ν_1 (a_2)	46	45	17	23
ν_2 (b_2, a_1, b_2, b_2)	165	160	175	171
ν_3 (a_1, b_2, a_1, a_1)	191	168	206	198
ν_4 (a_1)	201	200	214	209
ν_5 (b_2)	273	296	275	272
ν_6 (b_1)	310	297	321	322
ν_7 (a_1)	498	487	522	514
ν_8 (a_2)	698	718	611	620
ν_9 (b_2)	712	762	635	655
ν_{10} (b_1)	798	802	794	801
ν_{11} (a_1)	824	864	834	848
ν_{12} (b_2)	934	946	997	993
ν_{13} (a_1)	2036	2032	1949	2014
ν_{14} (b_2)	3400	3370	3438	3423
ν_{15} (a_1)	3502	3477	3529	3523
A /GHz	3,304	3,338	3,345	3,294
B /GHz	2,266	2,260	2,277	2,271
C /GHz	1,344	1,348	1,355	1,344
ClBeCl /°	136,764	138,241	137,987	138,075
ClBeC /°	95,965	95,323	95,191	95,391
BeC /Å	2,234	2,244	2,241	2,262
HCC /°	177,152	177,811	176,866	177,035
BeCl /Å	1,858	1,851	1,844	1,847
CC /Å	1,205	1,204	1,221	1,214
CBeC /°	31,307	31,112	31,632	31,143
BeCC /°	74,347	74,444	74,184	74,429
CH /Å	1,065	1,067	1,067	1,068

IV. Energies and structural data for C_2H_4-BeH_2

Method/6-311+G(d,p)	B3LYP	M06	MP2	CCSD
μ /D	3,389	3,254	3,763	3,729
ZPVE /kcal/mol	42,49	42,09	42,99	42,79
-E /H/P	94,5	94,5	94,2	94,2
-E /Kcal/mol	59328,2	59271,4	59097,7	59123,8
$-E_t$ (E+ZPVE) /Kcal/mol	59285,7	59229,3	59054,7	59081,0
ΔH_{int} /Kcal/mol	3,1	3,8	3,7	2,2
ΔH_{int} /KJ/mol	13,0	15,7	15,5	9,2
ΔH_{vert} /Kcal/mol	11,3	10,7	9,8	8,0
ΔH_{vert} /KJ/mol	47,4	44,7	41,2	33,5
ν_1 (a_2)	267	230	216	194
ν_2 (a_1)	308	256	269	247
ν_3 (b_2)	350	340	322	303
ν_4 (b_2, b_1, b_1, b_1)	465	479	451	436
ν_5 (b_1, b_2, b_2, b_2)	502	486	532	536
ν_6 (b_1)	676	684	698	700
ν_7 (a_1, b_1, b_1, b_1)	810	794	825	829
ν_8 (b_1, a_1, a_1, a_1)	823	830	856	853
ν_9 (b_2)	975	958	965	976
ν_{10} (a_1)	995	976	1005	1014
ν_{11} (a_2)	1054	1046	1076	1067
ν_{12} (a_2)	1236	1200	1243	1249
ν_{13} (a_1)	1356	1341	1370	1376
ν_{14} (b_2)	1479	1434	1489	1496
ν_{15} (a_1)	1623	1624	1637	1659
ν_{16} (a_1)	1964	1972	2004	1988
ν_{17} (b_2)	2085	2104	2142	2126
ν_{18} (b_2)	3143	3124	3187	3168
ν_{19} (a_1)	3151	3134	3199	3182
ν_{20} (a_2)	3218	3205	3280	3253
ν_{21} (b_1)	3243	3228	3303	3276
A /GHz	21,204	21,274	21,063	21,071
B /GHz	13,540	13,330	12,674	12,304
C /GHz	9,297	9,213	8,867	8,686
HBeH /°	138,309	140,670	142,787	143,180
HBeC /°	91,869	91,008	90,358	90,486
BeC /Å	2,077	2,100	2,163	2,197
HCC /°	121,940	122,048	121,610	121,746
BeH /Å	1,351	1,344	1,355	1,352
CC /Å	115.891	115.759	116.700	116.436
HCH /°	1,347	1,347	1,347	1,348
CBeC /°	37,953	37,315	36,497	35,848
BeCC /°	71,024	71,343	71,752	72,076
CH /Å	1,084	1,085	1,085	1,086
HCCBe /°	92,861	92,292	91,671	91,598

V. Energies and structural data for C_2H_4-BeF_2

Method/6-311+G(d,p)	B3LYP	M06	MP2	CCSD
μ /D	3,613	3,655	4,012	4,027
ZPVE /kcal/mol	37,20	36,96	37,75	37,72
-E /H/P	293,3	293,1	292,6	292,6
-E /Kcal/mol	184045,0	183949,7	183584,0	183599,1
$-E_t$ (E+ZPVE) /Kcal/mol	184007,8	183912,8	183546,2	183561,4
ΔH_{int} /Kcal/mol	4,3	7,2	6,8	6,3
ΔH_{int} /KJ/mol	18,0	30,3	28,4	26,4
ΔH_{vert} /Kcal/mol	9,3	11,7	12,1	11,8
ΔH_{vert} /KJ/mol	38,9	49,0	50,8	49,3
ν_1 (a_2)	29	-13	56	60
ν_2 (b_2)	136	159	140	142
ν_3 (b_1, a_1, b_1, b_1)	162	179	196	198
ν_4 (a_1, b_1, a_1, a_1)	175	189	204	204
ν_5 (b_2)	276	289	272	284
ν_6 (a_1)	319	323	350	349
ν_7 (b_1)	374	374	389	390
ν_8 (a_1)	736	736	743	754
ν_9 (b_2)	843	815	842	846
ν_{10} (b_1)	1014	1004	998	1003
ν_{11} (a_1)	1034	1020	1031	1036
ν_{12} (a_2)	1072	1070	1082	1070
ν_{13} (a_2)	1247	1212	1254	1259
ν_{14} (a_1)	1375	1353	1379	1381
ν_{15} (b_2)	1385	1397	1380	1400
ν_{16} (b_1)	1473	1427	1483	1491
ν_{17} (a_1)	1662	1662	1653	1671
ν_{18} (b_1)	3130	3110	3181	3159
ν_{19} (a_1)	3138	3120	3192	3172
ν_{20} (a_2)	3211	3197	3280	3248
ν_{21} (b_2)	3236	3221	3303	3272
A /GHz	5,550	5,582	5,515	5,556
B /GHz	3,852	3,966	3,975	3,961
C /GHz	2,681	2,740	2,737	2,741
FBeF /°	150,329	150,819	149,545	149,189
FBeC /°	104,205	103,958	104,537	104,709
BeC /Å	2,344	2,311	2,291	2,293
HCC /°	121,348	121,328	120,901	121,129
BeF /Å	1,347	1,347	1,347	1,348
CC /Å	1,411	1,405	1,418	1,412
HCH /°	1,338	1,333	1,349	1,348
CBeC /°	33,166	33,524	34,243	34,199
BeCC /°	73,417	73,238	72,879	72,901
CH /Å	1,085	1,087	1,086	1,087
HCCBe /°	90,934	90,627	90,687	90,859

VI. Energies and structural data for C_2H_4-$BeCl_2$

Method/6-311+G(d,p)	B3LYP	M06	MP2	CCSD
μ /D	4,265	4,115	4,715	4,717
ZPVE /kcal/mol	36,12	35,83	36,64	36,56
-E /H/P	1014,0	1013,8	1012,5	1012,5
-E /Kcal/mol	636272,6	636177,8	635337,5	635368,9
$-E_t$ (E+ZPVE) /Kcal/mol	636236,5	636142,0	635300,9	635332,4
ΔH_{int} /Kcal/mol	1,8	5,6	6,5	4,5
ΔH_{int} /KJ/mol	7,7	23,4	27,1	19,0
ΔH_{vert} /Kcal/mol	9,5	12,3	14,1	12,3
ΔH_{vert} /KJ/mol	40,0	51,7	59,1	51,6
ν_1 (a_2)	70	56	82	81
ν_2 (a_1)	143	153	145	145
ν_3 (b_2)	165	167	177	176
ν_4 (b_2, b_1, b_1, b_1)	183	202	207	206
ν_5 (b_1, b_2, b_2, b_2)	212	206	244	235
ν_6 (b_1)	287	283	277	288
ν_7 (a_1, b_1, b_1, b_1)	300	314	307	306
ν_8 (b_1, a_1, a_1, a_1)	480	484	516	507
ν_9 (b_2)	843	814	841	844
ν_{10} (a_1)	967	985	996	1002
ν_{11} (a_2)	1019	1003	1020	1015
ν_{12} (a_2)	1044	1027	1033	1039
ν_{13} (a_1)	1072	1067	1075	1065
ν_{14} (b_2)	1247	1212	1254	1259
ν_{15} (a_1)	1375	1353	1379	1382
ν_{16} (a_1)	1475	1428	1485	1492
ν_{17} (b_2)	1656	1654	1649	1668
ν_{18} (b_2)	3134	3111	3179	3162
ν_{19} (a_1)	3141	3120	3189	3174
ν_{20} (a_2)	3216	3199	3278	3252
ν_{21} (b_1)	3240	3222	3300	3274
A /GHz	2,874	2,974	2,974	2,934
B /GHz	2,153	2,142	2,171	2,167
C /GHz	1,341	1,358	1,371	1,361
ClBeCl /°	142,674	144,318	142,924	142,795
ClBeC /°	107,839	107,045	107,674	107,750
BeC /Å	2,32	2,294	2,276	2,293
HCC /°	121,337	121,334	120,971	121,151
BeCl /Å	1,848	1,844	1,837	1,840
CC /Å	1,341	1,335	1,351	1,350
HCH /°	117.284	117.310	118.008	117.643
CBeC /°	33,597	33,829	34,535	34,249
BeCC /°	73,201	73,085	72,732	72,875
CH /Å	1,085	1,087	1,086	1,087
HCCBe /°	91,221	90,854	91,307	91,362

VII. Energies and structural data for BeH_2 in its equilibrium geometry.

Method/6-311+G(d,p)	B3LYP	M06	MP2	CCSD
μ /D	0,000	0,000	0,000	0,002
ZPVE /kcal/mol	8,26	8,25	8,26	8,13
-E /H/P	15,9228	15,9084	15,8232	15,8393
-E /Kcal/mol	9991,5	9982,5	9929,0	9939,2
$-E_t$ (E+ZPVE) /Kcal/mol	9983,3	9974,3	9920,8	9931,1
ν_1 (π)	739	724	711	688
ν_2 (π)	739	724	711	688
ν_3 (σ)	2042	2047	2070	2049
ν_4 (σ)	2259	2274	2285	2261
A /GHz	0,000	0,000	0,000	0,000
B /GHz	142,417	142,464	141,950	141,747
C /GHz	142,417	142,464	141,950	141,747
BeH /Å	1,327	1,327	1,329	1,330

VIII. Energies and structural data for BeF_2 in its equilibrium geometry

Method/6-311+G(d,p)	B3LYP	M06	MP2	CCSD
μ /D	0,000	0,000	0,000	0,004
ZPVE /kcal/mol	4,25	4,26	4,19	4,24
-E /H/P	214,6747	214,5952	214,2046	214,2017
-E /Kcal/mol	134708,4	134658,5	134413,4	134411,6
$-E_t$ (E+ZPVE) /Kcal/mol	134704,1	134654,2	134409,2	134407,4
ν_1 (π)	368	352	350	352
ν_2 (π)	368	352	350	352
ν_3 (σ)	708	717	705	714
ν_4 (σ)	1530	1558	1527	1546
A /GHz	0,000	0,000	0,000	0,000
B /GHz	6,916	6,980	6,858	6,911
C /GHz	6,916	6,980	6,858	6,911
BeF /Å	1,387	1,380	1,393	1,387

IX. Energies and structural data for $BeCl_2$ in its equilibrium geometry.

Method/6-311+G(d,p)	B3LYP	M06	MP2	CCSD
ZPVE /kcal/mol	2,92	3,01	2,98	2,97
-E /H/P	935,3597	935,2799	934,1310	934,1562
-E /Kcal/mol	586938,2	586888,1	586167,2	586183,0
$-E_t$ (E+ZPVE) /Kcal/mol	586935,3	586885,1	586164,2	586180,1
ν_1 (π)	254	262	246	246
ν_2 (π)	254	262	246	246
ν_3 (σ)	399	407	412	411
ν_4 (σ)	1137	1172	1180	1175
A /GHz	0,000	0,000	0,000	0,000
B /GHz	2,234	2,248	2,246	2,246
C /GHz	2,234	2,248	2,246	2,246
BeCl /Å	1,799	1,797	1,792	1,794

X. Energies and structural data for C_2H_2 in its equilibrium geometry.

Method/6-311+G(d,p)	B3LYP	M06	MP2	CCSD
ZPVE /kcal/mol	16,96	17,00	16,61	16,72
-E /H/P	77,3566	77,2889	77,1132	77,1278
-E /Kcal/mol	48541,3	48498,8	48388,6	48397,7
$-E_t$ (E+ZPVE) /Kcal/mol	48524,3	48481,8	48371,9	48381,0
ν_1 (π)	657	690	561	575
ν_2 (π)	657	690	561	575
ν_3 (π)	773	781	767	773
ν_4 (π)	773	781	767	773
ν_5 (σ)	2062	2062	1963	2026
ν_6 (σ)	3420	3388	3457	3437
ν_7 (σ)	3522	3497	3547	3536
A /GHz	0,000	0,000	0,000	0,000
B /GHz	35,581	35,658	34,812	35,082
C /GHz	35,581	35,658	34,812	35,082
CH /Å	1,063	1,064	1,065	1,066
CC /Å	1,199	1,197	1,216	1,210

XI. Energies and structural data for C_2H_4 in its equilibrium geometry.

Method/6-311+G(d,p)	B3LYP	M06	MP2	CCSD
ZPVE /kcal/mol	31,86875	31,6	32,09	31,97
-E /H/P	78,6155126	78,538467	78,346303	78,3740729
-E /Kcal/mol	49331,2	49282,9	49162,3	49179,7
$-E_t$ (E+ZPVE) /Kcal/mol	49299,4	49251,3	49130,2	49147,8
ν_1 (b_{2u})	835	807	829	832
ν_2 (b_{3u})	974	961	889	905
ν_3 (b_{2g})	977	970	966	966
ν_4 (a_u)	1058	1051	1061	1045
ν_5 (b_{3g})	1238	1206	1237	1242
ν_6 (a_g)	1378	1355	1382	1382
ν_7 (b_{1u})	1472	1431	1481	1487
ν_8 (a_g)	1684	1691	1675	1688
ν_9 (b_{1u})	3123	3109	3175	3153
ν_{10} (a_g)	3137	3126	3193	3172
ν_{11} (b_{3g})	3194	3188	3265	3234
ν_{12} (b_{2u})	3223	3214	3292	3260
A /GHz	147,300	147,146	146,103	146,128
B /GHz	30,177	30,367	29,886	29,808
C /GHz	25,046	25,172	24,811	24,758
HCH /°	116,482	116,3794	117,182	116,865
CH /Å	1,085	1,0862	1,0853	1,087
CC /Å	1,3288	1,3231	1,3391	1,340
HCC /°	121,759	121,8103	121,409	121,568

XII. Energies of the isolated molecules with their geometries fixed to those they have in the complex C_2H_2-BeH_2

Method/6-311+G(d,p)	B3LYP		M06		MP2		CCSD	
Molecule	BeH_2	C_2H_2	BeH_2	C_2H_2	BeH_2	C_2H_2	BeH_2	C_2H_2
ZPVE /kcal/mol	15,60	6,99	15,66	7,05	7,13	15,38	7,06	15,49
-E /H/P	77,3540	15,9081	77,2871	15,8947	15,8114	77,1124	15,8279	77,1271
-E /Kcal/mol	48.539,7	9.982,3	48.497,6	9.973,9	9.921,6	48.388,0	9.932,0	48.397,2
$-E_t$ (E+ZPVE) /Kcal/mol	48.524,1	9.975,3	48.482,0	9.966,9	9.914,5	48.372,7	9.924,9	48.381,7

XIII. Energies of the isolated molecules with their geometries fixed to those they have in the complex C_2H_2-BeH_2

Method/6-311+G(d,p)	B3LYP		M06		MP2		CCSD	
Molecule	BeF_2	C_2H_2	BeF_2	C_2H_2	BeF_2	C_2H_2	BeF_2	C_2H_2
ZPVE /kcal/mol	15,81	3,55	15,82	3,58	3,58	15,48	3,62	15,58
-E /H/P	77,3566	214,6643	77,2889	214,5854	214,1943	77,1132	214,1912	77,1277
-E /Kcal/mol	48.541,3	134.701,8	48.498,8	134.652,4	134.406,9	48.388,5	134.405,0	48.397,6
$-E_t$ (E+ZPVE) /Kcal/mol	48.525,5	134.698,3	48.483,0	134.648,8	134.403,4	48.373,1	134.401,4	48.382,1

XIV. Energies of the isolated molecules with their geometries fixed to those they have in the complex C_2H_2-BeH_2

Method/6-311+G(d,p)	B3LYP		M06		MP2		CCSD	
Molecule	$BeCl_2$	C_2H_2	$BeCl_2$	C_2H_2	$BeCl_2$	C_2H_2	$BeCl_2$	C_2H_2
ZPVE /kcal/mol	15,91	2,37	15,82	2,39	2,50	15,45	2,49	15,56
-E /H/P	77,3563	935,3420	77,2887	935,2640	934,1142	77,1129	934,1394	77,1275
-E /Kcal/mol	48.541,1	586.927,1	48.498,7	586.878,1	586.156,7	48.388,4	586.172,5	48.397,5
$-E_t$ (E+ZPVE) /Kcal/mol	48.525,2	586.924,8	48.482,9	586.875,8	586.154,2	48.372,9	586.170,0	48.381,9

XV. Energies of the isolated molecules with their geometries fixed to those they have in the complex C_2H_4-BeH_2

Method/6-311+G(d,p)	B3LYP		M06		MP2		CCSD	
Molecule	BeH_2	C_2H_4	BeH_2	C_2H_4	BeH_2	C_2H_4	BeH_2	C_2H_4
ZPVE /kcal/mol	31,70	6,99	31,43	7,04	31,95	7,13	31,87	7,07
-E /H/P	78,6145	15,9084	78,5377	15,8959	78,3459	15,8118	78,3737	15,8286
-E /Kcal/mol	49.330,6	9.982,5	49.282,4	9.974,7	49.162,0	9.921,9	49.179,5	9.932,4
$-E_t$ (E+ZPVE) /Kcal/mol	49.298,9	9.975,5	49.251,0	9.967,7	49.130,1	9.914,8	49.147,6	9.925,4

XVI. Energies of the isolated molecules with their geometries fixed to those they have in the complex C_2H_4-BeF_2

Method/6-311+G(d,p)	B3LYP		M06		MP2		CCSD	
Molecule	BeF_2	C_2H_4	BeF_2	C_2H_4	BeF_2	C_2H_4	BeF_2	C_2H_4
ZPVE /kcal/mol	31,79	3,57	31,51	3,59	31,98	3,58	31,88	3,63
-E /H/P	78,6154	214,6657	78,5383	214,5870	78,3461	214,1951	78,3739	214,1920
-E /Kcal/mol	49.331,1	134.702,7	49.282,8	134.653,3	49.162,2	134.407,4	49.179,6	134.405,5
$-E_t$ (E+ZPVE) /Kcal/mol	49.299,3	134.699,1	49.251,3	134.649,8	49.130,2	134.403,9	49.147,8	134.401,9

XVII. Energies of the isolated molecules with their geometries fixed to those they have in the complex C_2H_4-$BeCl_2$

Method/6-311+G(d,p)	B3LYP		M06		MP2		CCSD	
Molecule	$BeCl_2$	C_2H_4	$BeCl_2$	C_2H_4	$BeCl_2$	C_2H_4	$BeCl_2$	C_2H_4
ZPVE /kcal/mol	31,77	2,40	31,49	2,44	31,96	2,53	31,87	2,51
-E /H/P	78,6153	935,3467	78,5383	935,2682	78,3460	934,1181	78,3738	934,1432
-E /Kcal/mol	49.331,1	586.930,0	49.282,8	586.880,8	49.162,1	586.159,1	49.179,6	586.174,8
$-E_t$ (E+ZPVE) /Kcal/mol	49.299,3	586.927,6	49.251,3	586.878,4	49.130,2	586.156,6	49.147,7	586.172,3

XVIII. Energies of the acetylene complexes at the MP2 and CCSD(T) methods with the aug-cc-pVTZ basis set. (a) Data from a CCSD/6-311+G(d,p) calculation.

Complex	C_2H_2-BeH_2		C_2H_2-BeF_2		C_2H_2-$BeCl_2$	
Method/aug-cc-pVTZ	MP2	CCSD(T)	MP2	CCSD(T)	MP2	CCSD(T)
ZPVE /kcal/mol	27,01	26,77	21,96	22,10[a]	19,90	20,85[a]
-E /H/P	93,0	93,1	291,5	291,6	1011,2	1011,5
-E /Kcal/mol	58364,9	58392,4	182926,0	182952,9	634555,0	634728,6
$-E_t$ (E+ZPVE) /Kcal/mol	58337,9	58365,6	182904,1	182930,8	634535,1	634707,7

XIX. Energies of the ethylene complexes at the MP2 and CCSD(T) methods with the aug-cc-pVTZ basis set. (a) Data from a CCSD/6-311+G(d,p) calculation.

Molecule	C_2H_4-BeH_2		C_2H_4-BeF_2		C_2H_4-$BeCl_2$	
Method/aug-cc-pVTZ	MP2	CCSD	MP2	CCSD	MP2	CCSD
ZPVE /kcal/mol	42,72	42,17	37,77	37,72[a]	36,54	36,56[a]
-E /H/P	94,2	94,3	292,8	292,8	1012,7	1012,8
-E /Kcal/mol	59141,5	59175,6	183704,5	183738,1	635459,4	635514,8
$-E_t$ (E+ZPVE) /Kcal/mol	59098,8	59133,5	183666,7	183700,3	635422,8	635478,2

XX. Energies of the isolated beryllium molecules in the equilibrium geometry at the MP2 and CCSD(T) methods with the aug-cc-pVTZ basis set.

Molecule	BeH_2		BeF_2		$BeCl_2$	
Method/aug-cc-pVTZ	MP2	CCSD	MP2	CCSD	MP2	CCSD
ZPVE /kcal/mol	8,24	8,14	4,19	4,25	2,91	2,90
-E /H/P	15,8	15,8	214,3	214,4	934,3	934,3
-E /Kcal/mol	9.935,5	9945,4	134497,3	134505,9	586250,9	586282,9
$-E_t$ (E+ZPVE) /Kcal/mol	9.927,3	9937,3	134493,1	134501,6	586248,0	586280,0

XXI. Energies of the isolated acetylene and ethylene molecules in the equilibrium geometry at the MP2 and CCSD(T) methods with the aug-cc-pVTZ basis set.

Molecule	C_2H_2		C_2H_4	
Method/aug-cc-pVTZ	MP2	CCSD	MP2	CCSD
ZPVE /kcal/mol	16,62	16,82	31,985	31,647
-E /H/P	77,2	77,2	78,4	78,4
-E /Kcal/mol	48.420,4	48438,1	49.198,8	49223,4
$-E_t$ (E+ZPVE) /Kcal/mol	48.403,8	48421,3	49.166,8	49191,8

XXII. Data from the topologycal analysis of C_2H_2-BeH_2

B3LYP/6-311+G(d,p)

BCP	ρ(r)	$-\nabla^2\rho(r)$	ε	λ_1	λ_2	λ_3
Be1 - C5	0.047560	+0.233101	4.091103	-0.081025	-0.015915	+0.330041
Be1 - H2	0.089584	+0.176662	0.151137	-0.184625	-0.160385	+0.521671
Be1 - H3	0.089584	+0.176662	0.151137	-0.184625	-0.160385	+0.521671
C4 - C5	0.401017	-1.190145	0.023259	-0.671271	-0.656012	+0.137137
C4 - H6	0.288997	-1.062823	0.002094	-0.825152	-0.823428	+0.585756
C5 - H7	0.288997	-1.062823	0.002094	-0.825152	-0.823428	+0.585756

M06/6-311+G(d,p)

BCP	ρ(r)	$-\nabla^2\rho(r)$	ε	λ_1	λ_2	λ_3
Be1 - C5	0.045369	+0.239976	3.940720	-0.078673	-0.015923	+0.334572
Be1 - H2	0.091744	+0.180140	0.120010	-0.190231	-0.169848	+0.540219
Be1 - H3	0.091744	+0.180140	0.120010	-0.190231	-0.169848	+0.540219
C4 - C5	0.393169	-1.075982	0.027072	-0.631043	-0.614410	+0.169471
C4 - H6	0.285499	-1.019070	0.003075	-0.807201	-0.804727	+0.592857
C5 - H7	0.285499	-1.019070	0.003075	-0.807201	-0.804727	+0.592857

MP2/6-311+G(d,p)

BCP	ρ(r)	$-\nabla^2\rho(r)$	ε	λ_1	λ_2	λ_3
Be1 - C5	0.034204	+0.038428	2.248883	-0.035969	-0.011071	+0.085468
Be1 - H2	0.088867	+0.205724	0.091187	-0.182447	-0.167201	+0.555372
Be1 - C4	0.034204	+0.038428	2.248883	-0.035969	-0.011071	+0.085468
Be1 - H3	0.088867	+0.205724	0.091187	-0.182447	-0.167201	+0.555372
Be1 - C5	0.034361	+0.185036	12.587705	-0.052924	-0.003895	+0.241855
C4 - C5	0.384505	-1.074687	0.017623	-0.609393	-0.598840	+0.133546
C4 - H6	0.285557	-1.056259	0.002175	-0.805067	-0.803320	+0.552129
C5 - H7	0.285557	-1.056259	0.002175	-0.805067	-0.803320	+0.552129

CCSD/6-311+G(d,p)

BCP	ρ(r)	$-\nabla^2\rho(r)$	ε	λ_1	λ_2	λ_3
Be1 - C5	0.033086	+0.038472	2.223705	-0.034550	-0.010717	+0.083739
Be1 - H2	0.088601	+0.202039	0.085841	-0.181113	-0.166795	+0.549946
Be1 - C4	0.033086	+0.038472	2.223705	-0.034550	-0.010717	+0.083739
Be1 - H3	0.088601	+0.202039	0.085841	-0.181113	-0.166795	+0.549946
Be1 - C4	0.033165	+0.176881	13.749168	-0.050304	-0.003411	+0.230596
C4 - C5	0.390660	-1.115323	0.021235	-0.619322	-0.606444	+0.110442
C4 - H6	0.285960	-1.047795	0.002813	-0.803327	-0.801073	+0.556605
C5 - H7	0.285960	-1.047795	0.002813	-0.803327	-0.801073	+0.556605

XXIII. Data from the topologycal analysis of C_2H_2-BeF_2

B3LYP/6-311+G(d,p)

BCP	ρ(r)	$-\nabla^2\rho(r)$	ε	λ_1	λ_2	λ_3
Be1 - F2	0.122778	+1.082980	0.012515	-0.341600	-0.337378	+1.761959
Be1 - F3	0.122778	+1.082980	0.012515	-0.341600	-0.337378	+1.761959
Be1 - C4	0.024247	+0.034218	1.953394	-0.021609	-0.007317	+0.063144
Be1 - C5	0.024247	+0.034218	1.953394	-0.021609	-0.007317	+0.063144
C4 - C5	0.409819	-1.232420	0.026593	-0.681813	-0.664151	+0.113544
C4 - H6	0.288821	-1.068121	0.004613	-0.829878	-0.826068	+0.587825
C5 - H7	0.288821	-1.068121	0.004613	-0.829878	-0.826068	+0.587825

M06/6-311+G(d,p)

BCP	ρ(r)	$-\nabla^2\rho(r)$	ε	λ_1	λ_2	λ_3
Be1 - F2	0.124129	+1.123402	0.012296	-0.354762	-0.350453	+1.828617
Be1 - F3	0.124129	+1.123402	0.012296	-0.354762	-0.350453	+1.828617
F3 - C4	0.024148	+0.037978	1.424855	-0.021251	-0.008764	+0.067994
F2 - C5	0.024148	+0.037978	1.424855	-0.021251	-0.008764	+0.067994
C4 - C5	0.401267	-1.110348	0.023573	-0.637798	-0.623109	+0.150559
C4 - H6	0.285166	-1.023502	0.004780	-0.811133	-0.807274	+0.594905
C5 - H7	0.285166	-1.023502	0.004780	-0.811133	-0.807274	+0.594905

MP2/6-311+G(d,p)

BCP	ρ(r)	$-\nabla^2\rho(r)$	ε	λ_1	λ_2	λ_3
Be1 - F2	0.118710	+1.091982	0.009452	-0.329640	-0.326553	+1.748175
Be1 - F3	0.118710	+1.091982	0.009452	-0.329640	-0.326553	+1.748175
F3 - C4	0.023532	+0.036600	1.001253	-0.020318	-0.010153	+0.067071
F2 - C5	0.023532	+0.036600	1.001253	-0.020318	-0.010153	+0.067071
C4 - C5	0.388461	-1.091477	0.021304	-0.613340	-0.600546	+0.122410
C4 - H6	0.284673	-1.051175	0.004637	-0.802770	-0.799065	+0.550661
C5 - H7	0.284673	-1.051175	0.004637	-0.802770	-0.799065	+0.550661

CCSD/6-311+G(d,p)

BCP	ρ(r)	$-\nabla^2\rho(r)$	ε	λ_1	λ_2	λ_3
Be1 - F2	0.120523	+1.118560	0.009020	-0.338810	-0.335781	+1.793151
Be1 - F3	0.120523	+1.118560	0.009020	-0.338810	-0.335781	+1.793151
F3 - C4	0.023449	+0.037247	1.066192	-0.020441	-0.009893	+0.067580
F2 - C5	0.023449	+0.037247	1.066192	-0.020441	-0.009893	+0.067580
C4 - C5	0.393961	-1.128493	0.022376	-0.621270	-0.607673	+0.100450
C4 - H6	0.285025	-1.042295	0.004915	-0.800797	-0.796881	+0.555383
C5 - H7	0.285025	-1.042295	0.004915	-0.800797	-0.796881	+0.555383

XXIV. Data from the topologycal analysis of C_2H_2-$BeCl_2$

B3LYP/6-311+G(d,p)

BCP	ρ(r)	$-\nabla^2\rho(r)$	ε	λ_1	λ_2	λ_3
Be1 - Cl2	0.081771	+0.289104	0.037310	-0.141404	-0.136318	+0.566827
Be1 - Cl3	0.081771	+0.289104	0.037310	-0.141404	-0.136318	+0.566827
Be1 - C4	0.028230	+0.089015	4.158417	-0.032413	-0.006284	+0.127712
C4 - C5	0.409404	-1.239670	0.045852	-0.694568	-0.664117	+0.119015
C4 - H6	0.289394	-1.075714	0.005147	-0.836240	-0.831958	+0.592484
C5 - H7	0.289394	-1.075714	0.005147	-0.836240	-0.831958	+0.592484

M06/6-311+G(d,p)

BCP	ρ(r)	$-\nabla^2\rho(r)$	ε	λ_1	λ_2	λ_3
Be1 - Cl2	0.083004	+0.291620	0.029324	-0.145147	-0.141012	+0.577780
Be1 - Cl3	0.083004	+0.291620	0.029324	-0.145147	-0.141012	+0.577780
Be1 - C4	0.026124	+0.097533	6.698441	-0.030086	-0.003908	+0.131527
C4 - C5	0.400726	-1.116378	0.038985	-0.647907	-0.623596	+0.155125
C4 - H6	0.285608	-1.028739	0.005006	-0.815732	-0.811669	+0.598662
C5 - H7	0.285608	-1.028739	0.005006	-0.815732	-0.811669	+0.598662

MP2/6-311+G(d,p)

BCP	ρ(r)	$-\nabla^2\rho(r)$	ε	λ_1	λ_2	λ_3
Be1 - Cl2	0.082485	+0.327658	0.024236	-0.144429	-0.141011	+0.613098
Be1 - Cl3	0.082485	+0.327658	0.024236	-0.144429	-0.141011	+0.613098
Be1 - C5	0.026128	+0.099629	7.712991	-0.029840	-0.003425	+0.132894
C4 - C5	0.388605	-1.102550	0.039372	-0.626608	-0.602872	+0.126930
C4 - H6	0.285454	-1.060131	0.005487	-0.809673	-0.805254	+0.554796
C5 - H7	0.285454	-1.060131	0.005487	-0.809673	-0.805254	+0.554796

CCSD/6-311+G(d,p)

BCP	ρ(r)	$-\nabla^2\rho(r)$	ε	λ_1	λ_2	λ_3
Be1 - Cl2	0.082507	+0.324241	0.020538	-0.144598	-0.141688	+0.610527
Be1 - Cl3	0.082507	+0.324241	0.020538	-0.144598	-0.141688	+0.610527
Be1 - C5	0.025196	+0.095569	8.439991	-0.028389	-0.003007	+0.126965
C4 - C5	0.394250	-1.139970	0.041338	-0.634903	-0.609699	+0.104631
C4 - H6	0.285912	-1.051170	0.005778	-0.807456	-0.802818	+0.559104
C5 - H7	0.285912	-1.051170	0.005778	-0.807456	-0.802818	+0.559104

XXV. Data from the topologycal analysis of C_2H_4-BeH_2

B3LYP/6-311+G(d,p)

BCP	ρ(r)	$-\nabla^2\rho(r)$	ε	λ_1	λ_2	λ_3
Be1 - C4	0.039009	+0.150425	11.706499	-0.063134	-0.004969	+0.218528
Be1 - H2	0.090112	+0.173729	0.135022	-0.186560	-0.164367	+0.524657
Be1 - H3	0.090112	+0.173729	0.135022	-0.186560	-0.164367	+0.524657
C4 - C5	0.328327	-0.937594	0.325682	-0.697456	-0.526111	+0.285974
C4 - H6	0.282498	-0.977433	0.010950	-0.760731	-0.752491	+0.535790
C4 - H7	0.282498	-0.977433	0.010950	-0.760731	-0.752491	+0.535790
C5 - H8	0.282498	-0.977433	0.010950	-0.760731	-0.752491	+0.535790
C5 - H9	0.282498	-0.977433	0.010950	-0.760731	-0.752491	+0.535790

M06/6-311+G(d,p)

BCP	ρ(r)	$-\nabla^2\rho(r)$	ε	λ_1	λ_2	λ_3
Be1 - C4	0.036049	+0.156489	16.308358	-0.057651	-0.003331	+0.217471
Be1 - H2	0.092184	+0.177659	0.100144	-0.191523	-0.174090	+0.543272
Be1 - H3	0.092184	+0.177659	0.100144	-0.191523	-0.174090	+0.543272
C4 - C5	0.327304	-0.900899	0.314947	-0.679953	-0.517095	+0.296148
C4 - H6	0.277357	-0.923800	0.000725	-0.731043	-0.730513	+0.537756
C4 - H7	0.277357	-0.923800	0.000725	-0.731043	-0.730513	+0.537756
C5 - H8	0.277357	-0.923800	0.000725	-0.731043	-0.730513	+0.537756
C5 - H9	0.277357	-0.923800	0.000725	-0.731043	-0.730513	+0.537756

MP2/6-311+G(d,p)

BCP	ρ(r)	$-\nabla^2\rho(r)$	ε	λ_1	λ_2	λ_3
Be1 - C4	0.031705	+0.022903	1.254163	-0.032681	-0.014498	+0.070083
Be1 - C5	0.031705	+0.022903	1.254163	-0.032681	-0.014498	+0.070083
Be1 - H2	0.089035	+0.203577	0.088072	-0.183112	-0.168290	+0.554979
Be1 - H3	0.089035	+0.203577	0.088072	-0.183112	-0.168290	+0.554979
C4 - C5	0.324450	-0.919559	0.354646	-0.681685	-0.503220	+0.265345
C4 - H6	0.280746	-0.980606	0.012610	-0.747068	-0.737764	+0.504226
C4 - H7	0.280746	-0.980606	0.012610	-0.747068	-0.737764	+0.504226
C5 - H8	0.280746	-0.980606	0.012610	-0.747068	-0.737764	+0.504226
C5 - H9	0.280746	-0.980606	0.012610	-0.747068	-0.737764	+0.504226

CCSD/6-311+G(d,p)

BCP	ρ(r)	$-\nabla^2\rho(r)$	ε	λ_1	λ_2	λ_3
Be1 - C4	0.030019	+0.021129	0.979185	-0.030142	-0.015229	+0.066500
Be1 - C5	0.030019	+0.021129	0.979185	-0.030142	-0.015229	+0.066500
Be1 - H2	0.088976	+0.200081	0.078837	-0.182214	-0.168899	+0.551194
Be1 - H3	0.088976	+0.200081	0.078837	-0.182214	-0.168899	+0.551194
C4 - C5	0.327225	-0.944279	0.365209	-0.692804	-0.507471	+0.255996
C4 - H6	0.280403	-0.971200	0.013244	-0.741946	-0.732248	+0.502994
C4 - H7	0.280403	-0.971200	0.013244	-0.741946	-0.732248	+0.502994
C5 - H8	0.280403	-0.971200	0.013244	-0.741946	-0.732248	+0.502994
C5 - H9	0.280403	-0.971200	0.013244	-0.741946	-0.732248	+0.502994

XXVI. Data from the topologycal analysis of C_2H_4-BeF_2

B3LYP/6-311+G(d,p)

BCP	ρ(r)	$-\nabla^2\rho(r)$	ε	λ_1	λ_2	λ_3
Be1 - C4	0.023869	+0.053625	2.883861	-0.017170	-0.004421	+0.075216
Be1 - F2	0.123755	+1.100520	0.009496	-0.344568	-0.341327	+1.786416
Be1 - F3	0.123755	+1.100520	0.009496	-0.344568	-0.341327	+1.786416
C4 - C5	0.338621	-1.003816	0.307079	-0.727193	-0.556349	+0.279726
C4 - H6	0.282480	-0.979541	0.009947	-0.762747	-0.755234	+0.538440
C4 - H7	0.282480	-0.979541	0.009947	-0.762747	-0.755234	+0.538440
C5 - H8	0.282480	-0.979541	0.009947	-0.762747	-0.755234	+0.538440
C5 - H9	0.282480	-0.979541	0.009947	-0.762747	-0.755234	+0.538440

M06/6-311+G(d,p)

BCP	ρ(r)	$-\nabla^2\rho(r)$	ε	λ_1	λ_2	λ_3
Be1 - C5	0.024395	+0.069234	2.865309	-0.018597	-0.004811	+0.092643
Be1 - F2	0.125065	+1.138949	0.010418	-0.357740	-0.354051	+1.850739
Be1 - F3	0.125065	+1.138949	0.010418	-0.357740	-0.354051	+1.850739
C4 - C5	0.336706	-0.961481	0.300206	-0.707151	-0.543876	+0.289546
C4 - H6	0.277215	-0.924481	0.005987	-0.735107	-0.730732	+0.541358
C4 - H7	0.277215	-0.924481	0.005987	-0.735107	-0.730732	+0.541358
C5 - H8	0.277215	-0.924481	0.005987	-0.735107	-0.730732	+0.541358
C5 - H9	0.277215	-0.924481	0.005987	-0.735107	-0.730732	+0.541358

MP2/6-311+G(d,p)

BCP	ρ(r)	$-\nabla^2\rho(r)$	ε	λ_1	λ_2	λ_3
Be1 - C5	0.024805	+0.079136	2.509926	-0.019385	-0.005523	+0.104044
Be1 - F2	0.118782	+1.099840	0.007097	-0.329307	-0.326986	+1.756133
Be1 - F3	0.118782	+1.099840	0.007097	-0.329307	-0.326986	+1.756133
C4 - C5	0.329333	-0.952354	0.337753	-0.695871	-0.520179	+0.263696
C4 - H6	0.280866	-0.982534	0.014146	-0.749639	-0.739182	+0.506287
C4 - H7	0.280866	-0.982534	0.014146	-0.749639	-0.739182	+0.506287
C5 - H8	0.280866	-0.982534	0.014146	-0.749639	-0.739182	+0.506287
C5 - H9	0.280866	-0.982534	0.014146	-0.749639	-0.739182	+0.506287

CCSD/6-311+G(d,p)

BCP	ρ(r)	$-\nabla^2\rho(r)$	ε	λ_1	λ_2	λ_3
Be1 - C5	0.024593	+0.080526	2.287989	-0.019619	-0.005967	+0.106111
Be1 - F2	0.120977	+1.131909	0.006764	-0.340070	-0.337785	+1.809764
Be1 - F3	0.120977	+1.131909	0.006764	-0.340070	-0.337785	+1.809764
C4 - C5	0.330869	-0.969917	0.349859	-0.703457	-0.521134	+0.254675
C4 - H6	0.280214	-0.970596	0.015309	-0.743525	-0.732314	+0.505242
C4 - H7	0.280214	-0.970596	0.015309	-0.743525	-0.732314	+0.505242
C5 - H8	0.280214	-0.970596	0.015309	-0.743525	-0.732314	+0.505242
C5 - H9	0.280214	-0.970596	0.015309	-0.743525	-0.732314	+0.505242

XXVII. Data from the topologycal analysis of C_2H_4-$BeCl_2$

B3LYP/6-311+G(d,p)

BCP	ρ(r)	$-\nabla^2\rho(r)$	ε	λ_1	λ_2	λ_3
Be1 - C5	0.026458	+0.055462	0.940075	-0.019737	-0.010173	+0.085371
Be1 - Cl2	0.083456	+0.299551	0.021677	-0.144827	-0.141755	+0.586133
Be1 - Cl3	0.083456	+0.299551	0.021677	-0.144827	-0.141755	+0.586133
C4 - C5	0.337185	-0.997545	0.296157	-0.722072	-0.557087	+0.281613
C4 - H6	0.283157	-0.984839	0.009577	-0.767579	-0.760298	+0.543038
C4 - H7	0.283157	-0.984839	0.009577	-0.767579	-0.760298	+0.543038
C5 - H8	0.283157	-0.984839	0.009577	-0.767579	-0.760298	+0.543038
C5 - H9	0.283157	-0.984839	0.009577	-0.767579	-0.760298	+0.543038

M06/6-311+G(d,p)

BCP	ρ(r)	$-\nabla^2\rho(r)$	ε	λ_1	λ_2	λ_3
Be1 - C4	0.026569	+0.070672	1.103054	-0.020986	-0.009979	+0.101636
Be1 - Cl2	0.084137	+0.298842	0.018868	-0.147475	-0.144744	+0.591061
Be1 - Cl3	0.084137	+0.298842	0.018868	-0.147475	-0.144744	+0.591061
C4 - C5	0.335283	-0.955248	0.290305	-0.702206	-0.544217	+0.291175
C4 - H6	0.277520	-0.927192	0.007580	-0.739197	-0.733636	+0.545642
C4 - H7	0.277520	-0.927192	0.007580	-0.739197	-0.733636	+0.545642
C5 - H8	0.277520	-0.927192	0.007580	-0.739197	-0.733636	+0.545642
C5 - H9	0.277520	-0.927192	0.007580	-0.739197	-0.733636	+0.545642

MP2/6-311+G(d,p)

BCP	ρ(r)	$-\nabla^2\rho(r)$	ε	λ_1	λ_2	λ_3
Be1 - C4	0.027149	+0.079183	0.977880	-0.021627	-0.010934	+0.111745
Be1 - Cl2	0.083593	+0.336660	0.013733	-0.146748	-0.144760	+0.628167
Be1 - Cl3	0.083593	+0.336660	0.013733	-0.146748	-0.144760	+0.628167
C4 - C5	0.328152	-0.947744	0.325763	-0.691263	-0.521408	+0.264926
C4 - H6	0.281087	-0.984703	0.013504	-0.752553	-0.742526	+0.510376
C4 - H7	0.281087	-0.984703	0.013504	-0.752553	-0.742526	+0.510376
C5 - H8	0.281087	-0.984703	0.013504	-0.752553	-0.742526	+0.510376
C5 - H9	0.281087	-0.984703	0.013504	-0.752553	-0.742526	+0.510376

CCSD/6-311+G(d,p)

BCP	ρ(r)	$-\nabla^2\rho(r)$	ε	λ_1	λ_2	λ_3
Be1 - C5	0.026199	+0.077499	1.136194	-0.020875	-0.009772	+0.108146
Be1 - Cl2	0.083568	+0.332620	0.011042	-0.146854	-0.145251	+0.624725
Be1 - Cl3	0.083568	+0.332620	0.011042	-0.146854	-0.145251	+0.624725
C4 - C5	0.329999	-0.966765	0.339055	-0.699959	-0.522726	+0.255921
C4 - H6	0.280740	-0.974603	0.014440	-0.747154	-0.736518	+0.509069
C4 - H7	0.280740	-0.974603	0.014440	-0.747154	-0.736518	+0.509069
C5 - H8	0.280740	-0.974603	0.014440	-0.747154	-0.736518	+0.509069
C5 - H9	0.280740	-0.974603	0.014440	-0.747154	-0.736518	+0.509069

XXVIII. AIMAll density plots for C_2H_2-BeH_2 at the B3LYP (up left), M06 (up right), MP2 (down left) and CCSD (down right) levels of theory with the 6-311+G(d,p) basis set.

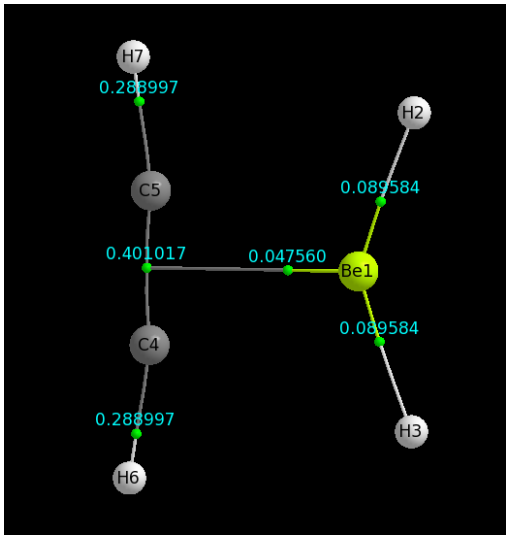

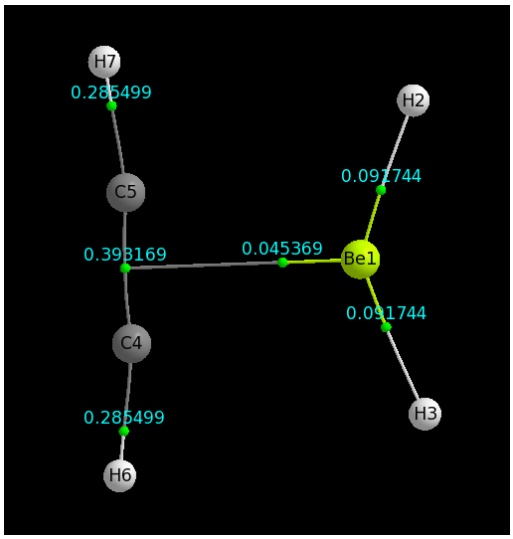

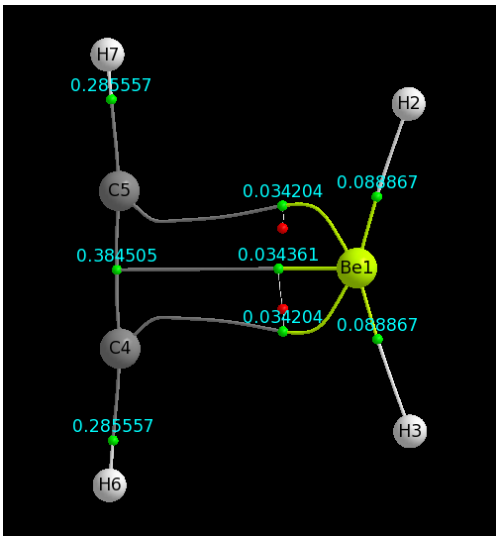

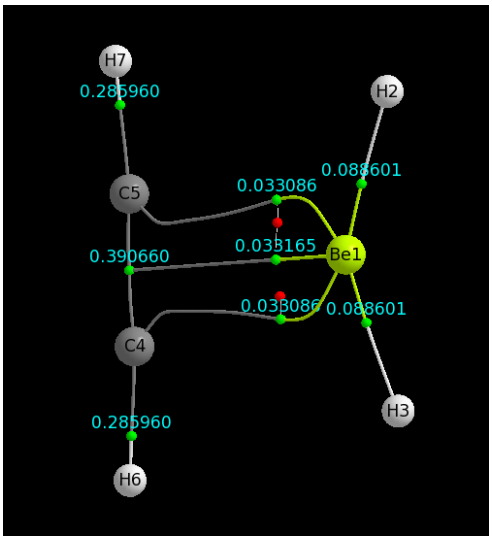

XXIX. AIMAll density plots for C_2H_2-BeF_2 at the B3LYP (up left), M06 (up right), MP2 (down left) and CCSD (down right) levels of theory with the 6-311+G(d,p) basis set.

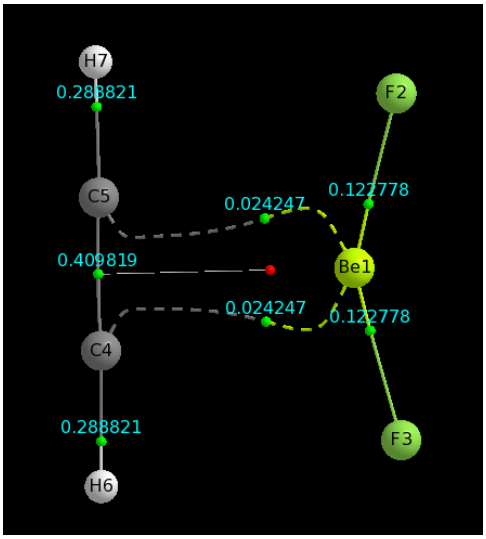

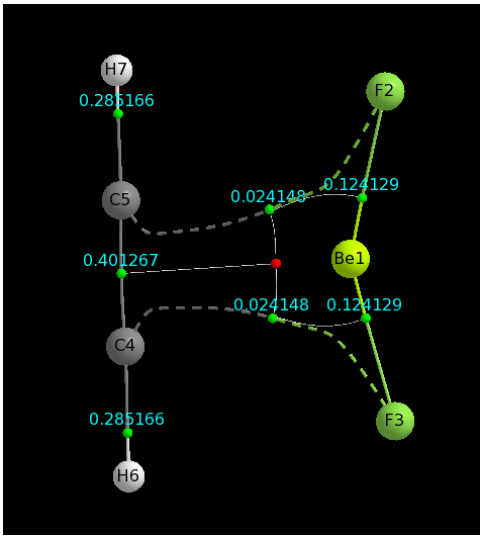

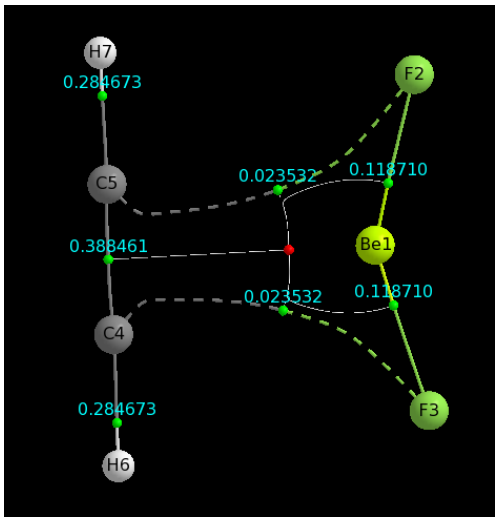

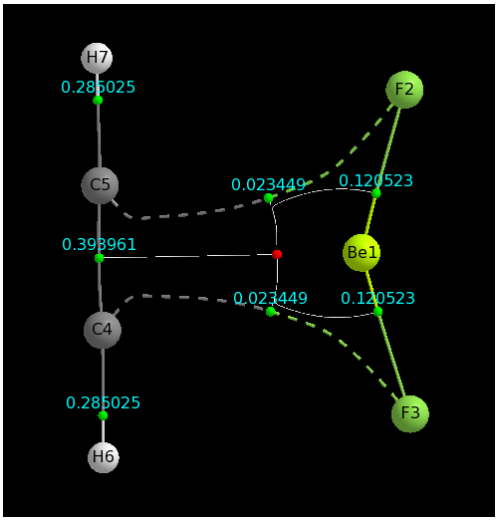

XXX. AIMAll density plots for C_2H_2-$BeCl_2$ at the B3LYP (up left), M06 (up right), MP2 (down left) and CCSD (down right) levels of theory with the 6-311+G(d,p) basis set.

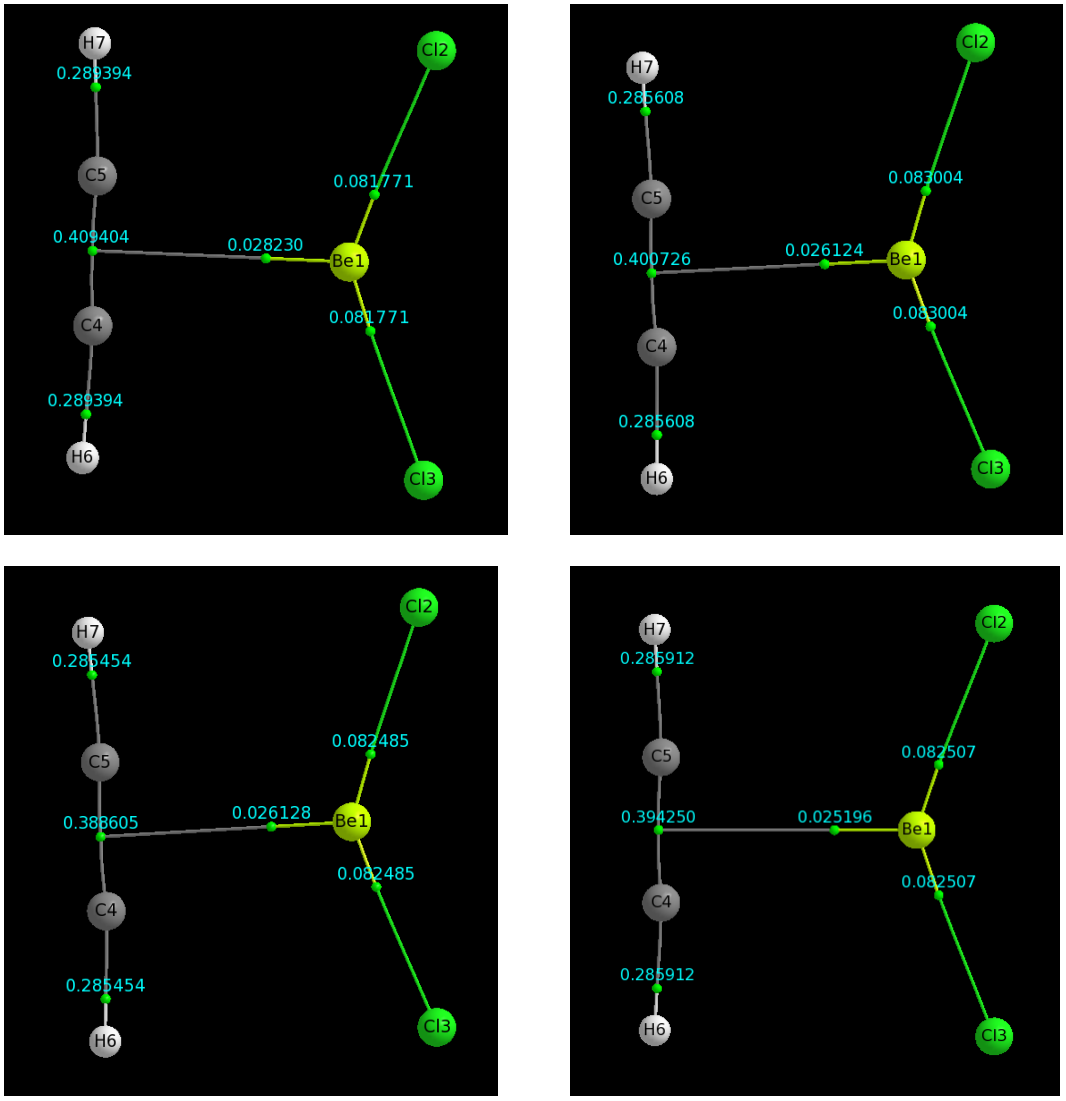

XXXI. AIMAll density plots for C_2H_4-BeH_2 at the B3LYP (up left), M06 (up right), MP2 (down left) and CCSD (down right) levels of theory with the 6-311+G(d,p) basis set.

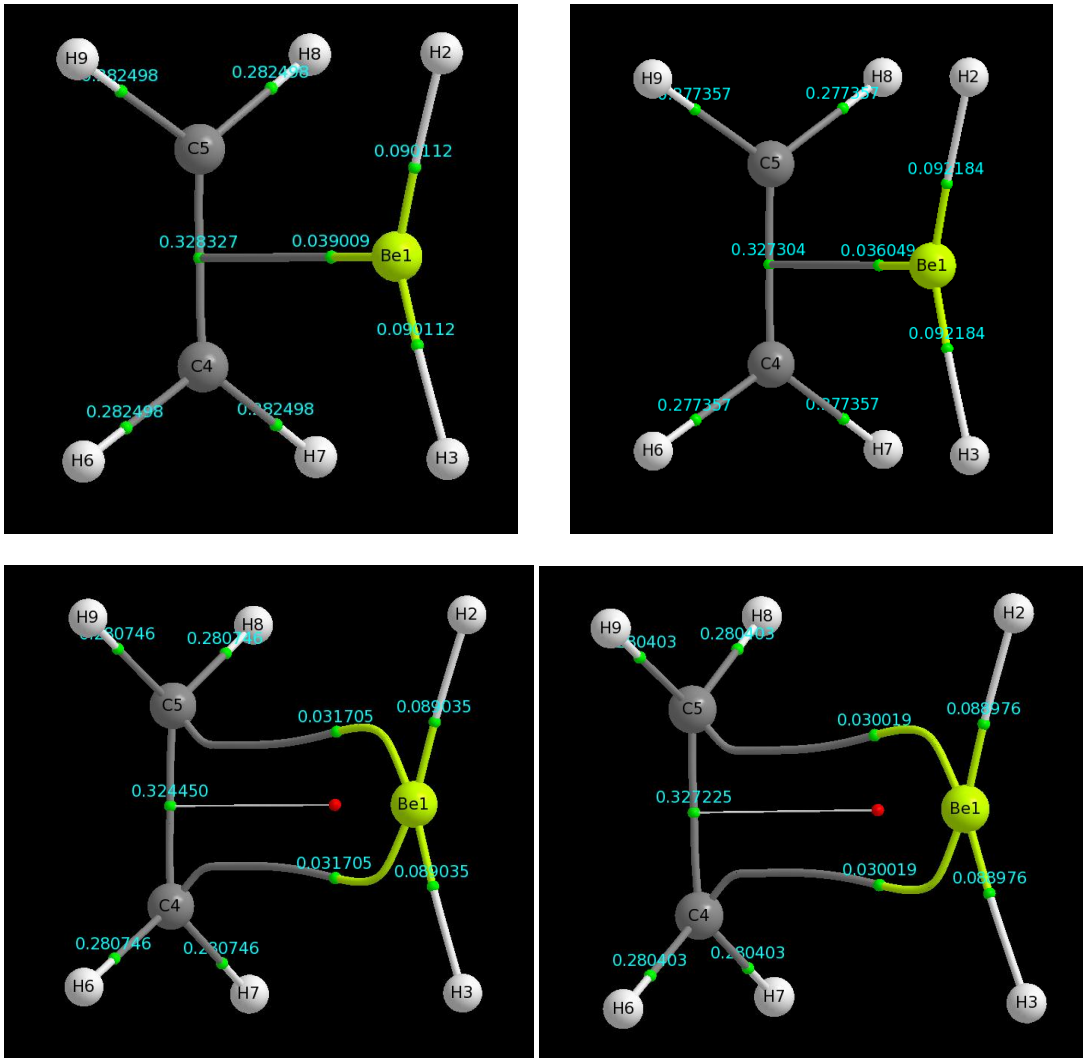

XXXII. AIMAll density plots for C_2H_4-BeF_2 at the B3LYP (up left), M06 (up right), MP2 (down left) and CCSD (down right) levels of theory with the 6-311+G(d,p) basis set.

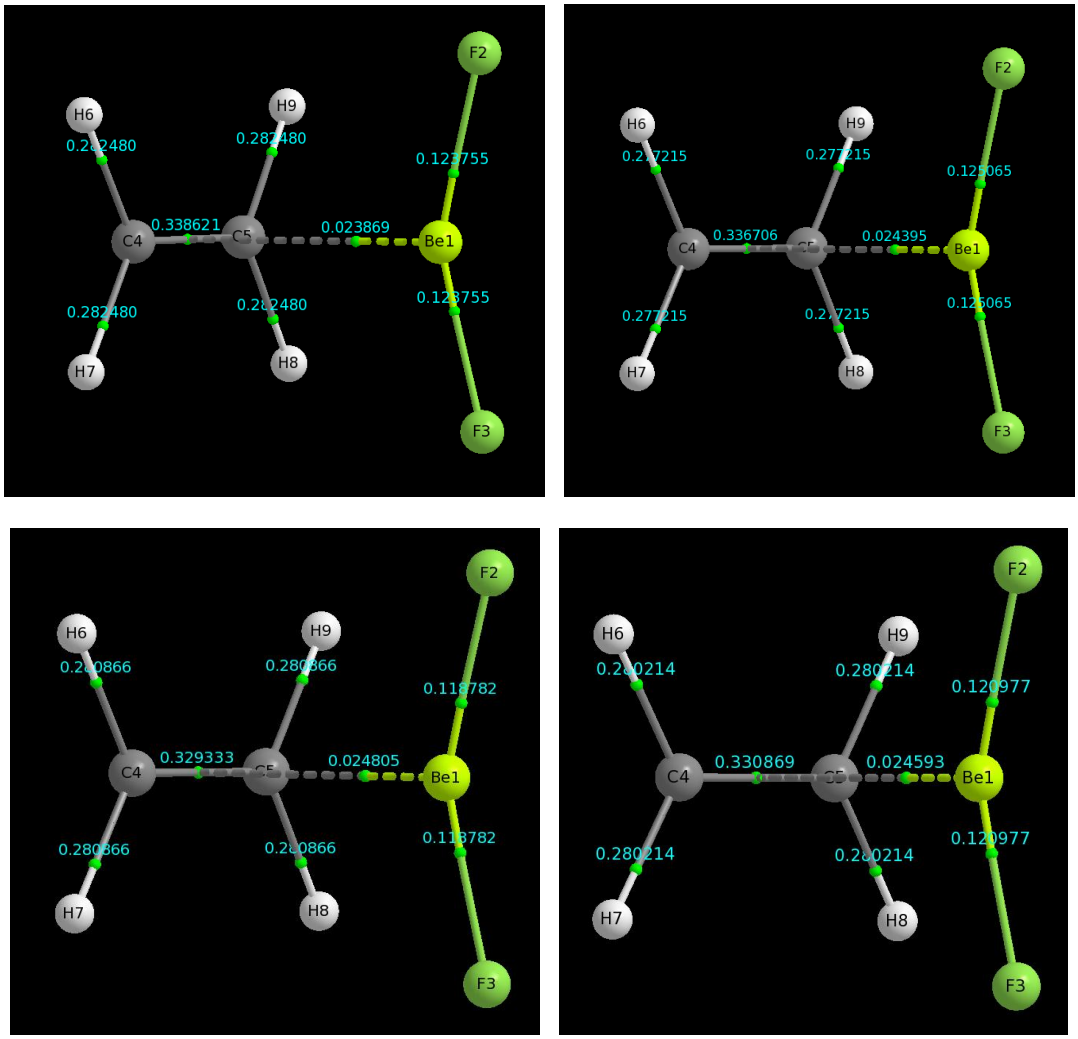

XXXIII. AIMAll density plots for C_2H_4-$BeCl_2$ at the B3LYP (up left), M06 (up right), MP2 (down left) and CCSD (down right) levels of theory with the 6-311+G(d,p) basis set.